J. Fluid Mech. (1973), *vol.* 61, *part* 4, *pp.* 625–706
Printed in Great Britain

A theory of turbulent flow round two-dimensional bluff bodies

By J. C. R. HUNT

Department of Applied Mathematics and Theoretical Physics,† University of Cambridge

(Received 31 October 1972)

By generalizing the theory of 'rapid distortion' of turbulence developed by Batchelor & Proudman (1954) it is shown in this paper that the turbulent velocity around a bluff body placed in a turbulent flow can be calculated outside and upstream of the regions of separated flow, if the incident turbulent flow satisfies the following conditions: (i) if $a/L_x \ll 1$ or $= O(1)$, $Re^{-1}\, u'_\infty/\bar{u}_\infty \ll 1 \ll Re^{\frac{1}{2}}$; (ii) if $a/L_x \gg 1$, $Re^{-1} \ll u'_\infty/\bar{u}_\infty \ll 1/(a/L_x)$ and $Re \gg (a/L_x)^2$, where $Re = \bar{u}_\infty a/\nu$, $\bar{u}_\infty$ is the mean uniform incident velocity, u'_∞ is the r.m.s. velocity of the homogeneous incident turbulence, a is a transverse dimension of the body (the radius in the case of a circular cylinder), L_x is the integral scale of the incident turbulence and ν is the kinematic viscosity.

Detailed calculations are given for the flow around a circular cylinder with particular emphasis on the turbulence very close to the surface. (The results can be generalized to other cylindrical bodies.) Mean-square values and spectra of velocity have been found only in the limiting situations where the turbulence scale is very much larger or smaller than the size of the body, i.e. $L_x \gg a$ or $L_x \ll a$. But, whatever the value of a/L_x, if the frequency is sufficiently large the results for spectra tend to those of the limiting situation where $L_x \ll a$. The reason why the turbulence velocities have not been calculated for intermediate values of a/L_x is that closed-form solutions cannot be found and that the computing time then required is quite excessive. However, some computed results are used in the paper to suggest the qualitative behaviour of the turbulence when L_x is of order a. An important result of the theory is that it illuminates and distinguishes between the governing physical processes of distortion of the turbulence by the mean flow, the direct 'blocking' of the turbulence by the body, and concentration of vortex lines at the body's surface.

The results of the theory have many applications, for example in calculating turbulent dispersion and fluctuating pressures on the body, as shown elsewhere by Hunt & Mulhearn (1973) and Hunt (1973).

In conclusion the theoretical results are briefly compared with experimental measurements of turbulent flows round non-circular cylinders. A detailed comparison with measurements round circular cylinders will be published later by Petty (1974).

† Also: Department of Engineering.

CONTENTS

1. Introduction

The changes in the turbulent velocities of a fluid flowing round a bluff body provide an interesting problem for a number of reasons. First, from a fundamental point of view this is an interesting case of distortion of a turbulent flow which is

different from the other examples which have been studied: distortion by a contraction in a wind tunnel (Ribner & Tucker 1953; Batchelor & Proudman 1954) and the distortion by a shear flow (Deissler 1965; Moffatt 1965; Townsend 1970). Second, this phenomenon must be understood if other important fluid dynamic phenomena are to be explained such as the effects of turbulence in the incident stream on boundary-layer transition and separation (Bearman 1968), vortex shedding (Petty 1974) and stagnation-point heat transfer (Kestin & Wood 1970). Third, since in most situations (whether natural or man-made) where a fluid flows round an obstacle the flow is turbulent, there are many practical problems whose solutions require better understanding of these turbulent flows: for example, calculating heat transfer to heat exchanger tubes (Kestin 1966); calculating fluctuating loads and fluctuating local pressures on buildings (Davenport 1971) and heat exchanger tubes (Owen 1965); predicting gustiness in the vicinity of tall buildings or the effect of turbulence near buildings on dispersion of airborne pollutants (Halitsky 1968); or estimating how a tower or a building, onto which anemometers are fixed, affects the turbulence near it (Cermak & Horn 1968).

The basis of our approach is the 'rapid-distortion theory' due to Prandtl (1933), Taylor (1935) and particularly developed by Batchelor & Proudman (1954), which provides a means of calculating the effect on an initially turbulent flow of a change in the mean velocity. For example, in the original application of the theory r.m.s. values, spectra and other characteristics of the turbulence were calculated downstream of a wind-tunnel contraction, in terms of the upstream values. The theory is only applicable if the time taken for a fluid particle to pass through the zone in which the mean velocity changes is very much less than the time taken for the turbulence to change of its own accord owing to its own viscous and nonlinear inertial forces; in other words, each Fourier component (or eddy) is affected by the mean flow before it has time to exchange energy with other Fourier components. For this approximation to be justified it has to be assumed that the intensity of the turbulence is small enough and the scale large enough. These assumptions also imply that the turbulence is of low enough intensity for the mean flow outside the boundary layers and wake to be only slightly distorted by the turbulence; the mean velocity may therefore be assumed known. It follows from these assumptions that this problem involving a random process is linear and therefore tractable by straightforward mathematical methods. In its application to wind-tunnel contractions Batchelor & Proudman's theory did not agree well with the experimental results of Townsend (1954), but Uberoi (1956) and more recently Tucker & Reynolds (1968) have shown that the theory does describe the distortion of turbulence provided that the assumptions of the theory are well satisfied by the experiments. The application by Townsend (1970) to shear flow also shows the success of the theory in interpreting experimental results. The essential differences between our theory and that of Batchelor & Proudman (1954) and Townsend (1970) are that, first, non-homogeneous distortions are considered (that is to say the turbulence may be of such a scale that the non-homogeneities in the mean flow velocity gradients are of importance) and second a boundary condition is imposed on the turbulence that the velocity

normal to the surface of the body be zero. (We do not consider eddy sizes of the order of the boundary-layer thickness, for which matching with the turbulence in the boundary layers may be necessary.) The analysis consists of calculating the velocity field for each wavenumber $\boldsymbol{\kappa}^*$ of the incident turbulence. As a particular example we take the case of a circular cylinder. It is found that closed-form solutions are not possible except when $a|\boldsymbol{\kappa}^*| \ll 1$ or $a|\boldsymbol{\kappa}^*| \gg 1$, where a is the radius of the body. For a few values of $|\boldsymbol{\kappa}^*|$ of order $1/a$ the velocity field has been computed to examine the trends between the limiting cases of large and small wavenumber. However, calculating the velocity for enough values of $\boldsymbol{\kappa}^*$ for r.m.s. values and spectra of the velocity to be calculated for scales of incident turbulence L_x of order a requires excessive computer time. Therefore results for r.m.s. values and spectra can only be obtained when $L_x \gg a$ or $L_x \ll a$. Despite this serious limitation on the usefulness of the theory, the analysis reveals how various physical processes combine to affect the turbulence near a bluff body, and explains, at least qualitatively, the main experimental results so far discovered.

There have been some previous theoretical studies relating to the problem considered here. Sutera, Maeder & Kestin (1963) analysed the effect of a simple spatially varying fluctuation on the mean velocity in stagnation-point boundary-layer (Hiemenz) flow. By considering a Fourier component with wavenumber κ_3^* in the direction parallel to the axis of the cylinder which receives the maximum amplification, they then calculated the effect of this disturbance on the mean velocity. The paper demonstrated the importance of vorticity amplification and provided some explanation for the effect of turbulence on heat transfer. However, as the authors were well aware, such an approach is not a realistic way of representing turbulence, especially as the only scales of disturbance considered were of order δ_b, the Hiemenz boundary-layer thickness. The analysis of this paper was extended by Sadeh, Sutera & Maeder (1970*a*), who considered a similar kind of fluctuation but now analysed its behaviour outside the boundary layer. Taking disturbances with κ_3^* of order δ_b^{-1} they showed that some disturbances starting upstream decay owing to viscous dissipation before they are amplified near the stagnation point. Note that in neither of these two papers were time-dependent disturbances considered. One paper where such disturbances are considered is that of Lighthill (1954), where the upstream velocity is assumed to be uniform in space but varying in time, so that the only changes which are not quasi-steady occur in the boundary layer. Lighthill's analysis is relevant to acoustically generated velocity fluctuations but not to turbulence. The only previous paper using statistical methods and rapid-distortion theory is that of Deissler (1967). Deissler calculated the changes in r.m.s. turbulent velocities and spectra along the stagnation line of an axisymmetric body, assuming that the turbulence scale is very small and that the effects of the boundary conditions on the body's surface can be ignored. Unlike the analysis of this paper he included the effects of viscosity, using the results of Pearson (1959), and also calculated the turbulent heat flux in the direction of the mean velocity. However, no attempt was made to justify the small-scale rapid-distortion analysis or to point out its limitations. Consequently, in this paper the analysis is stated *ab initio*.

There have by now been a number of experiments to measure mean and fluctuating velocities around a bluff body when the incident stream is turbulent or non-turbulent. The pioneering work of Piercy & Richardson (1930) and all the other relevant experiments have been reviewed by Bearman (1972) and Sadeh *et al.* (1970*a*). In this paper the only discussion of experiments is left to §7.3, where some experimental results are briefly compared with the theory.

The mathematical analysis of this paper is lengthy but straightforward. It is simple by comparison with many recent papers on turbulence theory. However, some readers may prefer just to concentrate on the physical assumptions of the analysis, the important results and their physical interpretation. In that case they are advised to read §§2, 5.3, 6.1, 6.2, 6.3, 6.4 and 7 and to look at all the diagrams.

2. Formulation of the theoretical problem

2.1. *Equations, definitions and assumptions*

If the fluid is assumed to be incompressible and of uniform density and viscosity, the governing equations are

$$\frac{\partial \mathbf{u}^*}{\partial t^*} + (\mathbf{u}^* . \nabla)\,\mathbf{u}^* = -\frac{1}{\rho}\nabla p^* + \nu \nabla^2 \mathbf{u}^*, \tag{2.1}$$

$$\nabla . \mathbf{u}^* = 0, \tag{2.2}$$

where $\mathbf{u}^*$, p^*, ρ and ν are the velocity, pressure, density and kinematic viscosity respectively. To avoid using p^*, we concentrate on $\mathbf{u}^*$ and the vorticity $\boldsymbol{\omega}^*$, by taking the curl of (2.1):

$$\frac{D\boldsymbol{\omega}^*}{Dt^*} = \frac{\partial \boldsymbol{\omega}^*}{\partial t^*} + (\mathbf{u}^* . \nabla)\,\boldsymbol{\omega}^* = (\boldsymbol{\omega}^* . \nabla)\,\mathbf{u}^* + \nu \nabla^2 \boldsymbol{\omega}^*, \tag{2.3}$$

where

$$\boldsymbol{\omega}^* = \nabla \times \mathbf{u}^*. \tag{2.4}$$

Then (2.2)–(2.4) become the governing equations for our analysis.

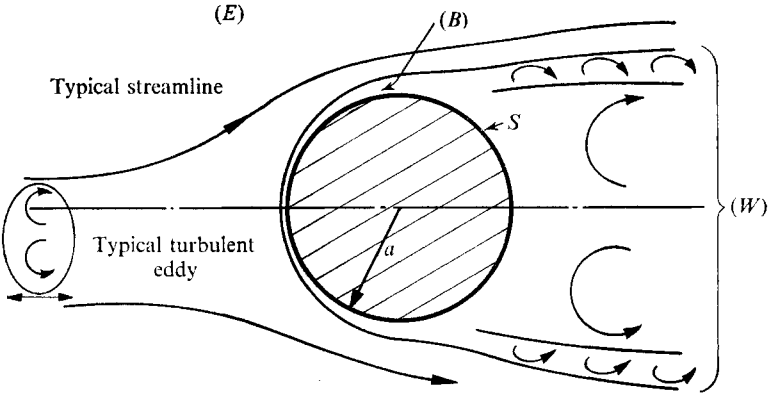

FIGURE 1. The regions of flow near a bluff body and the relevant length scales of the body and of the incident turbulence.

We have to find the solutions of these equations for the problem of a turbulent flow over a stationary bluff body (see figure 1). We assume that the turbulent flow upstream is in a statistical sense uniform in space and constant in time, at least to an extent sufficient for the validity of the subsequent theory. (The degree of uniformity required will be examined *a posteriori*.) It then follows that in the region of flow near the body although the turbulence varies from place to place it remains constant in time. In other words, the turbulent velocity and pressure field is a stationary random process, and thus it is convenient to express $\mathbf{u}^*$, p^* and $\boldsymbol{\omega}^*$ at a point in terms of their time-averaged, or Eulerian-mean, components (denoted by an overbar) and fluctuating components with zero mean; using the notation

$$\mathbf{u}^* = \overline{\mathbf{u}}(x^*, y^*, z^*) + \mathbf{u}'(x^*, y^*, z^*, t^*), \tag{2.5}$$

where
$$\overline{\mathbf{u}} = \lim_{T^* \to \infty} \left\{ \frac{1}{T^*} \int_0^{T^*} \mathbf{u}^*(x^*, y^*, z^*, t^*)\, dt^* \right\}$$

and
$$\overline{\mathbf{u}'} = \overline{\boldsymbol{\omega}'} = \overline{p'} = 0.$$

We can now express our assumptions about the upstream flow mathematically. First, as $x^* \to -\infty$,

$$\overline{\mathbf{u}} \sim (\overline{u}_\infty, 0, 0), \quad \overline{p} \sim \overline{p}_\infty, \tag{2.6a}$$

where $\overline{u}_\infty$ and $\overline{p}_\infty$ are constants. Thence, denoting upstream values by the suffix ∞,

$$\overline{\boldsymbol{\omega}}_\infty = 0.$$

Second, as $x^* \to -\infty$,

$$\mathbf{u}' \sim \mathbf{u}'_\infty(x^*, y^*, z^*, t^*), \quad p' \sim p'_\infty(x^*, y^*, z^*, t^*), \tag{2.6b}$$

where $\mathbf{u}'_\infty$ and p'_∞ are the turbulent velocity and static pressure in the absence of the body, and are therefore defined for all (x^*, y^*, z^*, t^*). Let

$$\mathbf{u}'_\infty = (u'_{\infty 1}, u'_{\infty 2}, u'_{\infty 3}), \quad u'_\infty = (\overline{(u'_{\infty 1})^2})^{\frac{1}{2}},$$

where u'_∞ is a constant which characterizes the intensity of the upstream turbulence. The upstream properties of $\boldsymbol{\omega}_\infty$ can be deduced from those of $\mathbf{u}_\infty$ by (2.4).

We also make the following further assumptions about the upstream flow and a dimension of the body a:

$$\overline{u}_\infty a/\nu = Re \gg 1, \quad u'_\infty l/\nu = \alpha Re \gg 1, \tag{2.7}$$

$$u'_\infty/\overline{u}_\infty = \alpha \ll 1 \tag{2.8}$$

and
$$u'_\infty a/(l\overline{u}_\infty) = \alpha a/l = \beta \ll 1, \tag{2.9}$$

where l is a length defining the scale of the turbulence (for example an integral scale in the x direction defined in (6.3a)). l and Re are also assumed to satisfy

$$l \gg a Re^{-\frac{1}{2}} \quad \text{if} \quad a/l \gg 1 \text{ or } O(1), \quad 1 \gg Re^{-\frac{1}{2}} \quad \text{if} \quad a/l \ll 1. \tag{2.10}$$

The conditions (2.7)–(2.10) can be expressed more compactly as

$$\text{if } a/l \ll 1 \text{ or } O(1) \quad \text{then} \quad Re^{-1} \ll \alpha \ll 1 \ll Re^{\frac{1}{2}},$$

$$\text{if } a/l \gg 1 \quad \text{then} \quad Re^{-1} \ll \alpha \ll (a/l)^{-1}, \quad Re^{\frac{1}{2}} \gg a/l.$$

Now consider an actual flow round a bluff body when $Re \gg 1$, and when there is no incident turbulence. Then analysis and experiments have shown that there are three main regions of the flow: (E) the external inviscid region where the flow is irrotational, (B) the thin boundary layers on the body, with thickness $\delta_b = O(aRe^{-\frac{1}{2}})$ near the stagnation region, part of which are steady and part unsteady or turbulent, and (W) the separated flow in the wake in which vorticity is non-zero everywhere and large fluctuations in velocity occur. Since the boundaries of (B) and (W) are fluctuating, and since fluid enters and leaves these regions *irrotational* velocity fluctuations occur in (E) which decay as $-x^*$ or $|y^*| \to \infty$. Let us denote this velocity by $\mathbf{u}'_w(x^*, y^*, z^*, t^*)$, where $\nabla \times \mathbf{u}'_w = 0$, with a reference velocity defined by $u'_w = |\mathbf{u}'_w|(\mathbf{x}_0)$ at some point close to the surface of the body, say on the centre-line $\mathbf{x}_0 = (0, 2a, 0)$. Let the characteristic length scale of this turbulence be l_w.

Thus when the incident flow is turbulent the fluctuating velocity in region (E) has two components $\mathbf{u}'$ and $\mathbf{u}'_w$. In order that these two components do not interact, as we shall show in § 2.2, we have to assume that

$$\alpha_w = u'_w/u_\infty \quad (\ll 1), \quad \beta_w = u'_w a/(l_w u_\infty) \quad (\ll 1), \tag{2.11}$$

which are good approximations upstream of the body's centre-line, but poor very close to the wake boundary, especially if vortex shedding occurs (Petty 1974).

In our subsequent analysis we shall concentrate on analysing the turbulence in region (E), in particular that part of the flow field upstream of the body's centre-line. Since the flow in the absence of incident turbulence cannot be analysed exactly, it cannot be expected that exact results will be obtained for a turbulent flow. In the next two subsections we reduce the problem to one which is tractable mathematically. This entails making further artificial assumptions about the boundary conditions.

2.2. *Order-of-magnitude analysis*

We first introduce the following non-dimensional variables:

$$\left.\begin{aligned} \mathbf{U}(x) = \overline{\mathbf{u}}/\overline{u}_\infty, \quad \Omega(\mathbf{x}) = \overline{\boldsymbol{\omega}} a/\overline{u}_\infty, \quad \mathbf{u}(\mathbf{x}, t) = \mathbf{u}'/u'_\infty, \quad \boldsymbol{\omega}(\mathbf{x}, t) = \boldsymbol{\omega}' a/u'_\infty, \\ \mathbf{u}_w(x, t) = \mathbf{u}'_w/u'_w, \quad p(x, t) = p' a/(\rho \overline{u}_\infty u'_\infty), \\ (x, y, z, t) = (x^*, y^*, z^*, t^* \overline{u}_\infty)/a. \end{aligned}\right\} \tag{2.12}$$

Substituting these new variables into (2.3) we have

$$\begin{aligned} \partial(\alpha\boldsymbol{\omega})/\partial t + ([\mathbf{U} + \alpha\mathbf{u} + \alpha_w \mathbf{u}_w] . \nabla)(\boldsymbol{\Omega} + \alpha\boldsymbol{\omega}) \\ = ([\boldsymbol{\Omega} + \alpha\boldsymbol{\omega}] . \nabla)(\mathbf{U} + \alpha\mathbf{u} + \alpha_w \mathbf{u}_w) + Re^{-1}\nabla^2(\boldsymbol{\Omega} + \alpha\boldsymbol{\omega}). \end{aligned} \tag{2.13}$$

We now use a heuristic argument to estimate the relative orders of magnitude of the various terms of (2.13) in region (E) as $\alpha, \beta, Re^{-1} \to 0$. The results of the analysis subsequently show that we may make two assumptions. First, we assume that

$$(\overline{u^2})^{\frac{1}{2}} = O(1).$$

Second, since in general the turbulent velocity at a point is induced by the vorticity within a sphere with a radius of order l around the point, we can assume that upstream of the body the length scale over which $\mathbf{u}$ or $\boldsymbol{\omega}$ varies is $O(l)$, and is also $O(l)$ near the body if $a/l \gg 1$. But when $a/l \ll 1$ or $O(1)$, then $\mathbf{u}$ or $\boldsymbol{\omega}$ varies over a distance of order a. Thus it follows that

$$\frac{\alpha(\mathbf{u}.\nabla)(\alpha\boldsymbol{\omega})}{(\mathbf{U}.\nabla)(\alpha\boldsymbol{\omega})} = O\left\{\frac{\alpha(\boldsymbol{\omega}.\nabla)(\alpha\mathbf{u})}{(\mathbf{U}.\nabla)(\alpha\boldsymbol{\omega})}\right\} = O(\alpha), \tag{2.14}$$

except in a small region $O(\alpha)$ from the stagnation point, where $\mathbf{U} = O(\alpha)$. But close to the stagnation point and elsewhere near the body the largest first-order term is $\alpha(\boldsymbol{\omega}.\nabla)\,\mathbf{U}$, so that the relevant ratios are

$$\frac{\alpha(\boldsymbol{\omega}.\nabla)(\alpha\mathbf{u})}{\alpha(\boldsymbol{\omega}.\nabla)\,\mathbf{U}} = O\left[\frac{\alpha(\mathbf{u}.\nabla)(\alpha\boldsymbol{\omega})}{\alpha(\boldsymbol{\omega}.\nabla)\,\mathbf{U}}\right] = \begin{cases} O(\beta) & \text{if} \quad a/l \gg 1, \\ O(\alpha) & \text{if} \quad a/l \ll 1 \text{ or } O(1). \end{cases} \tag{2.15}$$

This estimate is not always valid as shown in §5.3.1. The similar terms in (2.13) involving $\mathbf{u}_w$ are clearly $O(\alpha_w)$ and $O(\beta_w)$.

To consider the viscous terms we use the empirical result (Batchelor 1953, p. 103) that in a turbulent flow the energy dissipated per unit volume per unit time is

$$\varepsilon \propto \rho(\overline{\mathbf{u}'^2})^{\frac{3}{2}}/l, \quad \text{if} \quad (\overline{u'^2})^{\frac{1}{2}} l/\nu \gg 1.$$

Hence for turbulent eddies with a scale large compared with the Kolmogoroff dissipation length scale $(\nu^3/\varepsilon)^{\frac{1}{4}}$,

$$\frac{R^{-1}\nabla^2\boldsymbol{\omega}}{(\boldsymbol{\omega}.\nabla)\,\mathbf{U}} = O\left[\frac{\varepsilon/(\rho l u')}{(u'/l)\,(\bar{u}_\infty/a)}\right] = O\left[\frac{u'/l}{\bar{u}_\infty/a}\right] = O(\beta). \tag{2.16}$$

These order-of-magnitude results (2.14)–(2.16) show that for the zero-order mean variables (2.13) reduces to

$$(\mathbf{U}.\nabla)\,\boldsymbol{\Omega} = (\boldsymbol{\Omega}.\nabla)\,\mathbf{U} + O(\beta^2, \beta\beta_w, \beta\beta_w l_w/l, Re^{-1}). \tag{2.17}$$

Hence it follows that as β, β_w, $Re^{-1} \to 0$, if $\boldsymbol{\Omega} = 0$ upstream, then throughout (E)

$$\boldsymbol{\Omega} = 0. \tag{2.18}$$

Hence in (2.13) the first-order fluctuating terms and the error terms reduce to

$$\partial\boldsymbol{\omega}/\partial t + (\mathbf{U}.\nabla)\,\boldsymbol{\omega} = (\boldsymbol{\omega}.\nabla)\,\mathbf{U} + O(\alpha, \beta, \alpha_w, \beta_w). \tag{2.19}$$

Equation (2.19) is the basic equation for rapid-distortion analysis and was used by Batchelor & Proudman (1954). However, the order-of-magnitude estimate for the nonlinear terms in (2.19) is smaller than theirs, which was based on an estimate for the r.m.s. value of $\boldsymbol{\omega}'$, rather than the r.m.s. value of $\mathbf{u}'$ in our argument. No definitive estimate for these terms has been obtained, but we believe that Batchelor & Proudman's estimate is too large.

To calculate the fluctuating pressure p we use (2.1) subject to the assumptions made for (2.19), so that

$$-\nabla p = \partial\mathbf{u}/\partial t + (\mathbf{U}.\nabla)\,\mathbf{u} + (\mathbf{u}.\nabla)\,\mathbf{U} + \alpha\{(\mathbf{u}.\nabla)\,\mathbf{u}\} + O(\beta). \tag{2.20}$$

In order to use (2.20) to calculate p we must first concentrate on $\mathbf{u}$.

In order to solve (2.19) we assume that $\mathbf{U}$ has been found from (2.18) and the appropriate boundary conditions. Then $\boldsymbol{\omega}$ can be calculated in terms of $\boldsymbol{\omega}_\infty$. To find $\mathbf{u}$ we use (2.2) and (2.4)

2.3. *Boundary conditions*

To specify the mathematical problem we now have to state the boundary conditions on $\mathbf{U}$ and $\mathbf{u}$. Since we have already stated that our intention is to examine the turbulence in region (E) upstream of the body's centre-line, and therefore upstream of the separation point, we postulate that $\mathbf{U}$ will be adequately described in this region if we make the assumption (As 1) that no separation takes place.

Our justification is that for a steady flow round a circular cylinder potential-flow theory describes the pressure and velocity over a distance $\pm 30°$ from the stagnation point. It should be at least as good for a turbulent flow. Given that the scale of incident turbulence is large compared with the thickness of the boundary layer on the body (assumption (2.10)), the boundary condition on $\mathbf{u}$ on the surface S of that part of the body where the flow is unseparated, i.e. the boundary between (E) and (B), must be

$$\mathbf{u}.\mathbf{n} = 0, \tag{2.21}$$

where $\mathbf{n}$ is the outward normal from the body. Since we are not concerned with the flow in the region (E) where it impinges on (W), we need not consider the very complicated interaction between the incident and the wake-generated turbulence. Therefore to be consistent with our assumption (As 1) above we assume that the boundary condition (2.21) is valid all round the body.

As regards the boundary conditions far from the body we have already stated these in (2.6*b*) for $-x, |y|, |(z)| \to \infty$.† When $|x| \to \infty$ and $(y^2+(z)^2)^{\frac{1}{2}} \to \infty$ the turbulence is unaffected by the body, whence the boundary condition is also given by (2.6*b*). However, far downstream ($x \to +\infty$), even outside the wake in the external region (E), because vortex lines have been strained and rotated by their motion over the body, the turbulent velocity $\mathbf{u}'$ does not tend to $\mathbf{u}'_\infty$. Since this turbulence far downstream has a negligible effect on the turbulence upstream of the body and since our rapid-distortion analysis can only give a poor estimate of the turbulence at large distances from the beginning of the distortion, we do not attempt to calculate this part of the flow field. Therefore, we make the assumption (As 2) that, for $x > 0$,

$$\boldsymbol{\omega}' = \boldsymbol{\omega}'_\infty \quad \text{for} \quad (x^2+y^2+(z)^2)^{\frac{1}{2}} > R, \tag{2.22}$$

where $R \to \infty$, but it is assumed that in numerical calculations R is a large number (say 10). Also, for $x \gtrless 0$

$$\mathbf{u}' = \mathbf{u}'_\infty \quad \text{as} \quad (x^2+y^2+(z)^2)^{\frac{1}{2}} \to \infty. \tag{2.23}$$

Our last artificial assumption stems from (As 1). Since the time taken for a fluid particle to travel to the stagnation point is infinite, it follows that the straining and thence the vorticity is infinite on the streamline downstream of the rear

† In this section (z) refers to the co-ordinate z in the case of a three-dimensional body, but the term (z) should be ignored in the case of a two-dimensional body.

stagnation point, on $y = 0$. This difficulty is overcome through the assumption (As 3) that, within a small angle $\delta\theta$† either side of y, $(z) = 0, x > 0, \boldsymbol{\omega}$ is a linear function of θ determined by its values at $\theta = \pm\delta\theta$, for $r > 1$.

These expedient assumptions (As 1), (As 2) and (As 3) now render possible a formal statement of the mathematical problem.

(i) **U** is determined by (2.18) subject to the boundary conditions

$$\left.\begin{aligned} \mathbf{U} = (1,0,0) \quad \text{as} \quad (x^2+y^2+(z)^2)^{\frac{1}{2}} \to \infty, \\ \mathbf{U}.\mathbf{n} = 0 \quad \text{on} \quad S. \end{aligned}\right\} \tag{2.24}$$

(ii) $\boldsymbol{\omega}$ is determined by (2.19), using the predetermined value of **U** in the equation, and the assumptions (As 2) and (As 3).

(iii) **u** is calculated from (2.2) and (2.4) and is subject to the boundary conditions

$$\mathbf{u} \sim \mathbf{u}_\infty \quad \text{as} \quad x^2+y^2+(z)^2 \to \infty, \tag{2.25a}$$

$$\mathbf{u}.\mathbf{n} = 0 \quad \text{on} \quad S. \tag{2.25b}$$

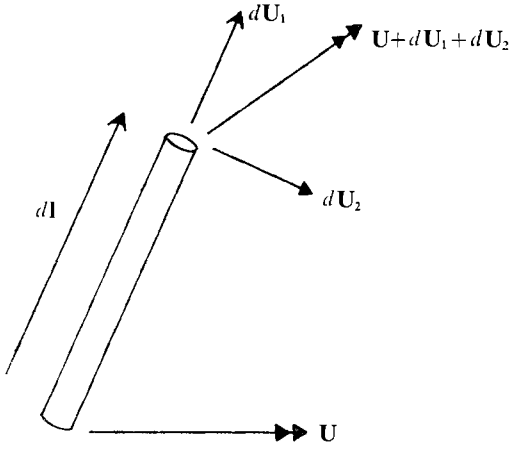

FIGURE 2. The components of mean velocity at each end of a fluid element undergoing stretching and rotation.

3. The methods of analysing flow round cylindrical bodies

3.1. *Calculation of* $\boldsymbol{\omega}$

$\boldsymbol{\omega}$ can be found in terms of $\boldsymbol{\omega}_\infty$ by means of Cauchy's solution of (2.19), which we derive with the aid of figure 2 (Batchelor 1967, p. 267). Equation (2.19) is the equation for the rate of change of vorticity of a fluid element. If we consider such an element to be a thin cylinder with a length $d\mathbf{l}$ parallel to $\boldsymbol{\omega}$, then the term $(\boldsymbol{\omega}.\nabla)\,\mathbf{U}$ may be expressed in the notation of figure 2 as

$$\lim_{d\mathbf{l}\to 0}[(|\boldsymbol{\omega}|/|d\mathbf{l}|)\,(d\mathbf{U}_1+d\mathbf{U}_2)],$$

† $\delta\theta$ refers to the angle measured from the x axis (the axis of symmetry) in spherical co-ordinates, for the case of a spherically symmetric three-dimensional body.

where $d\mathbf{U}_1 + d\mathbf{U}_2$ is the mean velocity of one end of the element relative to the other, $d\mathbf{U}_1$ being parallel to $\boldsymbol{\omega}$ (thus stretching the vortex lines) and $d\mathbf{U}_2$ being perpendicular (thus rotating the vortex lines). Thus $D\boldsymbol{\omega}/Dt$ is proportional to $d(d\mathbf{l})/dt$ and therefore if $\boldsymbol{\omega}$ is parallel to $d\mathbf{l}$ at time t_0, $\boldsymbol{\omega}$ remains parallel at all subsequent times, so that at time t_1

$$d\mathbf{l}(t_1)/|d\mathbf{l}(t_0)| = \boldsymbol{\omega}(t_1)/|\boldsymbol{\omega}(t_0)|. \tag{3.1}$$

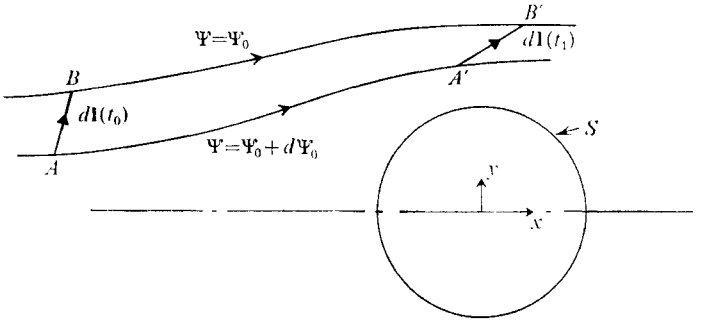

FIGURE 3. The motion of a fluid element in a flow round a bluff body showing how it is stretched and rotated.

The calculation of $d\mathbf{l}(t_1)$ in terms of its upstream value only requires a knowledge of $\mathbf{U}$. Let $d\mathbf{l}(t_0)$ to be the element AB (in figure 3) at time t_0 well upstream of the body and $d\mathbf{l}(t_1)$ be the same fluid element having travelled to $A'B'$ in the mean flow in a time $t_1 - t_0$. Then B and B' must lie on the same streamline, say $\Psi = \Psi_0$, and A and A' must lie on another, $\Psi = \Psi_0 + d\Psi_0$, where $\Psi(z, y)$ is defined by

$$\partial\Psi/\partial x = U_y, \quad \partial\Psi/\partial y = -U_x. \tag{3.2}$$

We now define a function $T_X(x, y)$ as the time for a particle to reach the point (x, y) from a point on the *same* streamline far upstream at $x = -X$, where $X \gg 1$. Then

$$T_X(x, y) = \int_{-X}^{x} dx'/U_x(x', y'), \tag{3.3}$$

where the integral is taken along the line $\Psi(x', y') = \Psi(x, y)$. Therefore, since the time taken to travel from B to B' is the same as that from A to A',

$$T_X(B') - T_X(B) = T_X(A') - T_X(A),$$

whence

$$T_X(B) - T_X(A) = T_X(B') - T_X(A') = dT \text{ (say)}. \tag{3.4}$$

We have only considered an element in the x, y plane. In general, AB or $A'B'$ is the component in this plane of an element with another component in the z direction, say AC or $A'C'$. In a two-dimensional flow the component in the z direction is *not* changed at all, so that $AC = A'C'$.

Expressing these results mathematically, if

$$d\mathbf{l}(t_0) = (dx_0, dy_0, dz_0),$$

and

$$d\mathbf{l}(t_1) = (dx_1, dy_1, dz_1),$$

then
$$d\Psi_0 = \frac{\partial \Psi}{dx} dx_1 + \frac{\partial \Psi}{dy} dy_1 = -dy_0, \tag{3.5}$$

since AB is well upstream of the body where $\partial\Psi/\partial x = 0$ and $\partial\Psi/\partial y = -1$. Also

$$dT = (\partial T_X/\partial x)\, dx_1 + (\partial T_X/\partial y)\, dy_1 = dx_0, \tag{3.6}$$

since upstream $\partial T_X/\partial y = 0$ and $\partial T_X/\partial x = 1$. On solving (3.5) and (3.6) for dx_1 and dy_1, using the easily derived result

$$\frac{\partial T_X}{\partial y}\frac{\partial \Psi}{\partial x} - \frac{\partial T_X}{\partial x}\frac{\partial \Psi}{\partial y} = 1,$$

and substituting for $\boldsymbol{\omega}$ in (3.1), it follows that

$$\left.\begin{aligned} \omega_x(t_1) &= U_x \omega_x(t_0) - \partial T_X/\partial y\, \omega_y(t_0), \\ \omega_y(t_1) &= U_y \omega_x(t_0) + \partial T_X/\partial x\, \omega_y(t_0). \end{aligned}\right\} \tag{3.7}$$

Also
$$\omega_z(t_1) = \omega_z(t_0).$$

To avoid the arbitrary value X in the definition of T_X, it is preferable to define a function

$$\begin{aligned} \Delta_T(x,y) &= \lim_{X\to\infty} [T_X(x,y) - (x+X)] \\ &= \int_{-\infty}^{x} \left(\frac{1}{U_x(x',y')} - 1\right) dx', \quad \text{where} \quad \Psi(x',y) = \Psi(x,y); \end{aligned} \tag{3.8}$$

physically $\Delta_T(x,y)$ is the time taken to travel from $(-\infty, y_0)$ to the point (x,y) *less* the time it would have taken to travel to the point (x,y_0) in the absence of the body. $\Delta_T(x,y)$ is related to Lighthill's (1956) 'drift' function, denoted here as $T(x,y)$, by the equation $T = x + \Delta_T$. Here y_0 is the value of y on the streamline through (x,y) when $x = -\infty$, so that

$$y_0 = -\Psi(x,y).$$

For later convenience we define the function $\Delta_y(x,y)$ as the change in the y co-ordinate of a fluid particle as it travels past the body:

$$\Delta_y = y - y_0 = y + \Psi. \tag{3.9}$$

For subsequent analysis it is convenient to use the suffix notation (1, 2, 3) for components (x,y,z). Then, taking the upstream values of ω_i at $x = -X$, it follows from (3.7) that

$$\omega_i(x,y,z,t_1) = \gamma_{ij}(x,y)\, \omega_{\infty j}(-X, y_0, z, t_1 - T_X(x,y)), \tag{3.10}$$

where
$$\gamma_{ij} = \begin{bmatrix} U_1 & -\partial\Delta_T/\partial y & 0 \\ U_2 & 1+\partial\Delta_T/\partial x & 0 \\ 0 & 0 & 1 \end{bmatrix} = \begin{bmatrix} U_1 & -\partial T/\partial y & 0 \\ U_2 & \partial T/\partial x & 0 \\ 0 & 0 & 1 \end{bmatrix}. \tag{3.11}$$

Note, that, as $x \to -\infty$, $\gamma_{ij} = \gamma_{\infty ij} = \delta_{ij}$. Note also that (3.10) is equivalent to the Lagrangian form, used by Batchelor & Proudman (1954),

$$\omega_i(\mathbf{x},t) = \omega_j(\mathbf{a},0)\, \partial x_i/\partial a_j \quad \text{where} \quad \mathbf{x} = \mathbf{a} \quad \text{at} \quad t = 0.$$

It follows immediately from (3.1) that in the absence of the body

$$\omega_{\infty j}(-X, y, z, t_0)$$

is related to $\omega_{\infty j}$ at (x, y, z) as follows:

$$\omega_{\infty j}(x, y, z, t_0 + x + X) = \omega_{\infty j}(-X, y, z, t_0). \tag{3.12}$$

Therefore (3.10) becomes, in the limit $X \to \infty$,

$$\omega_i(x, y, z, t) = \gamma_{ij}(x, y)\, \omega_{\infty j}(x, y - \Delta_y, z, t - \Delta_T). \tag{3.13}$$

It is worth noting that (3.12) could have been deduced by a direct appeal to Taylor's hypothesis, but there was no need because that hypothesis is implicitly contained in our assumptions (2.8) and (2.9).

3.2. *Calculation of* $\mathbf{u}$

Given $\boldsymbol{\omega}$ in (3.13), $\mathbf{u}$ now has to be calculated using (2.2), (2.4) and the boundary conditions (2.25). Since we know $\boldsymbol{\omega}_\infty$ and $\mathbf{u}_\infty$ at all values of (x, y, z, t) it is convenient to define the variables

$$\Delta\boldsymbol{\omega} = \boldsymbol{\omega} - \boldsymbol{\omega}_\infty, \quad \Delta\mathbf{u} = \mathbf{u} - \mathbf{u}_\infty.$$

Then $\Delta\boldsymbol{\omega}$ and $\Delta\mathbf{u}$ have to satisfy

$$\nabla \times \Delta\mathbf{u} = \Delta\boldsymbol{\omega}, \tag{3.14}$$

$\Delta\boldsymbol{\omega}$ being presumed known from (3.13), and

$$\nabla . \Delta\mathbf{u} = 0, \tag{3.15}$$

since $\nabla . \mathbf{u}_\infty = 0$. The boundary conditions on $\Delta\mathbf{u}$ are

$$\Delta\mathbf{u} \to 0 \quad \text{as} \quad x^2 + y^2 \to \infty, \tag{3.16a}$$

$$\Delta\mathbf{u} . \mathbf{n} = -\mathbf{u}_\infty . \mathbf{n} \quad \text{on} \quad S. \tag{3.16b}$$

Since it may be shown that there is a unique solution to (3.14) and (3.15) subject to (3.16), any solution which satisfies these equations must be the correct one. We begin by using the fact that any vector can be expressed as the sum of the gradient of a scalar and the curl of another vector. Let

$$\Delta\mathbf{u} = -\nabla\Phi + \nabla \times \boldsymbol{\psi}, \tag{3.17}$$

where Φ and $\boldsymbol{\psi}$ are functions of (x, y, z, t). Substituting this expression into (3.14) we find

$$\Delta\boldsymbol{\omega} = \nabla \times (\nabla \times \boldsymbol{\psi}). \tag{3.18}$$

$\boldsymbol{\psi}$ may be further specified (Batchelor 1967, p. 86) by the gauge condition

$$\nabla . \boldsymbol{\psi} = 0. \tag{3.19a}$$

Then, in Cartesian co-ordinates, (3.18) becomes

$$\nabla^2 \boldsymbol{\psi} = -\Delta\boldsymbol{\omega}. \tag{3.19b}$$

The solution to (3.19*b*) does not satisfy (3.19*a*) unless the correct boundary conditions are specified. The divergence of (3.19*b*) gives

$$\nabla^2(\nabla . \boldsymbol{\psi}) = 0,$$

whence, if $$\nabla.\boldsymbol{\psi} = 0 \quad \text{on} \quad S \quad \text{and as} \quad x^2+y^2 \to \infty, \tag{3.20a}$$

then (3.19a) is satisfied everywhere. The second set of boundary conditions for $\boldsymbol{\psi}$ is specified by (3.16). Since it is more convenient to satisfy (3.16) separately for $\nabla \times \boldsymbol{\psi}$ and $\nabla\Phi$ we have

$$\nabla \times \boldsymbol{\psi}.\mathbf{n} = 0 \quad \text{on} \quad S, \tag{3.20b}$$

$$|\nabla \times \boldsymbol{\psi}| \to 0 \quad \text{as} \quad x^2+y^2 \to \infty.$$

Since $\nabla.\mathbf{u} = 0$, Φ must satisfy

$$\nabla^2\Phi = 0, \tag{3.21}$$

subject to the boundary conditions determined by (3.16), namely

$$\nabla\Phi.\mathbf{n} = \mathbf{u}_\infty \quad \text{on} \quad S \tag{3.22}$$

and

$$|\nabla\Phi| \to 0 \quad \text{as} \quad x^2+y^2 \to \infty. \tag{3.23}$$

3.3. *Fourier analysis*

We assume that the upstream turbulence is stationary and homogeneous, and if, for mathematical convenience, we assume the turbulence only to exist within a large box with sides of non-dimensional lengths $2\mathscr{T}$, $2\mathscr{Y}$, $2\mathscr{Z}$, and within an interval of non-dimensional time $\mathscr{T}$, then we can express $\mathbf{u}_\infty$ and $\boldsymbol{\omega}_\infty$ by means of Fourier transforms:†

$$\begin{pmatrix} u_{\infty i} \\ \omega_{\infty i} \end{pmatrix}(x,y,z,t) = \iiint_{-\infty}^{\infty} \exp\{i[\kappa_1 x+\kappa_2 y+\kappa_3 z+\sigma t]\} \begin{pmatrix} S_{\infty i} \\ s_{\infty i} \end{pmatrix}(\kappa_1,\kappa_2,\kappa_3)\, d\kappa_1\, d\kappa_2\, d\kappa_3, \tag{3.24}$$

where $\sigma = -\kappa_1$, a consequence of (3.12) (or Taylor's hypothesis). Since $\boldsymbol{\omega}$ is related to $\mathbf{u}$ by (2.4), it follows that

$$s_{\infty i} = i\epsilon_{ijk}\kappa_j S_{\infty k}. \tag{3.25}$$

Since the mean velocity over the body is invariant in the z direction, the turbulence remains homogeneous in the z direction. Thus the turbulence near the body, which is inhomogeneous in the x and y directions, can be Fourier analysed as

$$u_i = \iint_{-\infty}^{\infty} \exp\{i(-\kappa_1 t+\kappa_3 z)\}\, \hat{\hat{u}}_i(x,y;\, \kappa_1\kappa_3)\, d\kappa_1\, d\kappa_3, \tag{3.26}$$

and similarly for all other quantities stationary in t and z, namely ω_i, ψ_i, Φ and p. The inverse transformation for $\hat{\hat{u}}_i$, for example, is

$$\hat{\hat{u}}_i(x,y,;\kappa_1,\kappa_3) = \frac{1}{(2\pi)^2}\int_{-\mathscr{T}}^{\mathscr{T}}\int_{\mathscr{Z}}^{\mathscr{Z}} u_i(x,y;z,t)\exp\{-i(-\kappa_1 t+\kappa_3 z)\}\, dt\, dz. \tag{3.27}$$

These Fourier transforms are only of use in so far as they enable us to calculate the spectra of the local turbulence in terms of that of the upstream turbulence.

† We could avoid introducing the unnecessary parameters $\mathscr{T}$, $\mathscr{Y}$, $\mathscr{Z}$, if we used Fourier–Stieltjes transforms (Batchelor 1953). But we prefer ordinary Fourier transforms on account of their greater familiarity to engineers, and because most real flows are finite in extent.

This requires expressing $\hat{\hat{u}}_i$ in terms of $S_{\infty i}$ by the introduction of a tensor M_{il} such that

$$\hat{\hat{u}}_i = \int_{-\infty}^{\infty} M_{il}(x, y; \kappa_1, \kappa_2, \kappa_3)\, S_{\infty l}(\kappa_1, \kappa_2, \kappa_3)\, d\kappa_2. \tag{3.28}$$

In §§4 and 5 this tensor is calculated by solving (3.18) and (3.21) for the Fourier transforms of ψ_i and Φ, i.e. $\hat{\hat{\psi}}_i$ and Φ. Similarly $\hat{\hat{p}}$ can be expressed in terms of $S_{\infty i}$ by a tensor defined by

$$\hat{\hat{p}} = \int_{-\infty}^{\infty} Q_n(x, y; \kappa_1, \kappa_2, \kappa_3)\, S_{\infty n}(\kappa_1, \kappa_2, \kappa_3)\, d\kappa_2. \tag{3.29}$$

The next problem is to use the solutions for M_{il} to calculate the spectra and covariances near the body in terms of the known three-dimensional spectrum $\Phi_{\infty ij}$ of the upstream turbulence, defined, following Batchelor (1953), as

$$\Phi_{\infty ij}(\boldsymbol{\kappa}) = \frac{1}{(2\pi)^3} \iiint_{-\infty}^{\infty} R_{\infty ij}(r_x, r_y, r_z, 0) \exp\{-i[\kappa_1 r_x + \kappa_2 r_y + \kappa_3 r_z]\}\, dr_x\, dr_y\, dr_z,$$

where $$\boldsymbol{\kappa} = (\kappa_1, \kappa_2, \kappa_3)$$

and $$R_{\infty ij}(r_x, r_y, r_z, \tau) = \overline{u_{\infty i}(x, y, z, t)\, u_{\infty j}(x + r_x, y + r_y, z + r_z, t + \tau)}.$$

Note that $$R_{\infty ij}(r_x, r_y, r_z, 0) = R_{\infty ij}(0, r_y, r_z, -r_x),$$

so that

$$\Phi_{\infty ij}(\boldsymbol{\kappa}) = \frac{1}{(2\pi)^3} \iiint_{-\infty}^{\infty} R_{\infty ij}(0, r_y, r_z, \tau) \exp\{-i[\kappa_2 r_y + \kappa_3 r_z - \kappa_1 \tau]\}\, dr_y\, dr_z\, d\tau. \tag{3.30}$$

The simplest spectrum to calculate near the body, but the most lengthy to obtain experimentally, is 'the two-dimensional spectrum'

$$\Psi_{ij}(x, y; x', y'; \kappa_1, \kappa_3) = \frac{1}{(2\pi)^2} \iint_{-\infty}^{\infty} R_{ij}(x, y; x', y'; r_z, \tau) \exp\{-i[\kappa_3 r_z - \kappa_1 \tau]\}\, dr_z\, d\tau, \tag{3.31}$$

where $$R_{ij}(x, y; x', y'; r_z, \tau) = \overline{u_i(x, y, z, t)\, u_j(x', y', z + r_z, t + \tau)}.$$

The most commonly measured spectrum is the 'one-dimensional spectrum'

$$\begin{aligned} \Theta_{ij}(x, y; x', y'; r_z; \kappa_1) &= \int_{-\infty}^{\infty} \Psi_{ij} \exp\{i(\kappa_3 r_z)\}\, d\kappa_3 \\ &= \frac{1}{2\pi} \int_{-\infty}^{\infty} R_{ij}(x, y; x', y'; r_z, \tau)\, e^{i\kappa_1 \tau}\, d\tau. \end{aligned} \tag{3.32}$$

If $(x', y') = (x, y)$ and $r_z = 0$, the spectrum is the 'power spectral density' at a point and is real. If $(x', y') = (x, y)$ and $r_z \neq 0$, it is called the 'coherence' and is real. But if $(x', y') \neq (x, y)$ it is usually called a 'cross-spectrum', and has real and imaginary parts. From Θ_{ij} can be found the cross-variance at two points:

$$\left.\begin{aligned} \text{with time delay} \quad & R_{ij}(x, y; x', y'; r_z, \tau) = \int_{-\infty}^{\infty} \Theta_{ij} e^{-i\kappa_1 \tau}\, d\kappa_1, \\ \text{and without} \quad & \overline{u_i(x, y, z)\, u_j(x', y', z + r_z)} = \int_{-\infty}^{\infty} \Theta_{ij}(\kappa_1)\, d\kappa_1, \end{aligned}\right\} \tag{3.33}$$

whence the mean-square turbulent velocity $\overline{u_i^2}(x, y, z)$ can be found. Other useful correlations can be derived once Ψ_{ij} and Θ_{ij} are known. Hereafter we shall assume that $(x, y) = (x', y')$ in Ψ_{ij}, Θ_{ij} and R_{ij} unless otherwise stated.

$\Phi_{\infty ij}$ and Ψ_{ij} are related to $S_{\infty i}$ and u_i, as a result of their definitions, as follows:

$$\overline{S^\dagger_{\infty i}(\kappa_1, \kappa_2, \kappa_3)\, S_{\infty j}(\kappa_1, \kappa_2, \kappa_3)} = (\mathscr{T}\mathscr{X}/\pi^2)\, \delta(\kappa_2 - \kappa_2')\, \Phi_{\infty ij}(\kappa_1, \kappa_2, \kappa_3), \tag{3.34}$$

where $\delta(\kappa_2 - \kappa_2')$ is the Dirac delta function and the dagger superscript denotes the complex conjugate. Also

$$\overline{\hat{\hat{u}}_i^\dagger(\kappa_1, \kappa_3)\, \hat{\hat{u}}_j(\kappa_1, \kappa_3)} = (\mathscr{T}\mathscr{X}/\pi^2)\, \Psi_{ij}(\kappa_1, \kappa_3). \tag{3.35}$$

Substituting the values for M_{il} found in (3.28) into (3.35) we have

$$\Psi_{ij}(\kappa_1, \kappa_3) = \int_{-\infty}^{\infty} M^\dagger_{il}(\boldsymbol{\kappa})\, M_{jm}(\boldsymbol{\kappa})\, \Phi_{\infty lm}(\boldsymbol{\kappa})\, d\kappa_2. \tag{3.36}$$

The important result for pressure calculations is the one-dimensional spectrum at one or two points, which by similar analysis is shown to be

$$\left.\begin{aligned} \Theta^{(p)}(x, y, z; x', y', z'; \kappa_1) = \int_{-\infty}^{\infty}\int_{-\infty}^{\infty} \exp\{i\kappa_3(z - z')\}\, Q_l(x, y; \kappa_1, \kappa_2, \kappa_3) \\ \times Q^\dagger_m(x', y'; \kappa_1, \kappa_2, \kappa_3)\, \Phi_{\infty lm}(\kappa_1, \kappa_2, \kappa_3)\, d\kappa_2, d\kappa_3, \end{aligned}\right\} \tag{3.37}$$

where

$$\Theta^{(p)} = \frac{1}{2\pi}\int_{-\infty}^{\infty} \overline{p(x, y, z, t)\, p(x', y', z', t+\tau)}\, e^{i\kappa_1 \tau}\, d\tau.$$

Thence

$$\overline{p(x, y, z)\, p(x', y', z')} = \int_{-\infty}^{\infty} \Theta^{(p)}(\kappa_1)\, d\kappa_1. \tag{3.38}$$

This section shows that the mathematical problem is to calculate M_{in} and Q_n, and then perform the necessary integrations to obtain whatever spectra may be needed.

4. Solution for the case of flow round a circular cylinder

4.1. *Exact solutions in terms of Fourier series*

To obtain the solutions to (3.18) and (3.21) for turbulent flow round a circular cylinder (shown in figure 3) we work with the Fourier transforms of ψ_i and Φ as defined in (3.26). In Cartesian tensor notation (3.18) becomes

$$\left(\frac{\partial^2}{\partial x^2} + \frac{\partial^2}{\partial y^2} - \kappa_3^2\right) \hat{\hat{\psi}}_i = -\left(\hat{\hat{\omega}}_i - \delta_{ij}\int_{-\infty}^{\infty} \exp\{i(\kappa_1 x + \kappa_2 y)\}\, s_{\infty j}\, d\kappa_2\right). \tag{4.1}$$

But from (3.13),

$$\hat{\hat{\omega}}_i = \gamma_{ij}(x, y) \exp\{i\kappa_1(\Delta_T + x)\} \int_{-\infty}^{\infty} \exp\{i\kappa_2(y - \Delta_y)\}\, s_{\infty j}\, d\kappa_2.$$

Therefore, if we define a new variable $\alpha_{ij}(x, y; \kappa_1, \kappa_2, \kappa_3)$ by

$$\hat{\hat{\psi}}_i = \int_{-\infty}^{\infty} \alpha_{ij} s_{\infty j}(\kappa_1, \kappa_2, \kappa_3)\, d\kappa_2,$$

(4.1) becomes $$(\partial^2/\partial x^2+\partial^2/\partial y^2-\kappa_3^2)\,\alpha_{ij}=-\Omega_{ij},$$
where $$\Omega_{ij}=[\gamma_{ij}\exp\{i(\kappa_1\Delta_T-\kappa_2\Delta_y)\}-\delta_{ij}]\exp\{i(\kappa_1 x+\kappa_2 y)\}. \tag{4.2}$$

It follows from their definitions in (3.8) and (3.9) that, as $x\to-\infty$ or $y\to\pm\infty$, Δ_T, $\Delta_y\to 0$ and $\gamma_{ij}\to\delta_{ij}$, so that $\Omega_{ij}\to 0$. However, when $x\to+\infty$ and $y=O(1)$ we have to use the artificial assumption (As 2), equation (2.22), in order that $\Omega_{ij}\to 0$.

Now the boundary conditions (3.20) can be expressed in terms of α_{ij}. To do this it is convenient to adopt the notation that, for the transforms specified in (3.26),

$$\partial/\partial x_3\equiv i\kappa_3.$$

Then for a circular cylinder (3.20) become

$$\partial\hat{\hat{\psi}}_i/\partial x_i=0 \quad \text{at} \quad r=1 \quad \text{and as} \quad r\to\infty,$$

$$n_i\epsilon_{ijk}\partial\hat{\hat{\psi}}_k/\partial x_j=0 \quad \text{at} \quad r=1; \quad \epsilon_{ijk}\partial\hat{\hat{\psi}}_k/\partial x_j=0 \quad \text{as} \quad r\to\infty.$$

To render these conditions applicable for α_{ij} we first note that, since

$$\nabla.\boldsymbol{\omega}_\infty=\partial\omega_{\infty i}/\partial x_i=0 \quad \text{and} \quad \nabla.\mathbf{u}_\infty=\partial u_{\infty i}/\partial x_i=0,$$

$$\kappa_i s_{\infty i}=\kappa_i S_{\infty i}=0.$$

Therefore the boundary conditions (3.20) for α_{ij} become

$$\partial\alpha_{ij}/\partial x_i=\lambda\kappa_j \quad \text{on} \quad r=1 \quad \text{and as} \quad r\to\infty, \tag{4.3a}$$

$$\epsilon_{ijk}\partial\alpha_{kl}/\partial x_j=\mu_l\kappa_l \quad \text{as} \quad r\to\infty, \tag{4.3b}$$

$$n_i\epsilon_{ijk}\partial\alpha_{kl}/\partial x_j=\mu\kappa_l \quad \text{at} \quad r=1, \tag{4.3c}$$

where λ and μ are scalars and μ_l is a vector. It may be proved that equating these functions to zero only affects the value of α_{ij} by an arbitrary constant.

To calculate the various terms in Ω_{ij} we first need to find the mean velocity $\mathbf{U}$, which has to satisfy (2.18) and the boundary conditions (2.25). For the case of a circular cylinder we have the standard potential-flow solution:

$$\mathbf{U}=(1-(x^2-y^2)/(x^2+y^2)^2,\ -2xy/(x^2+y^2)^2,\ 0). \tag{4.4a}$$

Hence $$\Psi=-y+y/(x^2+y^2), \quad \Delta_y=y/(x^2+y^2), \tag{4.4b}$$

and following Darwin (1953), if $\theta=\tan^{-1}(y/x)$,

$$\Delta_T(\theta,\Psi)=(1/\zeta)\{(1-\tfrac{1}{2}\zeta^2)\,[K(\zeta^2)\mp F(\theta-\tfrac{1}{2}\pi,\zeta^2)]-[E_L(\zeta^2)\mp E_L(\theta-\tfrac{1}{2}\pi,\zeta^2)]\}, \tag{4.4c}$$

for $\theta\gtrless\frac{1}{2}\pi$, where $$\zeta^2=4/(4+\Psi^2). \tag{4.4d}$$

Here $F(\theta-\frac{1}{2}\pi,\zeta^2)$ and $E_L(\theta-\frac{1}{2}\pi,\zeta^2)$ are elliptic integrals of the first and second kind, and $K(\zeta^2)$ and $E_L(\zeta^2)$ are complete elliptic integrals of the first and second kind. Although γ_{ij} can be calculated from the tabulated forms of these integrals, in general, it is as simple to compute $\Delta_T(x,y)$ directly by integrating $1/U_x$ along the streamlines, and thence to deduce γ_{ij} from $\partial T/\partial y$ and $\partial T/\partial x$. Lines of constant Δ_T and graphs of $\partial T/\partial r$ and $\partial T/(r\partial\theta)$ are shown in figures 4 and 5(*a*). Since

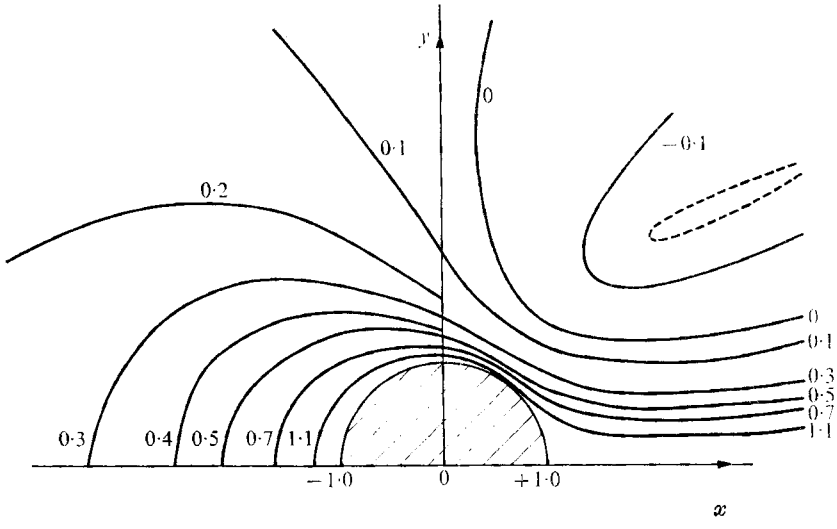

FIGURE 4. Lines of constant $\Delta_T(x, y)$, where Δ_T is the time taken to reach the point (x, y) less the time it would have taken in the absence of the body.

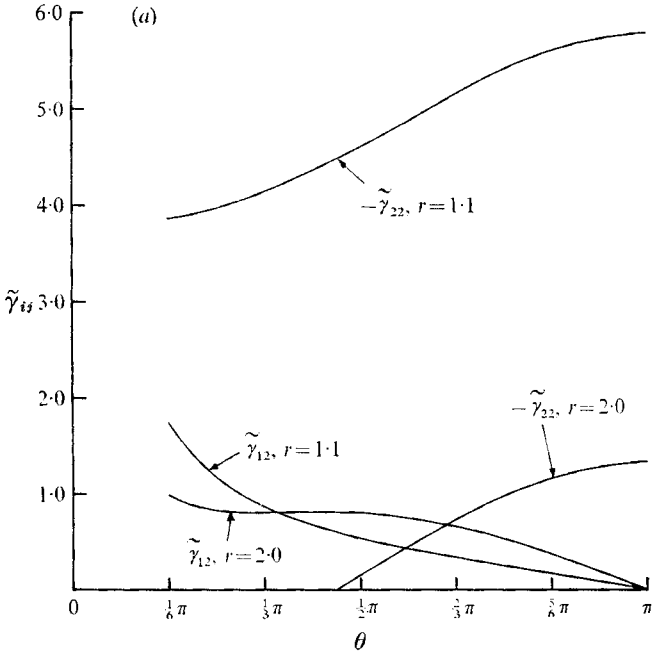

FIGURE 5(*a*). For legend see facing page.

$\gamma_{ij}-\delta_{ij}$ is small when $(x^2+y^2)^{\frac{1}{2}} > 10$, $x < 0$, for numerical (but not analytical) calculations we assume

$$\Omega_{ij} = 0 \quad \text{for} \quad (x^2+y^2)^{\frac{1}{2}} > R \quad (x \gtrless 0), \tag{4.5}$$

where $R = 10$. Hereafter we assume Ω_{ij} to be a known function.

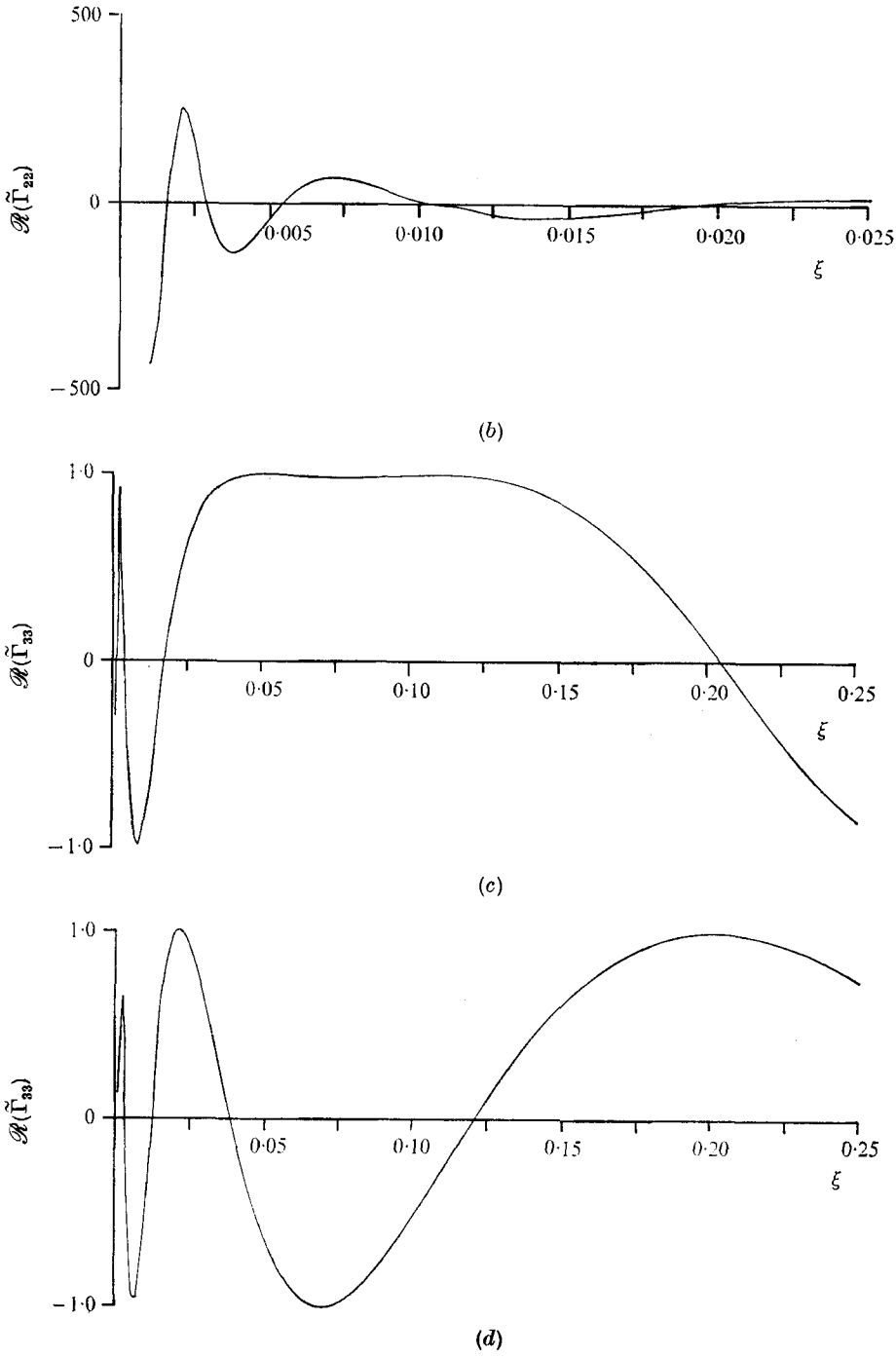

FIGURE 5. Graphs showing the distortion of the vorticity of the incident turbulence. (*a*) The vorticity tensors $\tilde{\gamma}_{12}$ ($= -\partial T/r\,\partial\theta$) and $\tilde{\gamma}_{22}$($= \partial T/\partial r$) as functions of θ at constant values of r. (*b*) the vorticity tensor $\tilde{\Gamma}_{22}$ (note $\tilde{\gamma}_{22} = |\tilde{\Gamma}_{22}|$) close to the surface of the cylinder when $\kappa_1 = \kappa_2 = 10$ at $\theta = \frac{3}{4}\pi$. (*c*) The vorticity tensor $\tilde{\Gamma}_{33}$ close to the surface of the cylinder away from the stagnation point $\theta = \frac{3}{4}\pi$ when $\kappa_1 = 5, \kappa_2 = 25$. (*d*) The vorticity tensor $\tilde{\Gamma}_{33}$ close to the surface of the cylinder on the stagnation line $\theta = \pi$ when $\kappa_1 = 5, \kappa_2 = 25$.

Since we are to consider the turbulent flow round a cylinder, it is convenient to use cylindrical co-ordinates (r, θ, z) and to write vectors in terms of (r, θ, z) components, with superscript tildes to denote this difference. For example

$$\tilde{\alpha}_{1j} = \alpha_{1j}\cos\theta + \alpha_{2j}\sin\theta,$$

$$\tilde{\alpha}_{2j} = -\alpha_{ij}\sin\theta + \alpha_{ij}\cos\theta, \quad \tilde{\alpha}_{3j} = \alpha_{3j}.$$

In this tensor notation the first suffix is used with (1, 2, 3) referring to (r, θ, z) components, but the second suffix always refers to *Cartesian* components of the relevant upstream variable. In the case of $\tilde{\alpha}_{ij}$, the upstream component is that of vorticity; in the case of $\tilde{M}_{il}$ (referred to later) it is velocity.

The turbulent stream function α_{ij}. In cylindrical co-ordinates (3.19*b*) becomes

$$\nabla^2\psi_r - (2/r^2)\,\partial\psi_\theta/\partial\theta - \psi_r/r_2 = -\Delta\omega_r, \tag{4.6a}$$

$$\nabla^2\psi_\theta + (2/r^2)\,\partial\psi_r/\partial\theta - \psi_\theta/r^2 = -\Delta\omega_\theta, \tag{4.6b}$$

$$\nabla^2\psi_z = -\Delta\omega_z, \tag{4.6c}$$

where $$\nabla^2 = \partial^2/\partial r^2 + (1/r)\,\partial/\partial r + (1/r^2)\,\partial^2/\partial\theta^2 + \partial^2/\partial z^2.$$

To find $\tilde{\alpha}_{ij}$, we express $\tilde{\alpha}_{ij}$ and $\tilde{\Omega}_{ij}$ as Fourier series:

$$\begin{pmatrix}\tilde{\alpha}_{ij}\\ \tilde{\Omega}_{ij}\end{pmatrix} = \sum_{n=0}^{\infty}\left\{\begin{pmatrix}\alpha_{ij}^{cn}\\ \Omega_{ij}^{cn}\end{pmatrix}(r;\kappa_1,\kappa_2,\kappa_3)\cos n\theta + \begin{pmatrix}\alpha_{ij}^{sn}\\ \Omega_{ij}^{sn}\end{pmatrix}(r;\kappa_1,\kappa_2,\kappa_3)\sin n\theta\right\}.$$

Note that $\tilde{\Omega}_{ij}$ has to be found from $\tilde{\gamma}_{ij}$ and $\tilde{\gamma}_{\infty ij}$, defined as

$$\tilde{\gamma}_{ij} = \begin{bmatrix} U_r & -\partial T/(r\,\partial\theta) & 0\\ U_\theta & \partial T/\partial r & 0\\ 0 & 0 & 1\end{bmatrix}, \quad \tilde{\gamma}_{\infty ij} = \begin{bmatrix}\cos\theta & -\sin\theta & 0\\ \sin\theta & \cos\theta & 0\\ 0 & 0 & 1\end{bmatrix}. \tag{4.7}$$

In cylindrical co-ordinates (4.2) has to be converted into equations for $\tilde{\alpha}_{ij}$ in the form (4.6). Thence α_{ij}^{cn} and α_{ij}^{sn} have to satisfy

$$\left\{\frac{\partial^2}{\partial r^2} + \frac{1}{r}\frac{\partial}{\partial r} - \frac{1}{r^2} - \left(\frac{n^2}{r^2} + \kappa_3^2\right)\right\}\begin{pmatrix}\alpha_{1j}^{cn}\\ \alpha_{1j}^{sn}\end{pmatrix} = -\begin{pmatrix}\Omega_{1j}^{cn}\\ \Omega_{1j}^{sn}\end{pmatrix} + \frac{2n}{r^2}\begin{pmatrix}\alpha_{2j}^{sn}\\ -\alpha_{2j}^{cn}\end{pmatrix}, \tag{4.8a}$$

$$\left\{\frac{\partial^2}{\partial r^2} + \frac{1}{r}\frac{\partial}{\partial r} - \frac{1}{r^2} - \left(\frac{n^2}{r^2} + \kappa_3^2\right)\right\}\begin{pmatrix}\alpha_{2j}^{cn}\\ \alpha_{2j}^{sn}\end{pmatrix} = -\begin{pmatrix}\Omega_{2j}^{cn}\\ \Omega_{2j}^{sn}\end{pmatrix} - \frac{2n}{r^2}\begin{pmatrix}\alpha_{1j}^{sn}\\ -\alpha_{1j}^{cn}\end{pmatrix}, \tag{4.8b}$$

$$\left\{\frac{\partial^2}{\partial r^2} + \frac{1}{r}\frac{\partial}{\partial r} - \left(\frac{n^2}{r^2} + \kappa_3^2\right)\right\}\begin{pmatrix}\alpha_{3j}^{cn}\\ \alpha_{3j}^{sn}\end{pmatrix} = -\begin{pmatrix}\Omega_{3j}^{cn}\\ \Omega_{3j}^{sn}\end{pmatrix}, \tag{4.8c}$$

subject to the boundary conditions resulting from (3.20) and (4.3),

$$\frac{1}{r}\frac{\partial}{\partial r}\left(r\begin{bmatrix}\alpha_{1j}^{cn}\\ \alpha_{1j}^{sn}\end{bmatrix}\right) + \frac{n}{r}\begin{pmatrix}\alpha_{2j}^{sn}\\ -\alpha_{2j}^{cn}\end{pmatrix} + i\kappa_3\begin{pmatrix}\alpha_{3j}^{cn}\\ \alpha_{3j}^{sn}\end{pmatrix} = 0 \quad \text{at} \quad r = 1, \tag{4.9a}$$

$$n\begin{pmatrix}\alpha_{3j}^{sn}\\ -\alpha_{3j}^{cn}\end{pmatrix} - i\kappa_3\begin{pmatrix}\alpha_{2j}^{cn}\\ \alpha_{2j}^{sn}\end{pmatrix} = 0. \tag{4.9b}$$

In (4.9) we have specified the functions λ, μ and μ_i defined in (4.3) to be zero. As $r \to \infty$

$$\left.\begin{aligned} \frac{n}{r}\begin{pmatrix} \alpha_{3j}^{sn} \\ -\alpha_{3j}^{cn} \end{pmatrix} - i\kappa_3 \begin{pmatrix} \alpha_{2j}^{cn} \\ \alpha_{2j}^{sn} \end{pmatrix} &= 0, \\ i\kappa_3 \begin{pmatrix} \alpha_{1j}^{cn} \\ \alpha_{1j}^{sn} \end{pmatrix} - \frac{\partial}{\partial r}\begin{pmatrix} n\alpha_{3j}^{cn} \\ n\alpha_{3j}^{sn} \end{pmatrix} &= 0, \\ \frac{1}{r}\frac{\partial}{\partial r}\left(r\begin{pmatrix} n\alpha_{2j}^{cn} \\ n\alpha_{2j}^{sn} \end{pmatrix}\right) - \frac{n}{r}\begin{pmatrix} \alpha_{1j}^{sn} \\ -\alpha_{1j}^{cn} \end{pmatrix} &= 0 \end{aligned}\right\} \tag{4.9c}$$

and (4.9*a*) is also valid. Equation (4.9*c*) implies that for finite κ_1, κ_2 and κ_3, as $r \to \infty$, $\alpha_{ij} \to 0$. An alternative method for finding $\tilde{\boldsymbol{\psi}}$ is to use the fact that $\nabla.\tilde{\boldsymbol{\psi}} = 0$ for all values of r. Then $\tilde{\psi}_1$ and $\tilde{\psi}_3$ can be calculated from (4.6*a*, *c*) and $\tilde{\psi}_2$ calculated from $\nabla.\tilde{\boldsymbol{\psi}} = 0$. It may be shown that $\tilde{\psi}_2$ calculated by this method satisfies (4.6*b*) identically. Since this is an easier method for calculating α_{ij}^{cn} and α_{ij}^{sn} when $n \geqslant 1$, it is one we adopt.

First, we calculate $\tilde{\alpha}_{3j}$ from (4.8*c*) directly, using the complementary functions $K_n(|r\kappa_3|)$ and $I_n(|r\kappa_3|)$ (modified Bessel functions) and the method of variation of parameters:

$$\begin{aligned} \begin{pmatrix} \alpha_{3j}^{cn} \\ \alpha_{3j}^{sn} \end{pmatrix} = K_n(|r\kappa_3|)\int_{r_1}^{r} r^{\times}\begin{pmatrix} \Omega_{3j}^{cn} \\ \Omega_{3j}^{sn} \end{pmatrix} I_n(|r^{\times}\kappa_3|)\,dr^{\times} \\ + I_n(|r\kappa_3|)\int_{r}^{r_2} r^{\times}\begin{pmatrix} \Omega_{3j}^{cn} \\ \Omega_{3j}^{sn} \end{pmatrix} K_n(|r^{\times}\kappa_3|)\,dr^{\times}. \end{aligned} \tag{4.10}$$

While the constant of integration r_2 is determined by (4.9*c*), the other constant r_1 is not determined by (4.9*b*). However, r_1 may be chosen at this stage to simplify the subsequent algebra. We find $r_1 = 1$, and $r_2 = R$ [defined in (2.22)]. Second, since we are using the fact that $\nabla.\tilde{\boldsymbol{\psi}} = 0$ [or (4.9*a*)] is valid for all r, $\tilde{\alpha}_{2j}$ can be found in terms of $\tilde{\alpha}_{1j}$ and $\tilde{\alpha}_{3j}$ (for $n \geqslant 1$);

$$\begin{pmatrix} \alpha_{2j}^{sn} \\ -\alpha_{2j}^{cn} \end{pmatrix} = -\frac{1}{n}\frac{\partial}{\partial r}\left(r\begin{bmatrix} \alpha_{1j}^{cn} \\ \alpha_{1j}^{sn} \end{bmatrix}\right) - \frac{i\kappa_3 r}{n}\begin{pmatrix} \alpha_{3j}^{cn} \\ \alpha_{3j}^{sn} \end{pmatrix}. \tag{4.11}$$

$\tilde{\alpha}_{2j}$ is then substituted into (4.8*a*), giving an equation for $\tilde{\alpha}_{1j}$ in terms of $\tilde{\Omega}_{1j}$ and $\tilde{\alpha}_{3j}$. For $n = 0$, we have

$$\left\{\frac{\partial^2}{\partial r^2} + \frac{1}{r}\frac{\partial}{\partial r} - \frac{1}{r^2} - \kappa_3^2\right\}\alpha_{1j}^{c0} = -\Omega_{1j}^{c0} \tag{4.12}$$

and for $n \geqslant 1$,

$$\left\{\frac{\partial^2}{\partial r^2} + \frac{3}{r}\frac{\partial}{\partial r} + \frac{1-n^2}{r^2} - \kappa_3^2\right\}\begin{pmatrix} \alpha_{1j}^{cn} \\ \alpha_{1j}^{sn} \end{pmatrix} = -\begin{pmatrix} F_{1j}^{cn} \\ F_{1j}^{sn} \end{pmatrix}, \tag{4.13}$$

where

$$\begin{pmatrix} F_{1j}^{cn} \\ F_{1j}^{sn} \end{pmatrix} = \begin{pmatrix} \Omega_{1j}^{cn} \\ \Omega_{1j}^{sn} \end{pmatrix} + \frac{2i\kappa_3}{r}\begin{pmatrix} \alpha_{3j}^{cn} \\ \alpha_{3j}^{sn} \end{pmatrix}.$$

The solution to (4.12) is

$$\begin{aligned} \alpha_{1j}^{c0} = K_1(|r\kappa_3|)\left\{C_{1j}^{c0} + \int_1^r r^{\times}\Omega_{1j}^{c0} I_1(|r^{\times}\kappa_3|)\,dr^{\times}\right\} \\ + I_1(|r\kappa_3|)\int_r^R r^{\times}\Omega_{1j}^{c0} K_1(|r^{\times}\kappa_3|)\,dr^{\times}, \end{aligned} \tag{4.14}$$

where $$C^{c0}_{1j} = I_0(|\kappa_3|)\,\Omega^{c0}_{1j}(r=1)/\kappa_3,$$

a result from (4.9a) and the fact that

$$\partial\Omega^{c0}_{1j}/\partial r + (\Omega^{c0}_{1j}/r) + i\kappa_3\,\Omega^{c0}_{3j} = 0.$$

From (4.13), for $n \geqslant 1$,

$$\begin{pmatrix}\alpha^{cn}_{1j}\\ \alpha^{sn}_{1j}\end{pmatrix} = \frac{1}{r}K_n(|r\kappa_3|)\left\{\begin{pmatrix}C^{cn}_{1j}\\ C^{sn}_{1j}\end{pmatrix} + \int_1^r r^{\times 2}\begin{pmatrix}F^{cn}_{1j}\\ F^{sn}_{1j}\end{pmatrix} I_n(|r^\times\kappa_3|)\,dr^\times\right\} + \frac{1}{r}I_n(|r\kappa_3|)\int_r^R r^{\times 2}\begin{pmatrix}F^{cn}_{1j}\\ F^{sn}_{1j}\end{pmatrix} K_n(|r^\times\kappa_3|)\,dr^\times. \quad (4.15)$$

To calculate $\tilde{\alpha}_{2j}$, we use (4.8b) for the case $n = 0$ to find

$$\alpha^{c0}_{2j} = K_1(|r\kappa_3|)\left[C^{c0}_{2j} + \int_1^r r^\times\Omega^{c0}_{2j}\,I_1(|r^\times\kappa_3|)\,dr^\times\right] + I_1(|r\kappa_3|)\int_r^R r^\times\Omega^{c0}_{2j}\,K_1(|r^\times\kappa_3|)\,dr^\times. \quad (4.16)$$

For $n \geqslant 1$, we use (4.10), (4.11) and (4.15) to obtain

$$\begin{aligned}\begin{pmatrix}\alpha^{sn}_{2j}\\ -\alpha^{cn}_{2j}\end{pmatrix} = \frac{1}{nr}\Bigg\{&-[nK_n(|r\kappa_3|) + r\kappa_3 K_{n-1}(|r\kappa_3|)]\\ &\times\left[\begin{pmatrix}C^{cn}_{1j}\\ C^{sn}_{1j}\end{pmatrix} + \int_1^r r^{\times 2}\begin{pmatrix}F^{cn}_{1j}\\ F^{sn}_{1j}\end{pmatrix} I_n(|r^\times\kappa_3|)\,dr^\times\right] + [r\kappa_3 I_{n-1}(|r\kappa_3|) - nI_n(|r\kappa_3|)]\\ &\times\int_r^R r^{\times 2}\begin{pmatrix}F^{cn}_{1j}\\ F^{sn}_{1j}\end{pmatrix} K_n(|r^\times\kappa_3|)\,dr^\times + i\kappa_3 r^2\begin{pmatrix}\alpha^{cn}_{3j}\\ \alpha^{sn}_{3j}\end{pmatrix}\Bigg\}. \quad (4.17)\end{aligned}$$

To satisfy (4.9b), it follows that, for $n = 0$,

$$C^{c0}_{2j} = -\frac{I_1(|\kappa_3|)}{K_1(|\kappa_3|)}\int_1^R r^\times\Omega^{c0}_{2j}\,K_1(|r^\times\kappa_3|)\,dr^\times, \quad (4.18a)$$

while for $n \geqslant 1$,

$$\begin{pmatrix}C^{cn}_{1j}\\ C^{sn}_{1j}\end{pmatrix} = \frac{i\frac{(\kappa_3^2+n^2)}{\kappa_3}I_n(|\kappa_3|)\begin{pmatrix}\Gamma^{cn}_{3j}\\ \Gamma^{sn}_{3j}\end{pmatrix} + [\kappa_3 I_{n-1}(|\kappa_3|) - nI_n(|\kappa_3|)]\begin{pmatrix}\Gamma^{cn}_{1j}\\ \Gamma^{sn}_{1j}\end{pmatrix}}{nK_n(|\kappa_3|) + \kappa_3 K_{n-1}(|\kappa_3|)}, \quad (4.18b)$$

where

$$\left.\begin{aligned}\begin{pmatrix}\Gamma^{cn}_{3j}\\ \Gamma^{sn}_{3j}\end{pmatrix} &= \int_1^\infty r^\times\begin{pmatrix}\Omega^{cn}_{3j}\\ \Omega^{sn}_{3j}\end{pmatrix} K_n(|r^\times\kappa_3|)\,dr^\times,\\ \begin{pmatrix}\Gamma^{cn}_{1j}\\ \Gamma^{sn}_{1j}\end{pmatrix} &= \int_0^\infty r^{\times 2}\begin{pmatrix}F^{cn}_{1j}\\ F^{sn}_{1j}\end{pmatrix} K_n(|r^\times\kappa_3|)\,dr^\times.\end{aligned}\right\} \quad (4.19)$$

Thus $\tilde{\alpha}_{ij}$ can now in principle be calculated with $\tilde{\alpha}_{3j}$ given by (4.10), $\tilde{\alpha}_{1j}$ by (4.14), (4.15), (4.18b) and (4.19), and $\tilde{\alpha}_{2j}$ by (4.16), (4.17) and (4.18). The problem of computing these integrals is left to §4.2.

Turbulent velocity potential β_i. To calculate $\hat{\hat{\Phi}}$, the Fourier transform of Φ, we have to solve (3.21). But first we express $\hat{\hat{\Phi}}$ in terms of a new function β_i, as before:

$$\hat{\hat{\Phi}}(x, y; \kappa_1, \kappa_3) = \int_{-\infty}^{\infty}\beta_i(x, y; \kappa_1, \kappa_2, \kappa_3)\,S_{\infty i}(\kappa_1, \kappa_2, \kappa_3)\,d\kappa_2. \quad (4.20)$$

β_i is now expressed as a Fourier series:

$$\beta_i = \sum_{n=0}^{\infty} \{\beta_i^{cn}(r;\kappa_1,\kappa_2,\kappa_3)\cos n\theta + \beta_i^{sn}(r;\kappa_1,\kappa_2,\kappa_3)\sin n\theta\}. \tag{4.21}$$

In cylindrical co-ordinates, (3.21) becomes

$$\left\{\frac{\partial^2}{\partial r^2}+\frac{1}{r}\frac{\partial}{\partial r}-\left(\frac{n^2}{r^2}+\kappa_3^2\right)\right\}\begin{pmatrix}\beta_i^{cn}\\ \beta_i^{sn}\end{pmatrix} = 0. \tag{4.22}$$

The boundary conditions (3.22) and (3.23) reduce to

$$\left.\begin{aligned}&\text{as}\quad r\to\infty,\quad \hat{\hat{\Phi}}\to 0,\quad \text{whence}\quad \beta_i\to 0,\\ &\text{at}\quad r=1,\quad \partial\beta_i/\partial r = (\cos\theta,\sin\theta,0)\exp\{i(\kappa_1\cos\theta+\kappa_2\sin\theta)\},\end{aligned}\right\} \tag{4.23}$$

whence

$$\frac{\partial}{\partial r}\begin{pmatrix}\beta_i^{cn}\\ \beta_i^{sn}\end{pmatrix} = \begin{pmatrix}G_i^{cn}\\ G_i^{sn}\end{pmatrix}, \tag{4.24}$$

where

$$\begin{pmatrix}G_i^{cn}\\ G_i^{sn}\end{pmatrix} = \frac{I}{2\pi}\int_0^{2\pi}\begin{pmatrix}\cos n\theta\\ \sin n\theta\end{pmatrix}(\cos\theta,\sin\theta,0)\exp\{i(\kappa_1\cos\theta+\kappa_2\sin\theta)\}\,d\theta. \tag{4.25}$$

Here $I = 1$ for $n = 0$ and $I = 2$ for $n \geqslant 1$. Thus $G_3^{cn} = 0$ and $G_3^{sn} = 0$.

Performing the integrals in (4.25) we find

$$\begin{pmatrix}G_1^{cn}\\ G_1^{sn}\\ G_2^{cn}\\ G_2^{sn}\end{pmatrix} = i^{n+1}(\tfrac{1}{2}I)\left\{\begin{pmatrix}\cos(n+1)\sigma_3\\ \sin(n+1)\sigma_3\\ \sin(n+1)\sigma_3\\ -\cos(n+1)\sigma_3\end{pmatrix}J_{n+1}(k_{12}) - \begin{pmatrix}\cos(n-1)\sigma_3\\ \sin(n-1)\sigma_3\\ -\sin(n-1)\sigma_3\\ -\cos(n-1)\sigma_3\end{pmatrix}J_{n-1}(k_{12})\right\}, \tag{4.26}$$

where $k_{12} = (\kappa_1^2+\kappa_2^2)^{\frac{1}{2}}$ and $\sigma_3 = \tan^{-1}(\kappa_2/\kappa_1)$. The solution to (4.22) subject to the conditions (4.23) and (4.24) is

$$\begin{pmatrix}\beta_i^{cn}\\ \beta_i^{sn}\end{pmatrix} = \begin{pmatrix}G_i^{cn}\\ G_i^{sn}\end{pmatrix}\frac{K_n(|r\kappa_3|)}{\kappa_3 K_{n+1}(|\kappa_3|)-nK_n(|\kappa_3|)}. \tag{4.27}$$

Calculating the tensor M_{in}. We now show how the solutions for α_{ij} and β_i can be used to calculate the tensor M_{in}. Since

$$\mathbf{u} = \Delta\mathbf{u}+\mathbf{u}_\infty = -\nabla\Phi+\nabla\times\boldsymbol{\psi}+\mathbf{u}_\infty,$$

it follows from the definitions of α_{ij} and β_i that, using Cartesian co-ordinates again,

$$\hat{u}_i(x,y,\kappa_1,\kappa_3) = \int_{-\infty}^{\infty}\sum_{j=1}^{3}\{(M_{ij}^{(s)}+M_{ij}^{(\infty)})S_{\infty j}+a_{ij}s_{\infty j}\}\,d\kappa_2, \tag{4.28}$$

where
$$M_{ij}^{(s)}(x, y, \kappa_1, \kappa_2, \kappa_3) = \left(-\frac{\partial \beta_j}{\partial x}, -\frac{\partial \beta_j}{\partial y}, -i\kappa_3 \beta_j\right), \quad M_{ij}^{(\infty)} = \delta_{ij} \exp\{i(\kappa_1 x + \kappa_2 y)\} \tag{4.29}$$

and
$$a_{ij} = \left(\frac{\partial \alpha_{3j}}{\partial y} - i\kappa_3 \alpha_{2j}, i\kappa_3 \alpha_{1j} - \frac{\partial \alpha_{3j}}{\partial x}, \frac{\partial \alpha_{2j}}{\partial x} - \frac{\partial \alpha_{1j}}{\partial y}\right). \tag{4.30}$$

Since $s_{\infty i} = \epsilon_{ijk}(i\kappa_j S_{\infty k})$, (4.28) reduces to the required form of (3.28), namely

$$\hat{\hat{u}}_i(x, y, \kappa_1, \kappa_3) = \int_{-\infty}^{\infty} \{M_{il}(x, y; \kappa_1, \kappa_2, \kappa_3)\, S_{\infty l}(\kappa_1 \kappa_2 \kappa_3)\}\, d\kappa_2, \tag{4.31}$$

where M_{il} is defined by

where
$$M_{il} = M_{il}^{(d)} + M_{il}^{(s)} + M_{il}^{(\infty)}, \quad M_{il}^{(d)} = i a_{ij} \epsilon_{jkl} \kappa_k. \tag{4.32}$$

4.2. *Numerical results*

The problem of computing M_{il}, as defined by (4.31), is fairly straightforward. However, it is worthwhile appreciating the salient features, the problems involved and the time taken in computing M_{il} in order to understand why we cannot realistically compute the turbulence except in some special types of flow.

The calculation of $\Omega_{ij}(x, y, \kappa_1, \kappa_2)$ is perfectly straightforward. $T_X(x, y)$ was computed by integrating $1/U_x$ along streamlines from $x = -X$ (in our case $X = 10$) to the point (x, y). Thence $\tilde{\gamma}_{22} = \partial T/\partial r$, $\tilde{\gamma}_{12} = -\partial T/r\,\partial\theta$ and Δ_T are found. The other terms in $\tilde{\Omega}_{ij}$ can be calculated directly from (4.3). $\tilde{\Omega}_{ij}$ was computed at 40 regularly spaced values of θ and 40 values of r from $r = 1{\cdot}01$ to $r = 10$, with spacings ranging from $0{\cdot}01$ near $r = 1{\cdot}01$ to spacings of $1{\cdot}0$ for $r > 6$. Since $\tilde{\Omega}_{ij}$ is calculated no closer to the body than at $r = 1{\cdot}01$ it was decided that M_{il} could not be calculated any closer than at $r = 1{\cdot}1$. Our second assumption (As 2) was used, taking $R = 10$, to justify calculating Ω_{ij} for values of $r < 10$. Then using (As 3) to calculate $\tilde{\Omega}_{ij}$ close to the line $\theta = 0$, taking $\delta\theta = \frac{1}{20}\pi$, the Fourier coefficients Ω_{ij}^{cn} and $\Omega_{ij}^{sn}(r)$ were calculated for $0 \leqslant n \leqslant 20$ at the same intervals from the values of $\tilde{\Omega}_{ij}$ at the 40 values of θ. For both Ω_{ij}^{cn} and other terms it is important to know how fast the Fourier series converge, taking as a crude measure of convergence the ratio λ_c of the moduli of the largest term and the last term in the series, i.e. the twenty-first. Table 3 in the appendix gives the largest term $|\Omega_{11}^{cn}|_{\max}$, its value of n and λ_c for various values of κ_1 and κ_2 at $r = 1{\cdot}01$ and $r = 3{\cdot}6$. The table shows up two trends, which are readily explicable. The first is the effect of κ_1 and κ_2 increasing, which is that when the variations in $\tilde{\Omega}_{ij}$ occur over smaller distances the terms in the series Ω_{11}^{cn} decrease with n more slowly. The second trend is that the series converges more slowly as r increases. The explanation for this is that the distance in the θ direction between the points at which $\tilde{\Omega}_{ij}$ is calculated increases as r increases, so that the Fourier series representation of $\tilde{\Omega}_{ij}$ becomes increasingly inaccurate and the errors involved take the form of spurious terms at the higher values of n.

In order to compute C_{1j}^{cn}, and thence α_{ij}^{cn}, it is first necessary to compute the functions Γ_{3j}^{cn} and Γ_{1j}^{cn}. The integrals in these functions and α_{ij}^{cn} and α_{ij}^{sn} involve integrating a function whose value is known at the the 40 values of r from $r = 1{\cdot}01$

to $r = 10$. This is done by dividing up this range into portions over which the function is known at equally spaced points, e.g. spaced at 0·01 from $r = 1{\cdot}01$ to $r = 1{\cdot}1$, or 1·0 from $r = 6{\cdot}0$ to $r = 10{\cdot}0$. Then the final integral is a sum of the integrals for each of these portions, obtained by using the five-point Newton–Cotes method of integration (the three-point method being Simpson's rule). The modified Bessel functions were calculated by a standard subroutine. Clearly this method is only reasonable if Ω_{ij} does not vary appreciably between the values of r at which it is calculated, which means that the method is limited to values of κ_1 and κ_2 less than 2 or 3. Instead of calculating $\tilde{\alpha}_{ij}$ from α_{ij}^{cn} and α_{ij}^{sn} by summing the Fourier series, and then calculating a_{ij} defined in (4.30), it is better to find the terms in the Fourier series expansion of $\tilde{a}_{ij}$, namely a_{ij}^{cn} and a_{ij}^{sn}. Then we can avoid differentiating $\tilde{\alpha}_{ij}$. The convergence for a_{ij}^{cn}, as a function of κ_1, κ_2 and κ_3, was very much better than the convergence for Ω_{ij}^{cn} because of the Bessel functions involved in the integrals. To substantiate this point we have given in table 4 the largest term $(a_{12}^{cn})_{\max}$, $n_{\max}$ and λ_c for a_{12}^{cn}, for various values of κ_1, κ_2 and κ_3. The only poor convergence occurs when κ_3 is small and κ_1 or κ_2 are large. Note that, though the convergence is rapid when $\kappa_1 = \kappa_2 = \kappa_3 = 3{\cdot}0$, the results are probably erroneous because of the coarseness of the r, θ grid for these values of κ_1 and κ_2.

The calculation of β_i^{cn} and β_i^{sn}, and thence $M_{il}^{(s)}$, is simply a matter of summing series of known functions. The convergence is always better than for a_{ij}.

Once a_{ij} and $M_{il}^{(s)}$ have been computed, M_{il} follows immediately. Results for $M_{il}^{(d)}$, $M_{il}^{(s)} + M_i^{(\infty)}$ and M_{il} are given in tables 1 and 2, in § 5.3.

The time taken to compute M_{il} for one set of values of κ_1, κ_2 and κ_3 at a given point (x, y) cannot be stated exactly. However, on an IBM 360 computer, to compute Ω_{ij}^{cn} and Ω_{ij}^{sn} for *one* pair of values of κ_1 and κ_2 at the necessary 40 values of r takes 70 s. To compute the constants C_{ij}^{cn} and C_{ij}^{sn} for one set of values of κ_1, κ_2 and κ_3 about 6 s are needed, and then to compute a_{ij} at some point (r, θ) a further 9 s. To compute $M_{il}^{(s)}$ only about 3 s are required. Thus if M_{il} is to be computed over a range of, say, 25 values of κ_3 at one pair of values of κ_1 and κ_2, at one point (x, y), the time for *each* value of κ_2 is about $\frac{1}{2}$ min.

From (3.32) and (3.33) we see that, to obtain the spectra and r.m.s. values of $\overline{u_i u_j}$, M_{in} has to be evaluated over all wavenumber space and then, after being multiplied by M_{jm} and $\Phi_{\infty nm}$, integrated. Thus, if M_{in} is calculated at say 25 values each for κ_1, κ_2 and κ_3, i.e. 15625 points, the overall time taken is about 87 h, clearly an unrealistic time.

The conclusion we draw from this fact is that asymptotic methods must be used to gain an understanding of the flow. But, as § 5 shows, computations of M_{in} are useful in that they show how the incident turbulence is distorted in the wavenumber region which cannot be analysed by asymptotic methods.

5. Asymptotic analysis

5.1. *Low wavenumber limit*

So far we have neither been able to obtain an analytical solution to our problem nor have we found it practical to compute a solution for other than a few

values of the wavenumber κ. Therefore we now look for asymptotic solutions in the limit $k(\equiv|\boldsymbol{\kappa}|)\to 0$ and $k\to\infty$. For both these limiting cases it is necessary to examine the original equations rather than to use the asymptotic forms of the Fourier series solutions of §4.1.

5.1.1. *Velocity tensor M_{il}.* We first attempt to find the solution to (4.2). Although we continue to use cylindrical co-ordinates, it is convenient to revert to Cartesian tensors α_{ij}, Ω_{ij}, etc. When $k\to 0$, Ω_{ij} can be expressed as an expansion which is uniformly valid for all values of r and θ.

$$\Omega_{ij}\sim[\Delta\gamma_{ij}(r,\theta)+i\kappa_k\nu_{ijk}(r,\theta)+O(k^2)]\exp\{ir(\kappa_1\cos\theta+\kappa_2\sin\theta)\}, \tag{5.1}$$

where

$$\Delta\gamma_{ij}=\gamma_{ij}-\delta_{ij},\quad \nu_{ij1}=\Delta_T\gamma_{ij},\quad \nu_{ij2}=-\Delta_y\gamma_{ij},\quad \text{and}\quad \nu_{ij3}=0.$$

γ_{ij} is defined in (3.11). The result is due to the fact that, as $r\to\infty$ with $\theta=O(1)$,

$$\Delta_T\sim-\cos\theta/r,\dagger \tag{5.2}$$

and

$$\Delta y=\sin\theta/r.$$

Equation (5.2) is easily proved by considering the flow when $x\to-\infty$ or when $\Psi\to\infty$. From (3.11) and (4.4) the functions $\Delta\gamma_{ij}(r,\theta)$ and $\nu_{ijk}(r,\theta)$ can only be expressed analytically in terms of elliptic integrals, but, as $r\to 1$ and $r\to\infty$, these expressions have simpler forms. From (4.4) it follows that, as $r\to 1$,

$$\left.\begin{aligned}\Delta_T&\sim-\tfrac{1}{2}\ln\xi-\ln[\sin(\tfrac{1}{2}\theta)]-(1+\cos\theta-\tfrac{1}{2}\ln 2)+\tfrac{1}{4}\xi+O(\xi^2\ln\xi),\\ \Delta_y&\sim(1-\xi)\sin\theta,\end{aligned}\right\} \tag{5.3}$$

where $\xi=r-1$. Hence as $r\to 1$, $\gamma_{ij}\sim g^{(1)}_{ij}(r,\theta)+\delta_{ij}$, where

$$g^{(1)}_{ij}(r,\theta)=\begin{bmatrix}-\cos 2\theta & \sin\theta/[2(r-1)] & 0\\ -\sin 2\theta & -\cos\theta/[2(r-1)] & 0\\ 0 & 0 & 0\end{bmatrix}. \tag{5.4}$$

Therefore, as $r\to 1$,

$$\Delta\gamma_{ij}\sim g^{(1)}_{ij}(r,\theta), \tag{5.5a}$$

whence from (5.1) and (5.3)

$$\kappa_k\nu_{ijk}\sim-\kappa_1[\tfrac{1}{2}\ln(r-1)\,(g^{(1)}_{ij}(r,\theta)+\delta_{ij})]. \tag{5.5b}$$

When $r\to\infty$,

$$\Delta\gamma_{ij}\sim-\frac{1}{r^2}g^{(\infty)}_{ij}(r,\theta), \tag{5.6a}$$

whence from (5.1) and (5.2)

$$\kappa_k\nu_{ijk}\sim-\frac{\kappa_1\cos\theta+\kappa_2\sin\theta}{r}\delta_{ij}+O(k/r^2), \tag{5.6b}$$

where

$$g^{(\infty)}_{ij}=\begin{bmatrix}\cos 2\theta & \sin 2\theta & 0\\ \sin 2\theta & -\cos 2\theta & 0\\ 0 & 0 & 0\end{bmatrix}.$$

† By taking $\theta=O(1)$ as $r\to\infty$, we are excluding the region near $y=0$, $x>+1$. Implicitly we are using assumptions (As 2) and (As 3) of §2.

Thus $\Delta\gamma_{ij} = O(1/r^2)$, whereas $\kappa_k \nu_{ijk} = O(k/r)$. Now consider two overlapping limiting cases when $r \to \infty$.

(*a*) $k \to 0$, $rk = \bar{r} \to \infty$. Let $\kappa_i = \kappa_i^\times k$ (where $\kappa_i^\times$ is $O(1)$); then in terms of $\bar{r}$ equation (4.2) becomes

$$\left(\frac{\partial^2}{\partial \bar{r}^2} + \frac{1}{r}\frac{\partial}{\partial \bar{r}} + \frac{1}{\bar{r}^2}\frac{\partial^2}{\partial \theta^2} - \kappa_3^{\times 2}\right)\alpha_{ij}$$
$$= \left\{\frac{g_{ij}^{(\infty)}}{\bar{r}^2} + \frac{i(\kappa_1^\times \cos\theta + \kappa_2^\times \sin\theta)}{\bar{r}}\delta_{ij}\right\} \exp\{i\bar{r}(\kappa_1^\times \cos\theta + \kappa_2^\times \sin\theta)\}.$$

Therefore, since $\kappa_i^\times$ is $O(1)$ as $\bar{r} \to \infty$, the solution is

$$\alpha_{ij} \sim -\left[\frac{i\delta_{ij}(\kappa_1^\times \cos\theta + \kappa_2^\times \sin\theta)/\bar{r} + g_{ij}^{(\infty)}/\bar{r}^2}{\kappa_1^{\times 2} + \kappa_2^{\times 2} + \kappa_3^{\times 2}}\right] \exp\{i\bar{r}(\kappa_1^\times \cos\theta + \kappa_2^\times \sin\theta)\},$$

or
$$\alpha_{ij} \sim -\left[\frac{i\delta_{ij}(\kappa_1 \cos\theta + \kappa_2 \sin\theta)}{k^2 r} + \frac{g_{ij}^{(\infty)}}{k^2 r^2}\right] \exp\{ir(\kappa_1 \cos\theta + \kappa_2 \sin\theta)\}. \tag{5.7}$$

In fact (5.7) is valid for all values of k if $rk \to \infty$, $r \to \infty$ and $k^2/r \to 0$.

(*b*) $k \to 0$, $r \to \infty$; $r\kappa_1$, $r\kappa_2 = o(1)$, $r\kappa_3$ arbitrary. Now (4.2) becomes

$$\left(\frac{\partial^2}{\partial r^2} + \frac{1}{r}\frac{\partial}{\partial r} + \frac{1}{r^2}\frac{\partial^2}{\partial \theta^2} - \kappa_3^2\right)\alpha_{ij} = -\Omega_{ij}, \tag{5.8}$$

where
$$\Omega_{ij} \sim -\frac{1}{r^2} g_{ij}^{(\infty)} - \frac{i(\kappa_1 \cos\theta + \kappa_2 \sin\theta)}{r}[\delta_{ij} + g_{ij}^{(\infty)}] + O(k^2).$$

Since we are looking for an asymptotic solution to $\nabla^2\boldsymbol{\psi} = -\Delta\boldsymbol{\omega}$ [i.e. (5.8)] as $r \to \infty$, we cannot satisfy the gauge condition $\nabla . \boldsymbol{\psi} = 0$ by specifying boundary conditions at $r = 1$. Instead we satisfy this condition directly by specifying that for all (x, y)

$$\partial\alpha_{ij}/\partial x_j = \lambda\kappa_j. \tag{5.9a}$$

(In this case the solution is simpler if λ is an arbitrary scalar.) The boundary condition on the velocity is the same as in (4.3*b*), namely

$$\epsilon_{ijk}\,\partial\alpha_{kl}/\partial x_j \to \mu_i\kappa_l \quad \text{as} \quad r \to \infty. \tag{5.9b}$$

Then if we also choose the complementary functions to (5.8) such that α_{ij} is finite or a constant when $\kappa_3 \to 0$, α_{ij} must have the form

$$\alpha_{ij} \sim -g_{ij}^{(\infty)}\left(\frac{1}{r^2\kappa_3^2} - \tfrac{1}{2}K_2(r\kappa_3)\right) - \frac{K_0(r\kappa_3)}{2}(\delta_{ij} + \delta_{i3}\delta_{3j})$$
$$+ \frac{\delta_{i3}\delta_{3j}}{2} + i\left\{\left(-\frac{1}{r\kappa_3^2} + \frac{1}{\kappa_3}K_1(r\kappa_3)\right)(\kappa_1 \cos\theta + \kappa_2 \sin\theta)\,\delta_{ij}\right.$$
$$\left. - \left(-\frac{1}{r\kappa_3^2} + \frac{1}{\kappa_3}K_1(r\kappa_3)\right)\left(\frac{\kappa_1\mu_{ij}^{(1)} + \kappa_2\mu_{ij}^{(2)}}{2}\right)\right\} + C_{ij}$$
$$+ \frac{i}{2}\{\kappa_1\mu_{ij}^{(3)} + \kappa_2\mu_{ij}^{(4)}\}\left[\frac{1}{r\kappa_3^2} - \frac{8}{r^3\kappa_3^4} + \frac{1}{\kappa_3}K_3(r\kappa_3)\right], \tag{5.10}$$

where $\mu_{ij}^{(1)} = \begin{bmatrix} \cos\theta & \sin\theta & 0 \\ \sin\theta & -\cos\theta & 0 \\ 0 & 0 & 0 \end{bmatrix}$, $\mu_{ij}^{(2)} = \begin{bmatrix} -\sin\theta & \cos\theta & 0 \\ \cos\theta & \sin\theta & 0 \\ 0 & 0 & 0 \end{bmatrix}$,

$\mu_{ij}^{(3)} = \begin{bmatrix} -\cos 3\theta & -\sin 3\theta & 0 \\ -\sin 3\theta & \cos 3\theta & 0 \\ 0 & 0 & 0 \end{bmatrix}$, $\mu_{ij}^{(4)} = \begin{bmatrix} -\sin 3\theta & \cos 3\theta & 0 \\ \cos 3\theta & \sin 3\theta & 0 \\ 0 & 0 & 0 \end{bmatrix}$

and C_{ij} is any constant tensor such that $C_{3j} = 0$. Note that the second and third terms are present in order that the gauge condition (5.9a) is satisfied, at least to $O(k)$. Note also that, as $r\kappa_3 \to \infty$ and $r\kappa_1, r\kappa_2 = o(1)$, α_{ij} tends to the limit given by (5.7).

Near the body we can only find α_{ij} ($k \to 0$) as a function of $\xi\,(= r-1)$:

$$\alpha_{ij} \sim f_{ij}(\theta) + \kappa_1 g_{ij1}(\theta) + \begin{bmatrix} 0 & -\sin\theta & 0 \\ 0 & \cos\theta & 0 \\ 0 & 0 & 0 \end{bmatrix} \times \{\tfrac{1}{2}\xi \ln \xi - \tfrac{1}{8}\kappa_1 [\xi \ln^2 \xi - 2\xi \ln \xi + 2\xi]\} + O(\xi, \xi^2 \ln \xi, k^2) \quad \text{as} \quad r \to 1,$$

where $f_{ij}(\theta)$ and $g_{ij1}(\theta)$ are unknown functions of θ.

To analyse the entire flow region as $k \to 0$, it is necessary to expand α_{ij} and a_{ij} [given by (4.30)] as asymptotic series of the form

$$\alpha_{ij} = \alpha_{ij}^{(0)} + \alpha_{ij}^{(L)} + \alpha_{ij}^{(1)} + \ldots, \tag{5.11}$$

where the terms are $O(1)$, $O(k \ln |\kappa_3|)$ and $O(k)$ respectively. By a fortunate quirk of the analysis, it turns out that we can find a_{ij} to $O(1)$ everywhere. We first calculate $\alpha_{3j}^{(0)}$ for all values of r, subject to the condition $rk = o(1)$. Since, to $O(1)$, $\Omega_{3j} = 0$, because $\Delta\gamma_{3j} = 0$,

$$(\partial^2/\partial x^2 + \partial^2/\partial y^2)\,\alpha_{3j} = 0. \tag{5.12}$$

The solution to (5.12) is determined by the boundary conditions as $r \to \infty$ (which are known from (5.10)) and at $r = 1$, for which the relevant condition is (4.3c):

$$r^{-1}\,\partial\alpha_{3j}^{(0)}/\partial\theta = 0 \quad \text{at} \quad r = 1. \tag{5.13}$$

The solution to (5.12), subject to (5.13) at $r = 1$ and (5.10) as $r \to \infty$ (with $rk = o(1)$), is unique and is

$$\alpha_{3j}^{(0)} = \tfrac{1}{4}[\ln (x^2 + y^2)\,(2\delta_{3j}) + \delta_{3j}]. \tag{5.14}$$

$\alpha_{3j}^{(0)}$ satisfies the condition (4.3a) at $r = 1$ in conjunction with $\alpha_{1j}^{(1)}$ and $\alpha_{2j}^{(1)}$. Since it may be proved that solutions to (5.8) for $\alpha_{1j}^{(1)}$ and $\alpha_{2j}^{(1)}$ which can also satisfy this condition do exist, the solution (5.14) for $\alpha_{3j}^{(0)}$ now satisfies all the necessary conditions. From (5.14) and (4.30) it follows that, as $k \to 0$,

$$a_{1j}^{(0)} \sim y\delta_{3j}/(x^2 + y^2), \quad a_{2j}^{(0)} \sim -x\delta_{3j}/(x^2 + y^2). \tag{5.15}$$

To calculate a_{3j} to $O(1)$, rather than solve for α_{ij} and α_{2j}, it is more convenient to take the curl of (4.2) and solve directly the equation

$$\left(\frac{\partial^2}{\partial x^2} + \frac{\partial^2}{\partial y^2}\right) a_{3j}^{(0)} = \frac{\partial \Omega_{2j}}{\partial x} - \frac{\partial \Omega_{1j}}{\partial y}, \tag{5.16}$$

where, to $O(1)$, $\Omega_{ij} = \gamma_{ij} - \gamma_{\infty ij} = \Delta\gamma_{ij}$. The boundary conditions are

$$a_{3j}^{(0)} = \partial\alpha_{2j}^{(0)}/\partial x - \partial\alpha_{1j}^{(0)}/\partial y \quad \text{as} \quad r \to \infty,$$

$\alpha_{ij}^{(0)}$ being given by (5.10), whence it follows that as $k \to 0$ and $r \to \infty$

$$a_{3j}^{(0)} \sim (y/(x^2+y^2), -x/(x^2+y^2), 0). \tag{5.17}$$

The exact solution to (5.16) as $k \to 0$ is similar to that found by Lighthill (1956) for a weak shear flow round a circular cylinder, and is easily deduced by inspecting the full expression for γ_{ij} in (3.11). We find that the solution to (5.16) satisfying (5.17) is

$$a_{3j}^{(0)} = (\Delta_y, \Delta_T, 0), \tag{5.18}$$

where Δ_y and Δ_T are defined by (3.8) and (3.9).

By considering the limit of (5.10) as $r\kappa_3 \to 0$, it follows that, in expanding α_{ij} as a power series in κ_i, there must be terms in $\kappa_i \ln|\kappa_3|$. This is the reason for the term $\alpha_{ij}^{(L)}(x, y)$ in (5.11), which is $O(k\ln|\kappa_3|)$. Since the expansion for

$$\Omega_{ij}(x, y, \kappa_1, \kappa_2, \kappa_3)$$

has no terms in $k\ln|\kappa_3|$, it follows that, equating terms $O(k\ln|\kappa_3|)$ in (5.8),

$$\nabla^2\alpha_{ij}^{(L)} = 0, \tag{5.19}$$

and the boundary conditions follow from (4.3) and (5.10):

$$\left.\begin{aligned} \alpha_{ij}^{(L)} \sim{}& \ln(\tfrac{1}{2}|\kappa_3|)(\delta_{ij} + \delta_{i3}\delta_{3j}) + (\tfrac{1}{4}ir\ln(\tfrac{1}{2}|\kappa_3|)) \\ &\times [2\delta_{ij}(\kappa_1\cos\theta + \kappa_2\sin\theta) + (\kappa_1\mu_{ij}^{(1)} + \kappa_2\mu_{ij}^{(2)})] + C_{ij} \quad \text{as} \quad r \to \infty, \\ &\partial\alpha_{3j}^{(L)}/r\,\partial\theta - i\kappa_3(\alpha_{2j}^{(L)}\cos\theta - \alpha_{1j}^{(L)}\sin\theta) = 0 \quad \text{at} \quad r = 1, \\ &\partial\alpha_{ij}^{(L)}/\partial x_i = \lambda\kappa_j, \quad \infty > r \geqslant 1, \quad \text{where} \quad \lambda = O(\ln\kappa_3). \end{aligned}\right\} \tag{5.20}$$

These conditions specify the constant C_{ij}, so that the solution is found to be

$$\begin{aligned} \alpha_{ij}^{(L)} = {}& \tfrac{1}{2}\ln(\tfrac{1}{2}|\kappa_3|)\,\delta_{i3}\delta_{3j} + \tfrac{1}{4}ir\ln(\tfrac{1}{2}|\kappa_3|) \\ &\times\{2(\kappa_1\cos\theta + \kappa_2\sin\theta)(\delta_{ij} - \delta_{i3}\delta_{3j}/r^2) + \kappa_1\mu_{ij}^{(1)} + \kappa_2\mu_{ij}^{(2)}\}. \end{aligned} \tag{5.21}$$

Thence the contribution to a_{ij} of order $k\ln|\kappa_3|$ is

$$a_{ij}^{(L)} = \begin{bmatrix} 0 & 0 & \tfrac{1}{2}i\ln(\tfrac{1}{2}|\kappa_3|)[\kappa_1\sin 2\theta/r^2 + \kappa_2(1-\cos 2\theta/r^2)] \\ 0 & 0 & -\tfrac{1}{2}i\ln(\tfrac{1}{2}|\kappa_3|)[\kappa_1(1+\cos 2\theta/r^2) + \kappa_2\sin 2\theta/r^2] \\ 0 & 0 & 0 \end{bmatrix}. \tag{5.22}$$

To find β_i (defined by (4.21)) and thence $M_{ij}^{(s)}$ (defined by (4.29)) as $k \to 0$ we use the asymptotic form of the Fourier series expressions for β_i. We have to consider the limiting cases (*a*) and (*b*) as before.

(*a*) $k \to 0$, $rk = \bar{r} \to \infty$. Then (4.27) shows that β_i, $M_{ij}^{(s)} = O(e^{-r\kappa_3})$. Therefore we can ignore β_i and $M_{ij}^{(s)}$ compared with α_{ij} and a_{ij}, which are $O[(kr)^{-1}]$.

(*b*) $k \to 0, rk = o(1)$. Calculating G_i^{cn} and G_i^{sn} directly from (4.25) and using the asymptotic forms for $K_n(r\kappa_3)$, as $k \to 0$, we find that if we retain terms up to $O(k^2)$ the Fourier series expansion for $\tilde{M}_{ij}^{(s)}$ terminates at $n = 2$. The detailed expression is given in the appendix.

M_{il} can now be found for small values of k_i from our knowledge of a_{ij} and $M_{ij}^{(s)}$ since, from (4.32),

$$M_{il} = M_{il}^{(d)} + M_{il}^{(s)} + \delta_{il} \exp\{i(\kappa_1 x + \kappa_2 y)\},$$

where $M_{il}^{(d)} = i\epsilon_{jkl}\kappa_k a_{ij}$. The results have shown that, as $k \to 0$, M_{il} can be expanded in powers of k. For the region of greatest interest where $rk = o(1)$ we find

$$M_{il} = M_{il}^{(0)} + M_{il}^{(1)} + M_{il}^{(L)} + M_{il}^{(2)} + \ldots, \tag{5.23}$$

where the various terms are $O(1)$, $O(k)$, $O(k^2 \ln|\kappa_3|)$ and $O(k^2)$ respectively. We assume a similar notation for $M_{il}^{(d)}$ and $M_{il}^{(s)}$. Since $a_{ij} = O(1)$ and $M_{il}^{(s)} = O(1)$ as $k \to 0$, $M_{il}^{(0)} = M_{il}^{(s,0)} + \delta_{il}$ where $M_{il}^{(s,0)}$ is deduced from the appendix, whence

$$M_{il}^{(0)} = \begin{bmatrix} 1-(x^2-y^2)/[(x^2+y^2)^2] & 2xy/[(x^2+y^2)^2] & 0 \\ -2xy/[(x^2+y^2)^2] & 1+(x^2-y^2)/[(x^2+y^2)^2] & 0 \\ 0 & 0 & 1 \end{bmatrix}. \tag{5.24}$$

Using the results (5.15) and (5.18) for a_{ij} and those in the appendix for $M_{il}^{(s,1)}$ it follows that

$$M_{il}^{(1)} = M_{il}^{(d,1)} + M_{il}^{(s,1)} + i(\kappa_1 x + \kappa_2 y)\,\delta_{il}, \tag{5.25}$$

where $M_{il}^{(d,1)} = i\epsilon_{jkl}\kappa_k a_{ij}$. Similarly, $a_{ij}^{(L)}$ is given by (5.22) and $M_{il}^{(s,L)}$ by the appendix, so that

$$M_{il}^{(L)} = i\epsilon_{jkl}\kappa_k a_{ij}^{(L)} + M_{il}^{(s,L)}.$$

For example, on the stagnation line $\theta = \pi$

$$M_{il}^{(L)} = \tfrac{1}{2}\ln(\tfrac{1}{2}|\kappa_3|) \begin{bmatrix} (\kappa_2^2+\kappa_3^2)(1-1/r^2) & -\kappa_1\kappa_2(1-1/r^2) & 0 \\ -\kappa_1\kappa_2(1+1/r^2) & (\kappa_1^2+\kappa_3^2)(1+1/r^2) & 0 \\ 0 & 0 & 0 \end{bmatrix}.$$

Although $M_{il}^{(s,2)}$ can be found for $\infty > r \geqslant 1$, a_{ij} can be calculated to $O(k)$ only when $r \gg 1$, so that $M_{il}^{(d,2)}$ and therefore $M_{il}^{(2)}$ are not known for the whole range $\infty > r \geqslant 1$.

An interpretation of the physical significance of the various terms in the expansion (5.23) is given in §5.3.3.

5.2. *High wavenumber limit*

5.2.1. *Velocity tensor* M_{il}. To find the solution to (4.2) when $k \gg 1$, it is first necessary to express $\Omega_{ij}(x, y)$ in terms of its value at a neighbouring point (x_1, y_1). Let

$$\Omega_{ij}(x,y) = \Gamma_{ij}(x,y) - \Gamma_{ij}^{(\infty)}(x,y), \tag{5.26}$$

where

$$\Gamma_{ij} = \gamma_{ij}(x,y)\exp\{i[\kappa_1(\Delta_T + x) + \kappa_2(y - \Delta_y)]\},$$

$$\Gamma_{ij}^{(\infty)} = \gamma_{\infty ij}\exp\{i[\kappa_1 x + \kappa_2 y]\}.$$

Then by Taylor's theorem

$$\Omega_{ij}(x,y) = \Gamma_{ij}(x_1,y_1)(1 + g_{ij}x' + h_{ij}y' + O(r'^2))\exp\{i[\chi_1 x' + \chi_2 y' + O(kr'^2)]\} - \Gamma_{ij}^{(\infty)}(x_1,y_1)\exp\{i[\kappa_1 x' + \kappa_2 y']\}, \tag{5.27}$$

where $$x' = x - x_1, \quad y' = y - y_1, \quad r' = (x'^2 + y'^2)^{\frac{1}{2}},$$

$$g_{ij} = \frac{1}{\gamma_{ij}} \frac{\partial \gamma_{ij}}{\partial x}(x_1, y_1), \quad h_{ij} = \frac{1}{\gamma_{ij}} \frac{\partial \gamma_{ij}}{\partial y}(x_1, y_1),$$

$$\chi_1(x_1, y_1) = \kappa_1[\partial \Delta_T/\partial x + 1] - \kappa_2 \partial \Delta_y/\partial x = \kappa_1 \partial T/\partial x - \kappa_2 U_2,$$

$$\chi_2(x_1, y_1) = \kappa_1 \partial \Delta_T/\partial y + \kappa_2(1 - \partial \Delta_y/\partial y) = \kappa_1 \partial T/\partial y + \kappa_2 U_1.$$

Stream function α_{ij} away from the body. It can either be proved by using the Green function solution (used later) or shown by inspection that the solution α_{ij} to (4.2) if k is sufficiently large must have the form

$$\alpha_{ij} = \alpha_{ij}^{(b)} + \alpha_{ij}^{(d)} - \alpha_{ij}^{(\infty)}. \tag{5.28}$$

Here $\alpha_{ij}^{(b)}$ is the complementary function (to be discussed later) arising from the boundary conditions and

$$\alpha_{ij}^{(d)} = f_1(x_1, y_1) \exp\{i[\chi_1 x' + \chi_2 y']\}, \quad \alpha_{ij}^{(\infty)} = f_2(x_1, y_1) \exp\{i[\kappa_1 x' + \kappa_2 y']\}.$$

These two solutions correspond to the two components of Ω_{ij} given by (5.32). Inspection of (4.2) and (5.27) then shows that $\alpha_{ij}^{(b)} = 0$, and if

$$|g_{ij} x'|, |h_{ij} y'| = o[k^{-1}] \tag{5.29}$$

as $k \to \infty$, then

$$\alpha_{ij} = \frac{\gamma_{ij}}{\chi^2} \exp\{i[\kappa_1(x + \Delta_T) + \kappa_2(y - \Delta_y)]\} - \frac{\delta_{ij}}{k^2} \exp\{i[\kappa_1 x + \kappa_2 y]\}, \tag{5.30}$$

where

$$\chi^2 = \chi_1^2 + \chi_2^2 + \chi_3^2, \quad \kappa_3 = \chi_3, \quad \chi^2 = \kappa_1^2(\nabla T)^2 + \kappa_2^2(\nabla \Psi)^2 + 2\kappa_1 \kappa_2(\nabla \Psi . \nabla T) + \kappa_3^2.$$

This is the solution to (4.2) used by Batchelor & Proudman (1954). It satisfies (4.3*a*) and from it a_{il} can be calculated; we find

$$a_{il} = a_{il}^{(d)} + a_{il}^{(\infty)} + a_{il}^{(b)},$$

where $$a_{il}^{(d)} = i\epsilon_{ijk}\{(\chi_j/\chi^2)\gamma_{kl} \exp i\{\kappa_1[x + \Delta_T] + \kappa_2[y - \Delta_y]\}\}, \tag{5.31}$$

$$a_{il}^{(b)} = 0, \quad a_{il}^{(\infty)} = i\epsilon_{ijk}\{-(\kappa_j \delta_{kl}/k^2) \exp[i(\kappa_1 x + \kappa_2 y)]\}.$$

Its limitation is that k^{-1} must be small compared with the distance over which the mean flow changes (i.e. (5.29) must be satisfied). This condition is violated near the body, where also the boundary condition (4.3*c*) must be satisfied, so that we must consider a new solution for this region of the flow.

Stream function α_{ij} near the body. To find α_{ij} near the surface of the body, we use the Green function solution to (4.2) re-expressed in terms of local Cartesian co-ordinates (ξ, η) in the (r, θ) directions, where $\xi = 0$ on $r = 1$ and $\eta = 0$ at some value of $\theta = \theta_1$. Then at a point (ξ_1, η_1)

$$\tilde{\alpha}_{ij}^{(d)}(\xi_1, \eta_1) = \frac{1}{2\pi} \int_{-X}^{X} \left\{ \int_{-Y}^{Y} \tilde{\Omega}_{ij}(\xi, \eta) K_0(|\kappa_3| \rho^{\times}) \, d\eta \right\} d\xi, \tag{5.32}$$

where $\rho^\times = (\xi^{\times 2}+\eta^{\times 2})^{\frac{1}{2}}$, $\xi^\times = \xi - \xi_1$ and $\eta^\times = \eta - \eta_1$ and the limits X and Y must satisfy the condition $k^{-1} \ll X, Y \ll 1$. In finding $\alpha_{ij}^{(d)}$ near $r = 1$, we have to ensure that the condition (4.3a) is satisfied, which implies that, since

$$\partial\Omega_{ij}/\partial x_i = \lambda\kappa_j,$$

$$\frac{\partial\tilde{\alpha}_{ij}}{\partial\xi_1}+\frac{\partial\tilde{\alpha}_{ij}}{\partial\eta_1}+i\kappa_3\tilde{\alpha}_{3j} = \frac{1}{2\pi}\int_{-X}^{X}\left\{\int_{-Y}^{Y}\frac{\partial}{\partial\xi}[\tilde{\Omega}_{1j}K_0(|\kappa_3|\rho')] + \frac{\partial}{\partial\eta}[\tilde{\Omega}_{2j}K_0(|\kappa_3|\rho')]\,d\eta\right\}d\xi - \lambda^\times\kappa_j,$$

where λ and $\lambda^\times$ are scalars in κ_i space. Thence (4.3a) is satisfied provided that a fictional $\tilde{\Omega}_{ij}$ is invented inside the body such that the normal component $\tilde{\Omega}_{1j}$ of $\tilde{\Omega}_{ij}$ is continuous across $\xi = 0$ in the sense

$$\lim_{\epsilon\to 0}(\tilde{\Omega}_{1j}(\xi = \epsilon) - \tilde{\Omega}_{1j}(\xi = -\epsilon)) = 0.$$

To find $\tilde{\Omega}_{ij}$ as $\xi \to 0$, we first need to know Δ_T and Δ_y. From (5.2) and (5.3), as $\xi \to 0$,

$$\left.\begin{aligned} y - \Delta_y &= 2\xi\sin\theta, \\ \Delta_T + x &\sim -\tfrac{1}{2}\ln\xi - \ln\sin\tfrac{1}{2}\theta - (1-\tfrac{1}{2}\ln 2) + \tfrac{1}{4}\xi(1+4\cos\theta). \end{aligned}\right\} \tag{5.33}$$

The simplest method of specifying $\tilde{\Omega}_{ij}$ when $\xi < 0$ is to assume $\tilde{\Omega}_{1j} = \tilde{\Omega}_{1j}(-\xi)$, so that by continuity $\tilde{\Omega}_{2j}(\xi) = -\tilde{\Omega}_{2j}(-\xi)$, and $\tilde{\Omega}_{3j}(\xi) = -\tilde{\Omega}_{3j}(-\xi)$. (Note that the solution for $\xi > 0$ will be unique when all the conditions are satisfied.) Thus when $|\xi| \to 0$,

$$\tilde{\Gamma}_{ij} \sim \tilde{\gamma}_{ij}\exp[i\{-\kappa_1(\ln\tfrac{1}{2}|\xi| + \ln|\sin\tfrac{1}{2}\theta| + A - \tfrac{1}{4}|\xi|(4\cos\theta+1)) + 2\kappa_2|\xi|\sin\theta\}], \tag{5.34}$$

where $\tilde{\gamma}_{ij} \sim \begin{bmatrix} 2|\xi|\cos\theta & |\xi|\sin\theta + (1-|\xi|)(1+\cos\theta)/2\sin\theta & 0 \\ \mp 2\sin\theta & \pm\tfrac{1}{4}(4\cos\theta+1) - 1/2\xi & 0 \\ 0 & 0 & \pm 1 \end{bmatrix}$ for $\xi \gtrless 0$,

and $A = 1 - \tfrac{1}{2}\ln 2$, $\tilde{\Gamma}_{ij}^{(\infty)} = \tilde{\gamma}_{\infty ij}\exp[i(1+\xi)(\kappa_1\cos\theta + \kappa_2\sin\theta)]$.

To demonstrate the irregular oscillations of $\tilde{\Gamma}_{ij}$ when $\theta = \pi$ and $\theta \neq \pi$, graphs of $\tilde{\Gamma}_{22}$ are shown in figure 5(b) and graphs of $\tilde{\Gamma}_{33}$ in figures 5(c) and (d). Their physical interpretation is left to § 5.3.3.

Considering the two components of $\tilde{\alpha}_{ij}$, given by (5.28), then as in (5.30)

$$\tilde{\alpha}_{ij}^{(\infty)} = -(\tilde{\gamma}_{\infty ij}/k^2)\exp[i(1+\xi_1)(\kappa_1\cos\theta + \kappa_2\sin\theta)]. \tag{5.35}$$

Substituting $\tilde{\Gamma}_{ij}$ into the integrand of (5.32), we can find $\tilde{\alpha}_{ij}^{(d)}$. If $\tilde{\gamma}_{ij}(\xi,\theta)$ is expanded as a Taylor series in $\eta = \theta - \theta_0$ near any value of θ_0, then at (ξ_1, η_1) $\tilde{\alpha}_{ij}^{(d)}$ is given to the lowest order by

$$\tilde{\alpha}_{ij}^{(d)}(\xi_1,\eta_1) = \frac{B(\theta_0)}{2\pi}\int_{-\infty}^{\infty}\left\{\int_{-\infty}^{\infty}\tilde{\gamma}_{ij}(\xi,0)\exp i[-\tfrac{1}{2}\kappa_1\ln|\xi| + \tilde{\chi}_1|\xi| + \tilde{\chi}_2\eta] \times K_0(|\kappa_3|(\eta^{\times 2}+\xi^{\times 2})^{\frac{1}{2}})\,d\eta\right\}d\xi, \tag{5.36}$$

where
$$B(\theta_0) = \exp i[-\kappa_1\{\ln|\sin\tfrac{1}{2}\theta_0| + A\}],$$
$$\tilde{\chi}_1(\theta_0) = 2\kappa_2\sin\theta_0 + \tfrac{1}{4}\kappa_1(4\cos\theta_0 + 1),$$
$$\tilde{\chi}_2(\theta_0) = |\xi|\partial\tilde{\chi}_1/\partial\theta - \tfrac{1}{2}\kappa_1\cot\tfrac{1}{2}\theta_0,$$
$$\eta^\times = \eta - \eta_1, \quad \xi^\times = \xi - \xi_1.$$

Taking the integral with respect to η, and using the result of Erdélyi, Magnus & Oberhettinger (1954, p. 56)

$$\int_{-\infty}^{\infty} \exp\{i\tilde{\chi}_2\eta\}\, K_0\{|\kappa_3|\,[(\eta-\eta_1)^2 + \xi^{\times 2}]^{\frac{1}{2}}\}\, d\eta = \frac{\pi\exp\{i\tilde{\chi}_2(\xi)\,\eta_1 - \tilde{\chi}_3|\xi-\xi_1|\}}{\tilde{\chi}_{23}(\xi,\theta_0)},$$

where
$$\tilde{\chi}_{23} = [\tilde{\chi}_2^2(\xi,\theta_0) + \kappa_3^2]^{\frac{1}{2}},$$

we find
$$\alpha_{ij}^{(d)}(\xi_1,\eta_1) = B(\theta_0)\exp\{-\tfrac{1}{2}i\kappa_1\eta_1\cot\tfrac{1}{2}\theta_0\}\, I_{ij}(\xi_1,\eta_1), \tag{5.37}$$

where
$$I_{ij}(\xi_1,\eta_1) = \int_{-\infty}^{\infty} \left\{\frac{\tilde{\gamma}_{ij}(\xi,0)\exp\{i[-\tfrac{1}{2}\kappa_1\ln|\xi| + |\xi|(\eta_1\partial\tilde{\chi}_1/\partial\theta + \tilde{\chi}_1)]\}}{2\tilde{\chi}_{23}(\xi,\theta_0)} \times\exp\{-|\xi-\xi_1|\tilde{\chi}_{23}\}\right\} d\xi. \tag{5.38}$$

The integral $I_{ij}(\xi_1,\eta_1)$ has to be considered carefully when $\xi\to 0$ and $k\to\infty$, but the following analytical expressions can be obtained when

$$k\xi \ll 1, \quad k \gg 1, \quad \kappa_1 \ll (\tilde{\chi}_1^2 + \tilde{\chi}_{23}^2)^{\frac{1}{2}}. \tag{5.39}$$

Of course when $k\xi \gg 1$ and $k \gg 1$, (5.37) reduces to the expression for $\alpha_{ij}^{(d)}$ in (5.30). Given the condition (5.39), the physical and practical implication of which will be discussed in §6, it follows that (5.38) may be simplified to

$$I_{ij}(\xi_1,\eta_1) = (I_{Aij} + I_{Bij} + I_{Cij})/2\tilde{\gamma}_{23}(0,\theta_0), \tag{5.40a}$$

where
$$\left.\begin{aligned} I_{Aij} &= \exp\{\tilde{\chi}_{23}\xi_1\}\left\{\int_{\xi_1}^{\infty}\tilde{\gamma}_{ij}(\xi,0)\,\xi^{-\frac{1}{2}i\kappa_1}\exp\{-\tilde{\mu}^\dagger\xi\}\,d\xi\right\},\\ I_{Bij} &= \exp\{-\tilde{\chi}_{23}\xi_1\}\left\{\int_0^{\xi_1}\tilde{\gamma}_{ij}(\xi,\eta_1)\,\xi^{-\frac{1}{2}i\kappa_1}\exp\{\tilde{\mu}\xi\}\,d\xi\right\},\\ I_{Cij} &= \exp\{-\tilde{\chi}_{23}\xi_1\}\left\{\int_0^{\infty}\tilde{\gamma}_{ij}(-\xi,\eta_1)\,\xi^{-\frac{1}{2}i\kappa_1}\exp\{-\tilde{\mu}^\dagger\xi\}\,d\xi\right\}\end{aligned}\right\} \tag{5.40b}$$

and $\tilde{\mu}, \tilde{\mu}^\dagger = \tilde{\chi}_{23} \pm i\tilde{\chi}_1$. From the expressions for $\tilde{\gamma}_{ij}$ in (5.34) it follows that these integrals can be partly expressed in terms of gamma functions because

$$\int_0^{\infty}\xi^{m-\frac{1}{2}i\kappa_1}\exp\{-\tilde{\mu}^\dagger\xi\}\,d\xi = \tilde{\mu}^{\dagger-(m+1)+\frac{1}{2}i\kappa_1}\Gamma(m+1-\tfrac{1}{2}i\kappa_1),$$

where m is an integer and $\mathscr{R}(\mu^\dagger) > 0$. Thence, by splitting I_{Aij} into an infinite and a finite integral, using the assumptions (5.39), and adding all the integrals we obtain the following expressions for I_{ij} (ξ_1,η_1):

$$I_{11}(\xi_1,\eta_1) = 2\cos\theta\left[\frac{\exp\{i(2\phi + \tfrac{1}{2}\kappa_1\ln\tilde{\chi}) + \tfrac{1}{2}\kappa_1\phi\}}{\tilde{\chi}_{23}\tilde{\chi}^2}\Gamma(2-\tfrac{1}{2}i\kappa_1) + O(k^{-1}\xi_{S1}^2, k\xi_{S1}^3)\right],$$

$$I_{12} = \frac{1+\cos\theta}{2\sin\theta}\left[\frac{\exp\{i(\phi+\frac{1}{2}\kappa_1\ln\tilde{\chi})+\frac{1}{2}\kappa_1\phi\}}{\tilde{\chi}_{23}\tilde{\chi}}\Gamma(1-\tfrac{1}{2}i\kappa_1)-\frac{\xi_1^2\exp\{-\frac{1}{2}i\kappa_1\ln\xi_1\}}{(2-\frac{1}{2}i\kappa_1)(1-\frac{1}{2}i\kappa_1)}\right],$$

$$\begin{pmatrix}I_{21}\\ I_{33}\end{pmatrix} = \begin{pmatrix}-2\sin\theta\\ 1\end{pmatrix}\left[\frac{\xi_1\exp\{i(\phi+\frac{1}{2}\kappa_1\ln\tilde{\chi})+\frac{1}{2}\kappa_1\phi\}}{\tilde{\chi}}\right.$$
$$\left.\times\Gamma(1-\tfrac{1}{2}i\kappa_1)-\frac{\xi_1^2\exp\{-\frac{1}{2}i\kappa_1\ln\xi_1\}}{(2-\frac{1}{2}i\kappa_1)(1-\frac{1}{2}i\kappa_1)}\right],$$

$$I_{22} = -\frac{1}{2}\left[\xi_1\exp\{\tfrac{1}{2}i\kappa_1\ln\tilde{\chi}+\tfrac{1}{2}\kappa_1\phi\}\Gamma(-i\tfrac{1}{2}\kappa_1)-\frac{\xi_1\exp\{-\frac{1}{2}i\kappa_1\ln\xi_1\}}{(1-\frac{1}{2}i\kappa_1)(-\frac{1}{2}i\kappa_1)}+O(k^2\xi^2)\right]$$
$$+\frac{1+4\cos\theta}{4}\left[\frac{\xi_1}{\tilde{\chi}}\exp\{i(\phi+\tfrac{1}{2}\kappa_1\ln\tilde{\chi})+\tfrac{1}{2}\kappa_1\phi\}\right.$$
$$\left.\times\Gamma(1-\tfrac{1}{2}i\kappa_1)-\frac{\xi^2\exp\{-\frac{1}{2}i\kappa_1\ln\xi_1\}}{(2-\frac{1}{2}i\kappa_1)(1-\frac{1}{2}i\kappa_1)}\right], \quad (5.41)$$

where

$$\tilde{\mu},\tilde{\mu}^\dagger = \tilde{\chi}\exp\{\pm i\phi\}, \quad \tilde{\chi} = (\tilde{\chi}_{23}^2+\tilde{\chi}_1^2)^{\frac{1}{2}}, \quad \phi = \tan^{-1}(\tilde{\chi}_1/\tilde{\chi}_{23}) \quad (\tfrac{1}{2}\pi \geqslant \phi \geqslant -\tfrac{1}{2}\pi). \quad (5.42)$$

$\tilde{\chi}_1$ can be positive or negative but $\tilde{\chi}_{23} \geqslant 0$. Note that because I_{21}, I_{22} and $I_{33} = 0$ on $\xi_1 = 0$, the boundary condition (4.3*b*) is now satisfied for $\alpha_{ij}^{(d)}$. Subject to the conditions (5.39), it can be shown that the complete expression for $\alpha_{ij}^{(d)}$ does now satisfy (4.2) and also the condition (4.3*a*).

Since $\alpha_{ij}^{(\infty)}$ does not satisfy (4.3*c*), a complementary function to (4.2) has to be found, $\alpha_{ij}^{(b)}$, such that $\alpha_{ij}^{(\infty)}+\alpha_{ij}^{(b)}$ does satisfy the condition that $\mathbf{u}.\mathbf{n} = 0$ on the surface of the body.

Gathering all the results together we find that near the body, subject to (5.39), $\tilde{\alpha}_{ij}$ is given by

$$a_{ij} = a_{ij}^{(d)}+a_{ij}^{(\infty)}+a_{ij}^{(b)}, \quad (5.43)$$

where

$$a_{ij}^{(d)} = B(\theta_0)\exp\{-\tfrac{1}{2}i\kappa_1\eta_1\cot\tfrac{1}{2}\theta_0\}$$
$$\times\begin{bmatrix}-i\kappa_3 I_{21} & -i\kappa_3 I_{22} & -ik_1\cot(\frac{1}{2}\theta_0)\,I_{33}\\ O(k^{-2}) & +i\kappa_3 I_{12} & -\partial I_{33}/\partial\xi_1\\ \dfrac{\partial I_{21}}{\partial\xi_1} & \dfrac{\partial I_{22}}{\partial\xi_1}+i\kappa_1\cot(\frac{1}{2}\theta_0)\,I_{12} & 0\end{bmatrix},$$

$$a_{ij}^{(\infty)} = \frac{i\exp\{i(\kappa_1\cos\theta+\kappa_2\sin\theta)(1+\xi)\}}{k^2}$$
$$\times\begin{bmatrix}-\kappa_3\sin\theta & \kappa_3\cos\theta & -(\kappa_2\cos\theta-\kappa_1\sin\theta)\\ -\kappa_3\cos\theta & -\kappa_3\sin\theta & \kappa_1\cos\theta+\kappa_2\sin\theta\\ +\kappa_2 & -\kappa_1 & 0\end{bmatrix},$$

$$a_{ij}^{(b)} = \frac{\exp\{i(\kappa_1\cos\theta+\kappa_2\sin\theta)-\tilde{k}\xi\}}{k^2}$$
$$\times\begin{bmatrix}i\kappa_3\sin\theta & -i\kappa_3\cos\theta & i\tilde{\kappa}_2\\ (\kappa_3\tilde{\kappa}_2/\tilde{k})\sin\theta & -(\kappa_3\tilde{\kappa}_2/\tilde{k})\cos\theta & \tilde{\kappa}_2/k^2\\ (i\kappa_3^2/\tilde{k})\sin\theta & i(\tilde{\kappa}_3/k)\cos\theta & i\tilde{\kappa}_3\tilde{\kappa}_2/k^2\end{bmatrix},$$

where $$\tilde{\kappa}_2 = -\kappa_1\sin\theta+\kappa_2\cos\theta, \quad \tilde{k}^2 = \kappa_3^2+\tilde{\kappa}_2^2.$$

$M_{il}^{(q)}$ can now be calculated from (5.31) or (5.43) using its definition in (4.32).

To calculate $M_{il}^{(s)}$ when $k \gg 1$, we recalculate the solution to (4.22), rather than use the asymptotic form of the Fourier series solution (4.26) and (4.27). The boundary conditions (4.23) for β_i at a point $(r = 1, \theta)$ can be expressed in terms of the distance $\eta = \theta - \theta_0$ from a point θ_0, so that on $r = 1$,

$$\partial\beta_i/\partial r = (\cos\theta_0, \sin\theta_0, 0)\exp\{i(\kappa_1\cos\theta_0 + \kappa_2\sin\theta_0)\}\exp\{i\tilde{\kappa}_2\eta\}.$$

Thence the solution to (4.22) for β_i is

$$\beta_i(\xi, \theta) = -\tilde{k}^{-1}(\cos\theta, \sin\theta, 0)\exp\{i(\kappa_1\cos\theta + \kappa_2\sin\theta) - \tilde{k}\xi\},$$

where $\tilde{\kappa}_2$ and $\tilde{k}$ are defined in (5.43). From its definition in (4.29),

$$\tilde{M}_{il}^{(s)} = \begin{bmatrix} -\cos\theta & -\sin\theta & 0 \\ (i\tilde{\kappa}_2/\tilde{k})\cos\theta & -(i\tilde{\kappa}_2/\tilde{k})\sin\theta & 0 \\ (i\kappa_3/\tilde{k})\cos\theta & (i\kappa_3/\tilde{k})\sin\theta & 0 \end{bmatrix} \exp\{i(\kappa_1\cos\theta + \kappa_2\sin\theta) - \tilde{k}\xi\}. \quad (5.44)$$

Clearly $\tilde{M}_{il}^{(s)}$ is exponentially small when $k\xi \gg 1$.

The complete expression for M_{il} defined by (4.32), when $k \gg 1$, can now be found from (5.31) or (5.43) and (5.44). When $k\xi = O(1)$, the expression is too lengthy to be comprehended, but when $k\xi \gg 1$, we can ignore $M_{il}^{(s)}$ and we find that

$$M_{in} = -\epsilon_{lmn}\epsilon_{ijk}\left[\frac{\kappa_m\chi_j\gamma_{kl}}{\chi^2}\exp\{i[\kappa_1(x+\Delta_T) + \kappa_2(y-\Delta_y)]\}\right.$$
$$\left. - \frac{\kappa_m\kappa_j}{k^2}\delta_{kl}\exp\{i(\kappa_1 x + \kappa_2 y)\}\right] + \delta_{in}\exp\{i(\kappa_1 x + \kappa_2 y)\}, \quad (5.45a)$$

where χ_j and χ are defined in (5.27) and (5.30). Contracting the tensors and using the result from the continuity equation that $\kappa_n S_{\infty n} = 0$, so that any term like $\lambda\kappa_i\kappa_n$ gives no contribution to $\hat{\bar{u}}_i$, we find

$$M_{in} = -\epsilon_{lmn}\epsilon_{ijk}\kappa_m\chi_j\gamma_{kl}\exp\{i[\kappa_1(x+\Delta_T) + \kappa_2(y-\Delta_y)]\}/\chi^2. \quad (5.45b)$$

Some special cases are given below, and will be used in § 6 to calculate spectra etc., and used in § 5.3.3 to discuss the physical meaning of the results.

Consider the case of M_{1n} when $\kappa_1 = 0$. Then the integral (5.38) can be performed *exactly*, whence on $\theta = \pi$, if $\xi \ll 1$,

$$\left.\begin{aligned} M_{11} = \tfrac{1}{4}\kappa_3 f(\kappa_3\xi), \quad M_{12} = M_{13} = 0, \\ \text{and} \qquad M_{2j} = o(\xi), \end{aligned}\right\} \quad (5.46a)$$

where $f(b) = e^b E_1(b) + e^{-b}E_i(b)$, $E_1(b)$ and $E_i(b)$ being exponential integrals (see Abramowitz & Stegun 1964, p. 228). The expression agrees with that derived from (5.41) and (5.42), given the properties of $\Gamma(-\frac{1}{2}i\kappa_1)$ as $\kappa_1 \to 0$. We find that, as $k\xi \to 0$,

$$M_{11} \sim -\tfrac{1}{2}\kappa_3\xi[\ln(\kappa_3\xi) + \gamma - 1 + \ldots], \quad (5.46b)$$

but as $k\xi \to \infty$, $M_{11} \sim 1/(2\xi) = 1/U_1$, in agreement with (5.45*a*).

It is interesting to calculate $\tilde{M}_{2n}(r=1,\theta)$, a component of velocity *parallel* to the surface at the surface. We find

$$\tilde{M}_{2n} = i\exp\{i[\kappa_1\{1-\tfrac{1}{2}\ln 2-\ln(\sin\tfrac{1}{2}\theta)+\tfrac{1}{2}\ln\tilde{\chi}\}+\phi]\}\exp\{\tfrac{1}{2}\kappa_1\phi\}\,\Gamma(1-\tfrac{1}{2}i\kappa_1)/\tilde{\chi} \times \begin{bmatrix} i\kappa_3^2(1+\cos\theta)/2\tilde{\chi}_{23}\sin\theta+\kappa_2 \\ \kappa_1 \\ -i\kappa_1\kappa_3(1+\cos\theta)/2\tilde{\chi}_{23}\sin\theta \end{bmatrix}, \dagger \quad (5.47)$$

where $$\phi = \tan^{-1}(\tilde{\chi}_1/\tilde{\chi}_{23}), \quad \tilde{\chi}_1 = 2\kappa_2\sin\theta+\tfrac{1}{4}\kappa_1(4\cos\theta+1),$$

$$\tilde{\chi}_{23} = [\tfrac{1}{4}(\kappa_3^2+\kappa_1^2\cot^2\tfrac{1}{2}\theta)]^{\frac{1}{2}}, \quad \tilde{\chi} = (\tilde{\chi}_{23}^2+\tilde{\chi}_1^2)^{\frac{1}{2}}.$$

Thus on $\theta=\pi$, $\tilde{\chi}_1<0$ and therefore, since

$$\Gamma\left(1-\frac{i\kappa_1}{2}\right) \sim \frac{i\kappa_1^{\frac{1}{2}}\exp\{-\frac{1}{4}\pi\kappa_1\}}{2\sqrt{\pi}}\exp\{-i(\tfrac{1}{2}\kappa_1(\ln\tfrac{1}{2}\kappa_1-1)+\tfrac{1}{4}\pi)\} \quad \text{as} \quad \kappa_1\to\infty, \quad (5.48)$$

$$\tilde{M}_{2n} = O(\kappa_1^{\frac{3}{2}}e^{-\frac{1}{4}\pi\kappa_1}) \quad \text{on} \quad \theta=\pi \quad \text{as} \quad \kappa_1\to\infty. \quad (5.49)$$

Thus an exponential 'cut-off' occurs as κ_1 increases, which has significant practical consequences, to be seen later. This 'cut-off' also applies to $\tilde{M}_{1n}$ and $\tilde{M}_{3n}$.

For pressure calculations and comparison with the computed solutions it is useful to have the full expression for $\tilde{M}_{in}$ on $\theta=\pi$ when $k\xi\gg 1$ written out from (5.45*a*) (before contraction). We find

$$M_{in} = \frac{e^{i\kappa_1 x}}{k^2}\begin{bmatrix}\kappa_1^2\\ \kappa_1\kappa_2\\ \kappa_1\kappa_3\end{bmatrix} + \frac{e^{i\kappa_1(x+\Delta T)}}{\chi^2}\begin{bmatrix}\kappa_3^2/U_1+\kappa_2^2U_1\\ -\kappa_1\kappa_2U_1\\ -\kappa_1\kappa_3/U_1\end{bmatrix}, \quad (5.50)$$

$$M_{2n} = \frac{e^{i\kappa_1 x}}{k^2}\begin{bmatrix}\kappa_1\kappa_2\\ \kappa_2^2\\ \kappa_2\kappa_3\end{bmatrix} + \frac{e^{i\kappa_1(x+\Delta T)}}{\chi^2}\begin{bmatrix}-\kappa_1\kappa_2/U_1\\ \kappa_1^2/U_1+\kappa_3^2U_1\\ -\kappa_2\kappa_3U_1\end{bmatrix}, \quad (5.51)$$

where $\chi^2=\kappa_1^2/U_1^2+\kappa_2^2U_1^2+\kappa_3^2$, $k^2=\kappa_i\kappa_i$ and $U_1=1-1/r^2$. Thus when $r\to\infty$, $M_{in}\to\delta_{in}e^{i\kappa_1 x}$ as demanded by the boundary conditions. When $r\to 1$ and $\kappa_1=0$, (5.50) matches with (5.46) because as $\kappa_3\xi\to\infty$,

$$M_{11}\sim 2/\xi = 1/U_1.$$

5.3. *Discussion of solution for M_{ij}*

Before calculating the velocity spectra in §6, it is appropriate at this stage to consider various aspects of our results for M_{ij}; first, the validity of the solutions and whether they are consistent with the original assumptions, of §2; second, a comparison between the computed and asymptotic solutions; and third, the interesting features of the results and their physical explanation.

† On $\theta=\pi$ in the particular limit $\kappa_2\to\infty$, $\kappa_3\to 0$, $\kappa_1\to 0$ the expression (5.47) for $\tilde{M}_{2n}$ is singular and is invalid. The reason is that the approximation in (5.40*a*) that $\tilde{\chi}_{23}(\xi,\theta_0)=\tilde{\chi}_{23}(0,\theta_0)$ is always valid if (5.39) is satisfied, except in this particular limit. When this approximation is not valid, the integral (5.38) must be evaluated numerically. But we can deduce that for the particular case $\kappa_3=\kappa_1=0$, $\tilde{M}_{2n}=O(\kappa_2^{\frac{1}{2}})$.

5.3.1. *Validity of the solutions.* Given the artificial nature of the boundary conditions to the mathematical problem (2.4) and (2.5), which will be discussed in §7.2, the most important question about the mathematical validity of the solution is whether the nonlinear inertial terms and viscous terms omitted from (2.17) and (2.19) are in fact negligible. Consider first the effect of nonlinear terms in (2.17) on the mean velocity and vorticity in (2.17).

The largest inertial term omitted is $\beta^2\,\overline{(\mathbf{u}.\nabla)\boldsymbol{\omega}}$, which, as shown by the results for small-scale turbulence in §5.2, becomes at a distance ξ from the surface of order β^2/ξ^2. Therefore $\tilde{\Omega}_2$ becomes $O(\beta^2/\xi)$, so that when $\xi = O(\beta^2)$ the solution (2.18) and the assumption in (2.19) that $\boldsymbol{\Omega} = 0$ are both invalidated. However, if $\tilde{\Omega}_2 = O(\beta^2/\xi)$ as $\xi \to 0$, then from (2.4) $U_z = O(-\beta^2 \ln \xi)$. These changes in $\boldsymbol{\Omega}$ and $\mathbf{U}$ bring new terms into (2.19) like $\Omega_y\,\partial\mathbf{u}/\partial y$, of $O(\beta^2(a/l)\,\xi^{-1})$, and $U_z\,\partial\boldsymbol{\omega}/\partial z$, of $O(\beta^2(a/l)\,\xi^{-1}\ln\xi)$. In deriving (2.19) turbulent nonlinear terms like $(\boldsymbol{\omega}.\nabla)\,\mathbf{u}$ were assumed to be small everywhere. Consider the order of magnitude of this term near the surface of the body as $\xi \to 0$, when $a/l \gg 1$. It is difficult to estimate, even given the r.m.s. values of $\mathbf{u}$, but it is unlikely that the largest term $(\omega_y\partial/\partial y)\,\mathbf{u}$ is greater than $O[\beta\xi^{-1}(a/l)]$. Compare this with the order of magnitude of the linear terms in (2.19) as $\xi \to 0$; when $\kappa_1 = O(1)$, $D\tilde{\omega}_1/Dt$ and $D\tilde{\omega}_3/Dt$ are $O(a^2/l^2)$ and $D\tilde{\omega}_2/Dt$ is $O((a/l)\,\xi^{-1})$; when $\kappa_1 \gg 1$, $D\tilde{\omega}_1/Dt$ and $D\tilde{\omega}_3/Dt$ are $O(\kappa_1(a/l))$ and $D\tilde{\omega}_2/Dt$ is $O(\kappa_1\xi^{-1})$. Thus as $\xi \to 0$ for $\kappa_1 = O(a/l)$, $|D\boldsymbol{\omega}/Dt|$ calculated from (2.19) is $O(\xi^{-1}(a/l))$, whereas the magnitude of the largest nonlinear terms which have been neglected is $O(\beta\xi^{-1}(a/l))$. Therefore, since we assume $\beta \ll 1$, the nonlinear effects do not become dominant near the body. The reason for this surprising result is that although the potential solution has the property $\mathbf{n}.\mathbf{U} \to 0$ as $\xi \to 0$, $\partial U_y/\partial y$ remains $O(1)$, and therefore despite the fact that $|\mathbf{u}| \gg |\mathbf{U}|$ in this region, the stretching of the vortex lines by the mean velocity continues to be $O(\beta^{-1})$ greater than the stretching by the turbulent velocity. However, the equations for two components of $\boldsymbol{\omega}$ in (2.19) contain nonlinear terms which cannot be ignored as $\xi \to 0$, so that our results for ω_1 and ω_3 in (3.10) are only valid as $\xi \to 0$ for $\kappa_1 = O(1)$ if $\xi \gg \alpha$ and for $\kappa_1 \gg 1$ if $\xi \gg \beta\kappa_1^{-1}$. It is not clear how these errors in $\tilde{\omega}_1$ and $\tilde{\omega}_3$ affects the validity of our results for $\tilde{M}_{1n}$ and $\tilde{M}_{2n}$ for small-scale turbulence as $\xi \to 0$. Since the body $\tilde{M}_{3n}$ is largely determined by the amplification of $\tilde{\omega}_2$, our expressions for $\tilde{M}_{3n}$ should be correct as $\xi \to 0$ provided that $\beta \ll 1$. For scales of turbulence comparable or larger than the size of the body the analysis is valid as $\xi \to 0$ provided that the original conditions (2.7)–(2.10) are satisfied.

The viscous terms were examined in terms of the r.m.s. values of the vorticity in §2, but now that it is known how the Fourier components of $\boldsymbol{\omega}$ vary, it is possible to be more precise in our criteria for neglecting these terms. From the Fourier transform of ω_y given by (4.2), we see that the viscous term $Re^{-1}\,\partial^2\omega_y/\partial x^2$ is $O(Re^{-1}/\xi^3)$ if κ_1 is $O(1)$, but is $O(Re^{-1}\kappa_1^2/\xi^3)$ if $\kappa_1 \gg 1$. Thence by comparing with the term $(\boldsymbol{\omega}.\nabla)\,\mathbf{U}$ it follows that the viscous terms are only negligible if

$$\xi \gg Re^{-\frac{1}{2}}, \quad \text{when} \quad \kappa_1 = O(1) \quad \text{or} \quad \kappa_1 \ll 1, \tag{5.52a}$$

and if

$$\xi \gg \kappa_1^{\frac{1}{2}} Re^{-\frac{1}{2}}, \quad \text{when} \quad \kappa_1 \gg 1. \tag{5.52b}$$

Equation (5.52a) implies that if the turbulence has an integral scale of order a over most of the wavenumber range, the theoretical solutions for M_{il} should be valid right up to the stagnation-point boundary layer. On the other hand, for very small-scale turbulence or high wavenumbers, the region of validity does not extend as far as this boundary layer. Both these results imply that as $Re \to \infty$ the range of validity of the solution comes closer to the body.

Less fundamental questions concern the range of validity in wavenumber space of the computed and asymptotic solutions. The computed solution described in §§4.1 and 4.3 has two main limitations. (i) When $\kappa_3 \to 0$ and $r = O(1)$ there should be a contribution to integrals like (4.10) from the region where $r \gg 1$, and therefore, since Ω_{ij} is assumed to be zero for $r > 10$ the value of α_{ij} and therefore $M_{in}^{(d)}$ must be incorrect for $\kappa_2 \lesssim 0{\cdot}1$. But $M_{in}^{(s)}$ is correct as $\kappa_3 \to 0$, and since $M_{in}^{(d)} = O(k)$ as $k \to 0$, computed solutions for M_{in} should be correct to a good approximation. (ii) When $\kappa_1, \kappa_2 \gg 1$, then the representation of Ω_{ij} and β_j as finite Fourier series with $n \leqslant 20$ becomes inaccurate. Thus our particular computations for M_{in} should be valid when κ_1, $\kappa_2 \lesssim 3$. The asymptotic solution for M_{in} when $k\xi \ll 1$ and $\xi \ll 1$ is, as stated in (5.39), only valid when $\kappa_1 \ll \tilde{\chi}$. This limitation is not, in fact, serious because when Θ_{ii} is evaluated, in §6, it will be found that this is the only range of wavenumber space of interest.

5.3.2. *Comparison with computed solutions.* In tables 1 and 2 the computed results for M_{in} are tabulated alongside values obtained from the asymptotic expressions for M_{in} in §§5.1.1 and 5.2.1. In the case where $k \ll 1$, M_{in} is valid to $O(k^2 \ln k)$. The three components of M_{in} have been grouped as $M_{in}^{(d)}$ and

$$M_{in}^{(s)} + M_{in}^{(\infty)}$$

in order to show how the relative magnitudes of these components vary as k increases. Detailed examination shows that, when $k \ll 1$, the small differences between the computed and asymptotic values of M_{in} are attributable to the differences in $M_{in}^{(d)}$ caused by the truncation of the computed integrals, as described in §5.3.1. The general conclusion to be drawn from these tables is that the asymptotic and computed solutions have the same qualitative trends as $\boldsymbol{\kappa}$ and (r, θ) vary, and also give results which are approximately equal when $k \lesssim 0{\cdot}3$ or $k \gtrsim 3{\cdot}0$. This implies that gross arithmetic or analytical errors have probably been avoided in the various solutions. It also implies that, in the region of wavenumber space where $3{\cdot}0 \gtrsim k \gtrsim 0{\cdot}3$ and where the asymptotic theory is not valid, the computed solutions should be fairly reliable.

5.3.3. *Physical implications.* We now attempt to find some physical meaning from all our computation and analysis, and begin by showing in figures 6(a)–(d) how M_{in} varies along a radius at $\theta = \pi$ and $\theta = 3\pi$, when $k \ll 1$, $k \sim 1$ and $k \gg 1$, using the results of §§5.1.1 and 5.2.1. In the case $k \gg 1$, the choice $\kappa_1 = \kappa_2 = 0$ is made to avoid the rapid oscillation in M_{in}, and because this part of the spectrum is of greatest interest.

Figures 6(a) and (b) show how for low wavenumbers of the turbulence, along the stagnation line, M_{11} decreases to zero and M_{22} increases to twice its incident value. M_{33} in fact remains constant. On the other hand, for high wavenumbers,

(*a*) $\kappa_1 = \kappa_2 = 0{\cdot}1, \quad r = 1{\cdot}1$

	Computed			Asymptotic
$\kappa_3 = 0{\cdot}1$	$M_{in}^{(d)}$	$M_{in}^{(s)} + M_{in}^{(\infty)}$	M_{in}	$M_{in}(k \to 0)$
$i, n = 1, 1$	0·00, 0·00	0·17, −0·03	0·17, −0·03	0·17, −0·03
1, 2	0·00, 0·00	0·00, 0·01	0·00, 0·01	0·00, 0·01
1, 3	0·00, 0·00	0·00, 0·00	0·00, 0·00	0·00, 0·00
2, 1	0·01, −0·05	0·00, −0·04	0·00, −0·09	0·03, −0·13
2, 2	−0·02, 0·05	1·80, −0·15	1·77, −0·06	1·77, −0·06
2, 3	0·02, 0·00	0·00, 0·00	0·02, 0·00	0·00, 0·00
$\kappa_3 = 0{\cdot}3$				
1, 1	0·01, 0·00	0·17, −0·03	0·18, −0·02	0·16, −0·03
1, 2	0·00, 0·00	0·00, 0·01	0·00, 0·01	0·00, 0·01
1, 3	0·00, 0·00	0·00, 0·00	0·00, 0·00	0·00, 0·00
2, 1	0·00, −0·05	−0·00, −0·04	0·01, −0·09	0·00, −0·13
2, 2	−0·10, 0·07	1·71, −0·15	1·61, −0·09	1·70, −0·06
2, 3	0·03, −0·01	0·00, 0·00	0·03, −0·01	0·00, 0·00
$\kappa_3 = 1{\cdot}0$				
1, 1	0·09, 0·01	0·19, −0·03	0·26, −0·02	
1, 2	0·00, 0·00	0·00, 0·00	0·00, 0·00	
1, 3	0·01, 0·00	0·00, 0·00	−0·01, 0·00	
2, 1	0·00, −0·04	0·00, −0·03	0·00, −0·07	
2, 2	−0·36, 0·10	1·45, −0·14	1·08, −0·04	
2, 3	0·04, −0·01	0·00, 0·00	0·04, −0·01	
$\kappa_3 = 1.6$				$M_{in}\ (k \to \infty,\ k\xi \ll 1)$
1, 1	0·20, 0·02	0·22, −0·03,	0·42, −0·02	0·40, 0·00
1, 2	0·00, 0·00	0·00, 0·004	0·00, 0·00	0·00, 0·00
1, 3	−0·01, 0·00	0·00, 0·00	−0·01, 0·00	0·02, 0·00
2, 1	0·00, −0·03	0·00, −0·03	0·00, −0·05	0·00, 0·00
2, 2	−0·49, 0·11	1·32, −0·14	0·83, −0·02	1·24, −0·01
2, 3	0·03, −0·01	0·00, 0·00	0·03, −0·01	−0·02, 0·00
$\kappa_3 = 3{\cdot}0$				
1, 1	0·56, 0·04	0·31, −0·04	0·87, 0·00	0·92, 0·02
1, 2	0·00, 0·00	0·00, 0·00	0·00, 0·00	0·00, 0·00
1, 3	−0·02, 0·00	0·00, 0·00	−0·02, 0·00	−0·02, 0·00
2, 1	0·00, −0·01	0·00, −0·02	0·00, −0·03	0·00, −0·02
2, 2	−0·64, 0·12	1.17, −0·13	0·53, 0·00	0·67, −0·03
2, 3	0·02, 0·00	0·00, 0·00	0·02, 0·00	0·01, 0·00
$\kappa_3 = 5{\cdot}0$				
1, 1	1.14, 0·09	0·43, −0·05	1·57, 0·03	1·67, 0·06
1, 2	0·00, 0·00	0·00, 0·00	0·00, 0·00	0·00, 0·00
1, 3	−0·02, 0·00	0·00, 0·00	−0·02, 0·00	−0·03, 0·00
2, 1	0·00, −0·01	0·00, −0·01	0·00, −0·02	0·00, −0·01
2, 2	−0·72, 0·12	1·09, −0·12	0·37, 0·00	0·40, 0·00
2, 3	0·01, 0·00	0·00, 0·00	0·01, 0·00	0·01, 0·00

TABLE 1(*a*). For legend see page 665.

(*b*) $\kappa_1 = \kappa_2 = 0{\cdot}1$; $r = 2{\cdot}0$, $\theta = \pi$

	Computed			Asymptotic
$\kappa_3 = 0{\cdot}1$	$M_{in}^{(d)}$	$M_{in}^{(s)} + M_{in}^{(\infty)}$	M_{in}	M_{in} $(k \to 0)$
$i, n = 1, 1$	0·00, 0·00	0·73, −0·17	0·73, −0·17	0·73, −0·17
1, 2	0·01, 0·00	0·00, 0·02	0·01, 0·02	0·01, 0·02
1, 3	0·00, 0·00	0·00, 0·00	0·00, 0·00	0·00, 0·00
2, 1	0·00, −0·03	0·00, −0·01	0·00, −0·03	0·02, −0·06
2, 2	−0·01, 0·03	1·22, −0·20	1·21, −0·17	1·21, −0·16
2, 3	0·01, −0·02	0·00, 0·00	0·01, 0·00	0·00, 0·00
$\kappa_3 = 0{\cdot}03$				
1, 1	0·02, 0·01	0·73, −0·17	0·75, −0·16	0·69, −0·17
1, 2	0·00, 0·00	0·00, 0·02	0·00, 0·01	0·01, 0·02
1, 3	−0·01, 0·00	0·00, 0·00	−0·01, 0·00	0·00, 0·00
2, 1	0·00, −0·03	0·00, −0·01	0·00, −0·04	0·01, −0·06
2, 2	−0·05, 0·04	1·17, −0·20	1·12, −0·16	1·13, −0·16
2, 3	0·02, 0·00	0·00, 0·00	0·02, 0·00	0·00, 0·00
$\kappa_3 = 1{\cdot}0$				
1, 1	0·15, 0·02	0·80, −0·18	0·96, −0·17	
1, 2	0·00, −0·01	0·00, 0·01	0·00, 0·00	
1, 3	−0·02, 0·00	0·00, 0·00	0·02, 0·00	
2, 1	0·00, −0·02	0·00, 0·00	0·00, −0·02	
2, 2	−0·17, 0·07	1·05, −0·02	0·88, −0·14	
2, 3	0·02, −0·01	0·00, 0·00	0·02, −0·01	
$\kappa_3 = 1{\cdot}6$				$M_{in}(k \to \infty, k\xi \gg 1)$
1, 1	0·26, 0·02	0·87, −0·19	1·13, −0·17	1·31, −0·19
1, 2	0·00, −0·01	0·00, 0·00	0·00, 0·00	0·00, 0·00
1, 3	−0·02, 0·00	0·00, 0·00	−0·02, 0·00	−0·02, 0·00
2, 1	0·00, −0·012	0·00, +0·00	−0·00, −0·01	0·00, 0·00
2, 2	−0·21, 0·08	1·01, −0·20	0·80, −0·12	0·74, −0·11
2, 3	0·01, 0·00	0·00, 0·00	0·01, 0·00	0·01, 0·00
$\kappa_3 = 3{\cdot}0$				
1, 1	0·36, 0·01	0·95, −0·20	1·31, −0·19	1·32, −0·19
1, 2	0·00, 0·00	0·00, 0·00	0·00, 0·00	0·00, 0·00
1, 3	−0·01, 0·00	0·00, 0·00	−0·01, 0·00	−0·01, 0·00
2, 1	0·00, −0·01	0·00, 0·00	0·00, −0·01	0·00, 0·00
2, 2	−0·24, 0·09	0·99, −0·20	0·75, −0·11	0·74, −0·11
2, 3	0·01, 0·00	0·00, 0·00	0·01, 0·00	0·00, 0·00
$\kappa_3 = 5{\cdot}0$				
1, 1	0·40, −0·01	0·98, −0·20	1·38, −0·20	1·32, −0·19
1, 2	0·00, 0·01	0·00, 0·00	0·00, 0·01	0·00, 0·00
1, 3	−0·01, 0·00	0·00, 0·00	−0·01, 0·00	−0·01, 0·00
2, 1	0·00, 0·00	0·00, 0·00	0·00, 0·00	0·00, 0·00
2, 2	−0·24, 0·09	0·98, −0·20	0·74, −0·11	0·74, −0·11
2, 3	0·01, 0·00	0·00, 0·00	0·01, 0·00	0·01, 0·00

TABLE 1(*b*). For legend see page 665.

(*c*) $\kappa_1 = \kappa_2 = 1{\cdot}0$, $r = 1{\cdot}1$, $\theta = \pi$

	Computed			Asymptotic
$\kappa_3 = 0{\cdot}1$	$M_{in}^{(d)}$	$M_{in}^{(s)} + M_{in}^{(\infty)}$	M_{in}	$M_{in}(k \to \infty, k\xi \ll 1)$
$i, n = 1, 1$	0·04, 0·03	0·00, −0·20	0·04, −0·17	−0·02, −0·06
1, 2	−0·04, −0·03	0·03, 0·05	−0·01, 0·02	−0·02, −0·06
1, 3	−0·01, 0·00	0·00, 0·00	−0·01, 0·00	−0·01, 0·00
2, 1	−0·02, −0·79	−0·31, −0·24	−0·33, −1·03	−1·32, −0·85
2, 2	0·02, 0·79	0·90, −0·17	0·93, −0·28	0·95, −0·49
2, 3	−0·01, −0·01	0·00, 0·00	−0·01, −0·01	0·69 −0·43
$K_3 = 1{\cdot}0$				
1, 1	0·14, 0·07	0·01, −0·23	0·15, −0·16	0·11, −0·08
1, 2	−0·04, −0·04	0·03, 0·03	−0·01, −0·01	−0·01, −0·05
1, 3	−0·10, −0·03	0·00, 0·00	−0·01, −0·03	−0·12, −0·03
2, 1	−0·05, −0·59	−0·23, −0·19	−0·27, −0·78	−0·73, −0·80
2, 2	0·09, 0·82	0·71, −1·12	0·80, −0·30	0·32, −0·76
2, 3	−0·04, −0·23	0·00, 0·00	−0·04, −0·23	0·35, 0·34
$\kappa_3 = 3{\cdot}0$				
1, 1	0·62, 0·33	0·08, −0·32	0·70, +0·01	0·71, 0·12
1, 2	−0·02, −0·03	0·01, 0·01	−0·01, −0·02	0·01, −0·03
1, 3	−0·20, −0·10	0·00, 0·00	−0·02, −0·10	−0·22, −0·13
2, 1	0·03, −0·28	−0·12, −0·09	−0·09, −0·37	−0·09, −0·29
2, 2	−0·04, 0·98	0·55, −1·01	0·51, −0·04	0·50, −0·26
2, 3	−0·03, −0·23	0·00, 0·00	−0·04, −0·23	−0·05, −0·16

(*d*) $\kappa_1 = \kappa_2 = 1{\cdot}0$; $r = 2{\cdot}0$, $\theta = \pi$

$K_3 = 0{\cdot}1$				$M_{in}(k \to \infty, k\xi \gg 1)$
$i, n = 1, 1$	0·20, −0·02	−0·56, −0·67	−0·36, −0·69	−0·17, −0·77
1, 2	−0·19, 0·02	0·04, 0·14	−0·15, 0·15	−0·25, −0·14
1, 3	−0·03, 0·03	0·00, 0·00	−0·03, 0·03	−0·03, 0·01
2, 1	−0·40, −0·10	−0·06, −0·04	−0·46, −0·15	−0·28, 0·11
2, 2	0·40, 0·10	−0·28, −0·95	0·12, −0·85	−0·14, −1·02
2, 3	−0·21, 0·36	0·00, 0·00	−0·21, 0·36	−0·02, −0·01
$\kappa_3 = 1{\cdot}0$				
1, 1	0·36, −0·13	−0·52, −0·78	−0·16, −0·91	−0·06, −0·92
1, 2	−0·17, −0·02	0·03, 0·05	−0·14, 0·03	−0·17, −0·08
1, 3	−0·19, 0·15	0·00, 0·00	−0·19, 0·15	−0·19, 0·09
2, 1	−0·33, −0·05	−0·02, −0·02	−0·32, −0·08	−0·19, 0·09
2, 2	0·44, 0·99	−0·38, −0·93	0·09, −0·85	−0·06 −0·92
2, 3	−0·12, −0·04	0·00, 0·00	−0·12, −0·04	−0·17, −0·08
$\kappa_3 = 3{\cdot}0$				
1, 1	0·58, −0·30	−0·43, −0·89	0·15, −1·19	0·10, −1·20
1, 2	−0·07, −0·04	0·00, 0·00	−0·06, −0·03	−0·05, −0·02
1, 3	−0·17, 0·11	0·00, 0·00	−0·17, 0·11	−0·16, 0·10
2, 1	−0·14, −0·03	0·00, 0·00	−0·14, 0·02	−0·05, 0·03
2, 2	0·50, 0·13	−0·41, −0·91	0·08, −0·78	0·05, −0·79
2, 3	−0·12, −0·04	0·00, 0·00	−0·12, −0·04	−0·14, −0·05

TABLE 1. A comparison of computed and asymptotic values for M_{in} at $\theta = \pi$. The two numbers for M_{in} at each value of $(\kappa_1, \kappa_2, \kappa_3)$ are the real and imaginary parts.

(a) $\kappa_1 = \kappa_2 = 0{\cdot}1$; $r = 1{\cdot}1$

$\kappa_3 = 0{\cdot}1$	Computed $M_{in}^{(d)}$	Computed $M_{in}^{(s)} + M_{in}^{(\infty)}$	Computed M_{in}	Asymptotic M_{in} $(k \to 0)$
$i, n = 1, 1$	−0·01, −0·03	0·99, −0·02	0·98, −0·05	0·99, −0·09
1, 2	0·00, 0·03	0·81, 0·03	0·81, 0·06	0·81, 0·10
1, 3	0·01, 0·00	0·00, 0·00	0·01, 0·00	0·00, 0·00
2, 1	−0·01, −0·03	0·81, −0·03	0·81, −0·06	0·82, −0·10
2, 2	0·00, 0·03	0·99, 0·02	0·98, 0·05	0·99, 0·09
2, 3	0·01, 0·00	0·00, 0·00	0·01, 0·00	0·00, 0·00
$\kappa_3 = 0{\cdot}3$				
1, 1	−0·02, −0·03	0·94, −0·02	0·92, −0·05	0·94, −0·09
1, 2	−0·04, 0·03	0·77, 0·03	0·73, 0·07	0·78, 0·10
1, 3	0·02, 0·00	0·00, 0·00	0·02, 0·00	0·00, 0·00
2, 1	−0·03, −0·03	0·77, −0·03	0·74, −0·06	0·78, −0·10
2, 2	−0·05, 0·04	0·94, 0·02	0·09, 0·06	0·94, 0·09
2, 3	0·03, 0·00	0·00, 0·00	0·03, 0·00	0·00, 0·00
$\kappa_3 = 1{\cdot}0$				
1, 1	−0·06, −0·01	0·82, −0·02	0·76, −0·03	
1, 2	−0·19, 0·03	0·63, 0·02	0·44, 0·05	
1, 3	0·02, 0·00	0·00, 0·00	0·02, 0·00	
2, 1	−0·19, −0·02	0·63, −0·02	0·45, 0·04	
2, 2	−0·18, 0·03	0·82, 0·02	0·54, 0·05	
2, 3	0·04, 0·00	0·00, 0·00	0·03, 0·00	
$\kappa_3 = 1{\cdot}6$				M_{in} $(k \to \infty, k\xi \ll 1)$
1, 1	−0·04, 0·00	0·77, −0·01	0·73, −0·01	0·54, −0·01
1, 2	−0·27, 0·02	0·55, 0·02	0·28, 0·04	0·48, 0·00
1, 3	0·02, 0·00	0·00, 0·00	0·02, 0·00	0·00, 0·00
2, 1	−0·33, −0·02	0·55, −0·02	0·22, −0·04	0·04, −0·04
2, 2	−0·23, 0·03	0·77, 0·01	0·55, 0·04	0·77, 0·01
2, 3	0·03, 0·00	0·00, 0·00	0·03, 0·00	0·01, 0·00
$\kappa_3 = 3{\cdot}0$				
1, 1	0·13, 0·03	0·74, −0·01	0·87, 0·02,	0·88, 0·04
1, 2	−0·38, 0·01	0·43, 0·01	0·05, 0·02	0·08, −0·02
1, 3	0·01, 0·00	0·00, 0·00	0·01, 0·00	0·00, 0·00
2, 1	−0·64, −0·02	0·43, −0·01	−0·20, −0·04	−0·32, −0·04
2, 2	−0·26, 0·02	0·74, 0·01	0·48, 0·03	0·59, 0·01
2, 3	0·03, 0·00	0·00, 0·00	0·03, 0·00	0·02, 0·00
$\kappa_3 = 5{\cdot}0$				
1, 1	0·50, 0·07	0·76, 0·00	1·27, 0·06	1·36, 0·10
1, 2	−0·48, 0·00	0·33, 0·01	−0·15, 0·00	−0·17, −0·02
1, 3	0·00, 0·00	0·00, 0·00	0·00, 0·00	0·00, 0·00
2, 1	−1·07, −0·05	0·33, −0·01	−0·74, −0·06	−0·84, −0·08
2, 2	−0·25, 0·02	0·76, 0·00	0·41, 0·03	0·57, 0·02
2, 3	0·03, 0·00	0·00, 0·00	0·03, 0·00	0·03, 0·00

TABLE 2(a). For legend see page 669.

(*b*) $\kappa_1 = \kappa_2 = 0{\cdot}1$; $r = 2{\cdot}0$, $\theta = \frac{3}{4}\pi$

	Computed			Asymptotic
$\kappa_3 = 0{\cdot}1$	$M_{in}^{(d)}$	$M_{in}^{(s)} + M_{in}^{(\infty)}$	M_{in}	M_{in} $(k \to 0)$
$i, n = 1, 1$	−0·01, −0·02	0·99, 0·01	0·98, 0·01	0·98, −0·03
1, 2	0·01, 0·02	0·24, 0·02	0·25, 0·03	0·24, 0·05
1, 3	0·01, 0·00	0·00, 0·00	0·00, 0·00	0·00, 0·00
2, 1	−0·01, −0·02	0·24, −0·02	0·24, −0·04	0·26, −0·05
2, 2	−0·01, 0·02	0·99, −0·01	0·99, 0·01	0·98, 0·03
2, 3	0·01, 0·00	0·00, 0·00	0·01, 0·00	0·00, 0·00
$\kappa_3 = 0{\cdot}3$				
1, 1	−0·01, −0·01	0·97, 0·01	0·96, −0·01	0·94, −0·03
1, 2	−0·02, 0·01	0·22, 0·02	0·20, 0·03	0·23, 0·05
1, 3	0·01, 0·00	0·00, 0·00	0·01, 0·00	0·00, 0·00
2, 1	−0·03, −0·02	0·22, −0·01	0·19, −0·03	0·24, −0·05
2, 2	−0·03, 0·02	0·97, −0·01	0·94, 0·02	0·94, 0·03
2, 3	0·02, 0·00	0·00, 0·00	0·02, 0·00	0·00, 0·00
$\kappa_3 = 1{\cdot}0$				
1, 1	0·03, −0·01	0·94, 0·00	0·97, 0·00	
1, 2	−0·12, 0·01	0·12, 0·01	0·00, 0·01	
1, 3	0·01, 0·00	0·00, 0·00	0·01, 0·00	
2, 1	−0·17, −0·01	0·12, −0·01	−0·05, −0·02	
2, 2	−0·05, 0·02	0·94, 0·00	0·89, 0·02	
2, 3	0·02, 0·00	0·00, 0·00	0·02, 0·00	
$\kappa_3 = 3{\cdot}0$				M_{in} $(k \to \infty, k\xi \gg 1)$
1, 1	0·10, 0·00	0·99, 0·00	1·09, 0·00	1·08, 0·01
1, 2	−0·24, 0·00	0·02, 0·00	−0·22, 0·00	−0·25, 0·00
1, 3	0·00, 0·00	0·00, 0·00	0·00, 0·00	0·01, 0·00
2, 1	−0·33, 0·00	0·02, 0·00	−0·31, 0·00	−0·31, 0·00
2, 2	−0·01, 0·01	0·99, 0·00	0·98, 0·01	1·00, 0·01
2, 3	0·01, 0·00	0·00, 0·00	0·01, 0·00	0·01, 0·00
$\kappa_3 = 5{\cdot}0$				
1, 1	0·11, 0·00	1·00, 0·00	1·11, 0·00	1·08, 0·01
1, 2	−0·28, 0·01	0·00, 0·00	−0·28, 0·01	−0·25, 0·00
1, 3	0·00, 0·00	0·00, 0·00	0·00, 0·00	0·00, 0·00
2, 1	−0·34, 0·00	0·00, 0·00	−0·34, 0·00	−0·31, 0·00
2, 2	0·02, 0·00	1·00, 0·00	1·02, 0·00	1·00, 0·01
2, 3	0·01, 0·00	0·00, 0·00	0·01, 0·00	0·01, 0·00

TABLE 2(*b*). For legend see page 669.

when $\kappa_1 = 0$, M_{22} decreases and M_{11} increases as the body is approached, but of course within a distance $O(k^{-1})$ of the surface M_{11} has to decrease to zero.

When $\kappa_1 \gg 1$ analytical solutions show that the amplification of M_{11} is greatly reduced and M_{22} increases slightly. M_{33} has not been plotted because, when $k \to 0$ and when $\kappa_3 \gg 1$ and $\kappa_1 = \kappa_2 = 0$, there is no change from its upstream value; $|M_{33}| = 1$ for $-\infty < x < -1$. For intermediate values of k it will be different.

In figures 6(*c*) and (*d*) graphs of $|M_{11}|$ and $|M_{22}|$ are given on the line $\theta = \frac{3}{4}\pi$. Now the differences in behaviour between high and low wavenumbers are very

(c) $\kappa_1 = \kappa_2 = 1{\cdot}0$; $r = 1{\cdot}1$, $\theta = \frac{3}{4}\pi$

$\kappa_3 = 0{\cdot}1$	Computed $M_{in}^{(d)}$	Computed $M_{in}^{(s)} + M_{in}^{(\infty)}$	Computed M_{in}	Asymptotic $M_{in}(k \to \infty, k\xi \ll 1)$
$i, n = 1, 1$	0·06, −0·29	0·81, −0·19	0·87, −0·48	1·23, −1·25
1, 2	−0·06, 0·29	0·61, 0·29	0·55, 0·58	−0·22, 0·43
1, 3	0·01, −0·01	0·00, 0·00	0·01, −0·01	−0·02, −0·45
2, 1	0·07, −0·31	0·61, −0·29	0·68, −0·60	1·20, −1·28
2, 2	−0·07, 0·31	0·81, 0·19	0·74, 0·50	−0·2, 0·46
2, 3	0·01, −0·01	0·00, 0·00	0·01, −0·01	−0·02, −0·45
$\kappa_3 = 0{\cdot}3$				
1, 1	0·07, −0·27	0·80, −0·19	0·87, −0·46	1·17, −1·15
1, 2	−0·08, 0·28	0·59, 0·28	0·51, 0·58	−0·13, 0·60
1, 3	0·02, −0·05	0·00, 0·00	0·02, −0·05	0·14, −0·99
2, 1	0·08, −0·30	0·59, −0·28	0·67, −0·58	1·12, −1·19
2, 2	−0·09, 0·31	0·80, 0·19	0·71, 0·50	−0·08, 0·65
2, 3	0·04, −0·05	0·00, 0·00	0·04, −0·05	−0·13, −0·99
$\kappa_3 = 1{\cdot}0$				
1, 1	0·08, −0·12	0·75, −0·17	0·83, −0·24	0·89, −0·59
1, 2	−0·14, 0·22	0·53, 0·23	0·39, 0·45	0·39, 0·49
1, 3	0·06, −0·10	0·00, 0·00	0·06, −0·10	−0·27, −0·59
2, 1	−0·01, −0·22	0·53, −0·23	0·52, −0·55	0·69, −0·73
2, 2	−0·13, 0·29	0·75, 0·17	0·62, 0·46	0·54, 0·59
2, 3	0·14, −0·07	0·00, 0·00	0·14, −0·07	−0·23, −0·54
$\kappa_3 = 1, 6$				
1, 1	0·08, 0·00	0·74, −0·14	0·82, −0·14	0·77, −0·21
1, 2	−0·21, 0·16	0·49, 0·19	0·28, 0·35	0·38, 0·15
1, 3	0·08, −0·10	0·00, 0·00	0·08, −0·10	−0·09, −0·30
2, 1	−0·13, −0·19	0·49, −0·19	0·36, −0·38	0·40, −0·48
2, 2	−0·18, 0·27	0·74, 0·14	0·56, 0·41	0·64, 0·28
2, 3	0·19, −0·05	0·00, 0·00	0·19, −0·05	−0·02, −0·21
$\kappa_3 = 3{\cdot}0$				
1, 1	0·13, 0·26	0·74, −0·09	0·87, 0·17	0·79, 0·29
1, 2	−0·35, 0·04	0·41, 0·12	0·06, 0·16	0·10, −0·11
1, 3	0·07, −0·10	0·00, 0·00	0·07, −0·10	0·04, −0·16
2, 1	−0·43, −0·26	0·41, −0·12	−0·02, −0·38	−0·05, −0·40
2, 2	−0·27, 0·24	0·74, 0·09	0·47, 0·33	0·55, 0·11
2, 3	0·23, 0·01	0·00, 0·00	0·23, 0·01	0·16, −0·01

TABLE 2(c). For legend see page 669.

much less than on the stagnation line $\theta = \pi$. In addition the differences between $|M_{11}|$ and $|M_{22}|$ are reduced. In fact $|M_{21}|$ is greater than $|M_{22}|$ and behaves like $|M_{11}|$.

Having seen the general way in which M_{in} varies with (r, θ) and k we now consider in more detail the physical mechanism involved and the asymptotic behaviour of M_{in} as $\xi(= r - 1) \to 0$ and $k \to 0$ or $k \to \infty$.

There are two ways in which the body affects the incident turbulent flow, as mentioned in § 1 and as implied mathematically by dividing M_{in} into the components $M_{in}^{(d)}$ and $M_{in}^{(s)}$.

(*d*) $\kappa_1 = \kappa_2 = 1{\cdot}0$; $r = 2{\cdot}0$, $\theta = \frac{3}{4}\pi$

	Computed			Asymptotic
$\kappa_3 = 0.1$	$M_{in}^{(d)}$	$M_{in}^{(s)} + M_{in}^{(\infty)}$	M_{in}	$M_{in}(k \to \infty,\ k\xi \gg 1)$
$i, n = 1, 1$	0·05, −0·08	0·94, 0·06	0·99, −0·02	1·09, 0·03
1, 2	0·05, 0·08	0·15, 0·14	0·20, 0·22	−0·09, −0·03
1, 3	−0·01, 0·00	0·00, 0·00	−0·01, 0·00	−0·02, 0·00
2, 1	0·01, −0·14	0·15, −0·14	0·16, −0·28	−0·21, −0·04
2, 2	−0·01, 0·14	0·94, −0·63	0·93, −0·49	−0·21, 0·04
2, 3	0·01, −0·01	0·00, 0·00	0·01, −0·01	−0·01, 0·00
$\kappa_3 = 0{\cdot}3$				
1, 1	0·03, −0·07	0·93, 0·05	0·96, −0·03	1·11, 0·4
1, 2	−0·03, 0·07	0·14, 0·12	0·11, 0·19	−0·09, −0·03
1, 3	−0·02, 0·00	0·00, 0·00	−0·02, 0·00	−0·05, −0·01
2, 1	−0·04, −0·14	0·14, −0·12	−0·18, −0·26	−0·20, −0·04
2, 2	0·03, 0·15	0·93, −0·05	0·96, 0·10	1·21, 0·04
2, 3	0·02, −0·04	0·00, 0·00	0·02, −0·04	−0·02, −0·01
$\kappa_3 = 1{\cdot}0$				
1, 1	0·11, −0·02	0·94, 0·02	0·95, 0·00	1·15, 0·05
1, 2	−0·09, 0·02	0·09, 0·06	0·00, 0·08	−0·10, −0·03
1, 3	−0·02, 0·00	0·00, 0·00	−0·02, 0·00	−0·05, −0·02
2, 1	−0·12, −0·11	0·09, −0·06	−0·03, −0·17	−0·19, −0·03
2, 2	0·04, 0·17	0·94, −0·02	0·98, 0·15	0·18, 0·05
2, 3	0·08, −0·06	0·00, 0·00	0·08, −0·06	0·01, −0·02
$\kappa_3 = 1{\cdot}6$				
1, 1	0·15, 0·01	0·96, 0·01	1·11, 0·02	1·14, 0·05
1, 2	−0·14, −0·13	0·06, 0·03	−0·08, −0·10	−0·13, −0·02
1, 3	−0·01, 0·00	0·00, 0·00	−0·01, 0·00	0·00, −0·02
2, 1	−0·18, −0·09	0·06, −0·03	−0·12, −0·12	−0·21, −0·03
2, 2	0·03, 0·17	0·96, −0·01	0·99, 0·16	1.13, 0·05
2, 3	0·10, −0·05	0·00, 0·00	0·10, −0·05	0·05, −0·02
$\kappa_3 = 3{\cdot}0$				
1, 1	0·16, 0·06	0·99, 0·00	1·15, 0·06	1·11, 0·06
1, 2	−0·21, −0·04	0·02, 0·00	−0·19, −0·04	−0·20, −0·02
1, 3	0·17, 0·00	0·00, 0·00	0·17, 0·00	0·03, −0·01
2, 1	0·27, −0·08	0·02, 0·00	0·29, −0·08	−0·26, −0·02
2, 2	0·01, 0·15	0·99, 0·00	1·00, 0·15	1·06, 0·06
2, 3	0·09, −0·02	0·00, 0·00	0·09, −0·02	0·07, −0·01

TABLE 2. A comparison of computed and asymptotic values of M_{in} at $\theta = \frac{3}{4}\pi$

(i) *Distortion of vorticity field by mean flow.* The first effect is that the body creates a different mean velocity field around it and upstream of it, which, as shown in §3, leads to the distortion of the random vorticity field of the incident turbulence. Consider an eddy in the incident flow with a velocity $\mathbf{u}_\infty$, vorticity $\boldsymbol{\omega}_\infty$ and length l (or wavenumber $k = 1/l$). The vorticity of the eddy when distorted by the mean flow induces a velocity $\mathbf{u}^{(d)}$, in addition to the incident velocity $\mathbf{u}_\infty$. If $l \gtrsim a$ changes in $\boldsymbol{\omega}$ occur over a distance of order (denoted by $\sim$) a, so that $|\mathbf{u}^{(d)}| \sim |a\boldsymbol{\omega}_\infty|$. But if $l \ll a$ these changes occur over a distance $\sim l$, so that $|\mathbf{u}^{(d)}| \sim |l\boldsymbol{\omega}_\infty|$. Since $\mathbf{u}_\infty \sim l\boldsymbol{\omega}_\infty$, then, if $l \gtrsim a$, the ratio $|\mathbf{u}^{(d)}|/|\mathbf{u}_\infty| \sim a/l$ and if

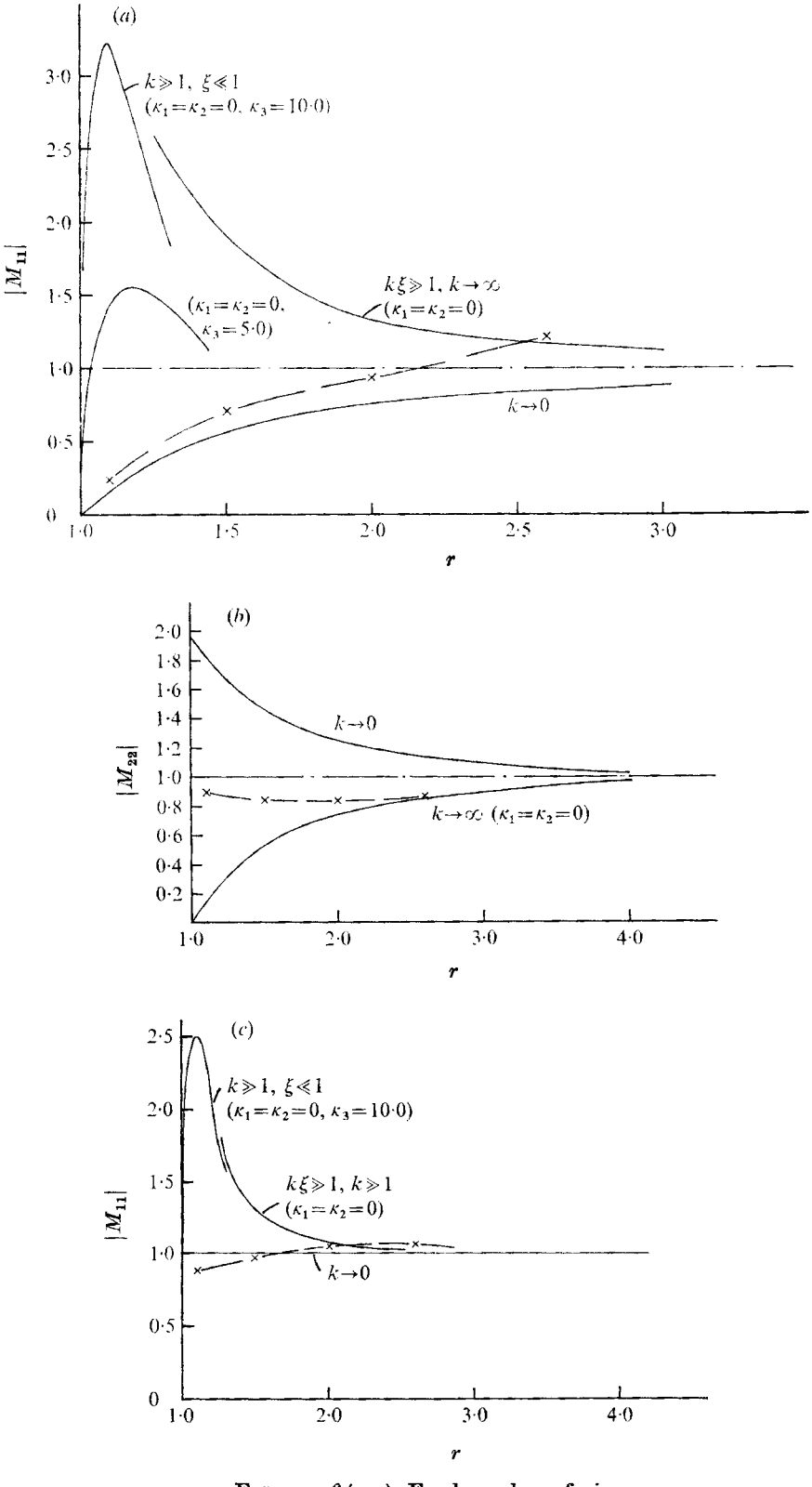

FIGURES 6 (*a–c*). For legend see facing page.

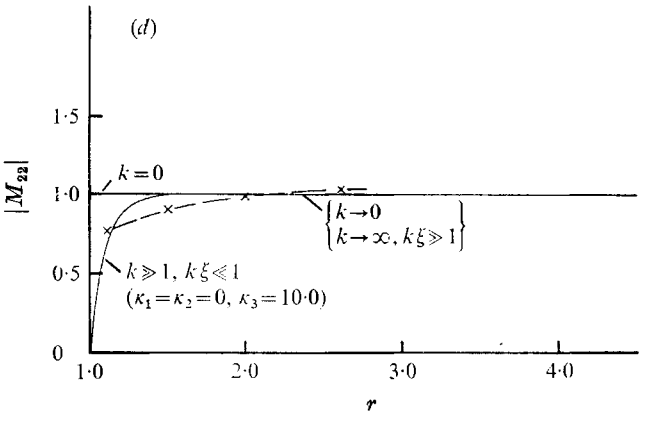

FIGURE 6. Asymptotic solutions for $|M_{11}|$ and $|M_{22}|$ when $k \ll 1$ and $k \gg 1$ and computed solutions (crosses) when $\kappa_1 = \kappa_2 = \kappa_3 = 1{\cdot}0$. (*a*) $|M_{11}|(r)$ on $\theta = \pi$. (*b*) $|M_{22}|(r)$ on $\theta = \pi$. (*c*) $|M_{11}|(r)$ on $\theta = \frac{3}{4}\pi$. (*d*) $|M_{22}|(r)$ on $\theta = \frac{3}{4}\pi$.

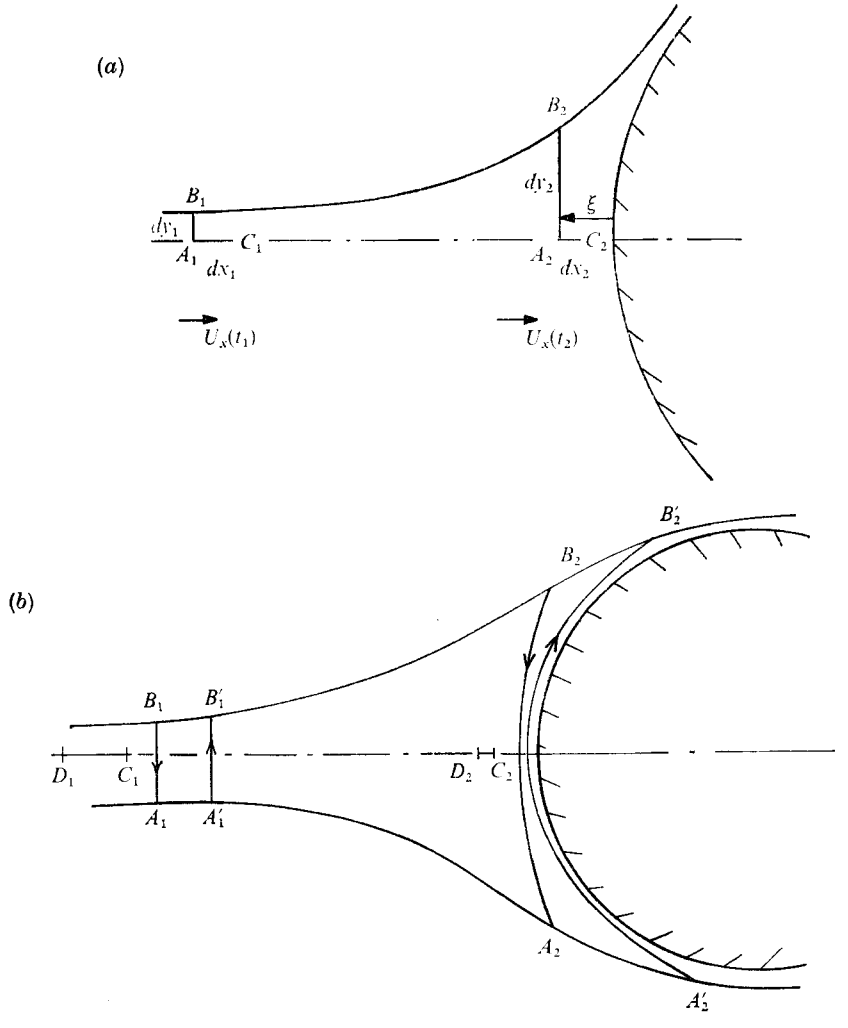

FIGURE 7. (*a*) Stretching of fluid elements near the stagnation point. (*b*) Stretching and 'piling-up' of vortex lines around the cylinder.

$l \ll a$, $|\mathbf{u}^{(d)}|/|\mathbf{u}_\infty| \sim 1$. Thus the velocity of turbulent eddies with wavelengths large compared with the body's dimension (or $k \ll 1$) is relatively unaffected by their vorticity being distorted by the mean flow. However, the velocities of small-scale eddies (or $k \gg 1$) can be amplified or diminished in proportion to the stretching or shortening of the vortex lines. Thus to understand how the velocity of small-scale eddies (or wavenumber components of the incident turbulence where $k \gg 1$) is changed it is necessary to examine how a vortex line in the incident flow is stretched as it is convected round the body by the mean flow. Figure 7 (*a*) shows how the lengths of two vortex elements which are parallel and perpendicular to the stagnation line upstream are changed from (dx_1, dy_1) at time t_1 to (dx_2, dy_2) at time t_2, where $dy_2/dy_1 = 1/U_x(t_2)$, if $U_x(t_1) = 1$. This result follows from (3.11). The physical implication is obviously that as the fluid element approaches the body, the length of the fluid element AC is reduced to zero while that of the element AB is stretched by an infinite amount. The effect on the local velocity, if $k \gg 1$, is equally dramatic, but depends critically on the value of the wavenumber κ_1 (which is also the frequency).

If $\kappa_1 = 0$, then the vortex line AB is one of an identical sequence of vortex lines produced by a velocity $u_{\infty 1} = S_1 \exp\{i\kappa_3 z\}$ and the stretching of the vortex line leads to an amplification of u_1, near the stagnation point (see figure 7*a*). (This phenomenon was fully discussed by Sutera *et al.* 1963.) The vortex line AC can be produced by a velocity field of the form $\mathbf{u} = (0, S_2 \exp\{i\kappa_3 z\}, S_3\{\exp\{i\kappa_2 y\}\})$, so that the implication of AC being reduced is that u_2 and u_3 decrease. Both these results are confirmed by inspection of the results in (5.50) and (5.51) for M_{in} on the line $\theta = \pi$, where we see that, if $\kappa_1/\xi \to 0$, as $\xi \to 0$ and $k\xi \to \infty$,

$$M_{11} = O(1/\xi), \quad M_{22} = O(\xi), \quad M_{33} = O(\xi^2). \tag{5.53}$$

On the other hand, if $\kappa_1 \neq 0$ then the incident velocity $\mathbf{u}_\infty$ must be partly generated by a sinusoidal distribution of vortex lines such as A_1B_1 and $A_1'B_1'$ in figure 7 (*b*), whose vorticities have opposite signs, e.g.

$$\mathbf{u}_\infty = (S_1 \exp\{i(\kappa_1 x + \kappa_3 z)\}, 0, S_3 \exp\{i(\kappa_1 x + \kappa_3 z)\}).$$

Since the vortex lines cannot slip round the two-dimensional body, it follows now that vortex lines are 'piled up' at the stagnation point and along the whole surface of the body; both in this case and the previous case viscous effects at the surface ensure that a steady situation is maintained. The velocity induced by this 'pile-up' of vortex lines with differing signs is likely to be much less than in the case of $\kappa_1 = 0$. The results of the analysis in (5.50) and (5.51) show that this is a reasonable physical picture because if $\kappa_1 = O(k)$, as $\xi \to 0$ and $k\xi \to \infty$

$$M_{11} = O(\xi), \quad M_{22} = O(\xi), \quad M_{33} = O(1). \tag{5.54}$$

In considering the induced velocities given by (5.53) and (5.54), we have assumed that locally the vorticity field varies sinusoidally over several wavelengths, which is true if $k\xi \gg 1$. However, at the body surface the vorticity field ceases, unless we imagine that there is a vorticity field inside the body. This is the analytical device adopted in § 5.2.1, which is further complicated by the fact that $\tilde{\omega}_2 \to \infty$ as $\xi \to 0$, and that if $\kappa_1 \neq 0$ there is a 'pile-up' of an infinite number of vortex lines of varying strengths in an infinitesimal distance, as shown by the

graphs of $\tilde{\Gamma}_{22}$ and $\tilde{\Gamma}_{33}$ in figures 5(*b*)–(*d*). Because the θ and z components of vorticity inside the body are assumed to be of the opposite sign to the vorticity outside, e.g. $\tilde{\omega}_2(-\xi) = -\tilde{\omega}_2(\xi)$, it follows that the normal velocity $\tilde{u}_1$ is zero at $\xi = 0$. But since the vorticity inside and outside the body both add to the turbulent velocity $\tilde{u}_3$ parallel to the axis of the cylinder, and since $\tilde{\omega}_2$ is singular as $\xi \to 0$ (as shown by figure 5*b*), it follows that for low frequencies $\tilde{u}_3$ is singular as $\xi \to 0$. The radial component of vorticity $\tilde{\omega}_1$ at the surface of the body is only zero at the stagnation point and retains the same sign inside the body. Since neither $\tilde{\omega}_1$ nor $\tilde{\omega}_3$ is singular at $\xi = 0$, the azimuthal velocity $\tilde{u}_2$ is of order unity for low frequencies, except at the stagnation point when $\kappa_3 = \kappa_1 = 0$. Thus as $\kappa_1 \to 0$ and $(\kappa_3^2 + \kappa_2^2)^{\frac{1}{2}} \to \infty$, such that $\kappa_1 |\ln \xi| \to 0$ as $\xi \to 0$,

$$|\tilde{M}_{11}| = O(-\xi \ln \xi), \quad |\tilde{M}_{21}| = O(1), \quad |\tilde{M}_{31}| = O(-\ln \xi).$$

However, when $\kappa_1 \gg 1$ the vortex lines are so concentrated near $\xi = 0$ that they cancel each other out and induce very small velocities. For example if

$$\theta = \pi \quad \text{and} \quad \kappa_1 \to \infty \quad \text{or} \quad \theta \neq \pi, \quad \kappa_1 \to \infty \quad \text{and} \quad (\kappa_3^2 + \kappa_1^2)^{\frac{1}{2}} \gg (\kappa_2^2 + \kappa_1^2)$$

$$|\tilde{M}_{11}| = O[k^{\frac{1}{2}} \xi \exp\{-\tfrac{1}{2}\pi\kappa_1\}], \quad |\tilde{M}_{21}| = O[\kappa_1^{\frac{1}{2}} \exp\{-\tfrac{1}{2}\pi\kappa_1\}],$$

$$|\tilde{M}_{31}| = O[\kappa_1^{\frac{1}{2}} \exp\{-\tfrac{1}{2}\pi\kappa_1\}].$$

Alternatively over a limited range of wavenumber space and away from the stagnation point this concentration of vortex lines can induce large velocities. For example if $\theta \neq \pi$ and $\kappa_2 \gg \kappa_3 \gg \kappa_1 \gg 1$,

$$|\tilde{M}_{11}| = O(\xi \kappa_1^{-\frac{1}{2}}), \quad |\tilde{M}_{21}| = O(\kappa_1^{\frac{1}{2}}), \quad |\tilde{M}_{31}| = O(\kappa_1^{\frac{1}{2}}).$$

The reason why this amplification can occur is because, when $\theta \neq \pi$ and $\kappa_1 \to \infty$, the term $e^{\frac{1}{2}\kappa_1 \phi} \Gamma(-\frac{1}{2} i \kappa_1)$ occurring in the expression for I_{ij} in (5.41) can be $O(\kappa_1^{-\frac{1}{2}})$ if $\tilde{\chi}_1 \gg \tilde{\chi}_{23}$, but at $\theta = \pi$ where $\phi < 0$ this term is at most $O(\kappa_1^{-\frac{1}{2}} e^{-\frac{1}{4}\pi\kappa_1})$. This difference is caused by the integrated effect of the vortex lines being much less at $\theta = \pi$ than when $\theta \neq \pi$, because of the different nature of the 'pile-up' of vortex lines at the stagnation point to elsewhere round the cylinder, which is demonstrated by figures 5(*c*) and (*d*). The physical explanation for this difference is that away from the stagnation region the variation of the incident vorticity between streamlines, i.e. the effect of κ_2, contributes an additional regular sinusoidal oscillation to the variation to the vorticity $\tilde{\Gamma}_{ij}$ with ξ. This differs from the effect of the variation of the incident vorticity with time (i.e. κ_1), which is to create an oscillation in $\tilde{\Gamma}_{ij}$ of ever decreasing scale near the surface owing to the logarithmic singularity of Δ_T, the time delay function. In fact these two effects counteract each other when $\kappa_2 \gg \kappa_1$ and $\theta \neq \pi$ because then at a point $\xi = \kappa_1/(4\kappa_2 \sin\theta)$, the phase of $\tilde{\Gamma}_{ij}$ is stationary, i.e. $\partial[\kappa_1(\Delta_T + x) + \kappa_2(y - \Delta_y)]/\partial\xi = 0$. This explains why the graph of $\tilde{\Gamma}_{33}$ in figure 5(*c*), unlike that in figure 5(*d*), has an extended maximum, and why therefore the integral for the induced velocity is so much greater than when $\theta = \pi$. From a mathematical point of view it is interesting that in this limit I_{ij} can also be calculated by the method of stationary phase.

The other implication of the 'pile-up' of vortex lines is that it not only affects the magnitude of the velocity but also ensures that the velocity oscillates

very rapidly close to the surface of the body. This means that when the velocity is integrated along a line normal to the surface to calculate the surface pressure, the result must be very small when $\kappa_1 \gg 1$, as shown in detail by Hunt (1973).

Note that we have concentrated on the cases where $k \gg 1$, so that there is a direct relation between local vorticity and velocity. In general the velocity at a point is induced by vorticity over a wide area of the flow, which is why it is so difficult to compute M_{il} when $k \sim 1$.

(ii) *Blocking of turbulent fluctuations by the pressure of the body.* The other important effect the body has on the turbulence is that it forces the component of turbulent velocity normal to the surface of the body to be zero. This effect can be present even if the body does not distort the mean flow, for example a flat plate parallel to the flow. This boundary condition (2.25*b*) can be satisfied if the body is replaced by a set of sources producing a velocity $\mathbf{u}^{(s)}$, so that in the flow field near the body

$$\mathbf{u} = \mathbf{u}_\infty + \mathbf{u}^{(d)} + \mathbf{u}^{(s)},$$

and on the body at $n = 0$,

$$\mathbf{u}^{(s)}.\mathbf{n} = -\mathbf{u}_\infty.\mathbf{n} - \mathbf{u}^{(d)}.\mathbf{n}.$$

These two velocity components $\mathbf{u}^{(d)}$ and $\mathbf{u}^{(s)}$, due to the distortion of vorticity and the body's replacement by a distribution of sources, correspond to the expressions $\nabla \times \boldsymbol{\psi}$ and $\nabla\Phi$ in (3.17) and to the tensors $M_{in}^{(d)}$ and $M_{in}^{(s)}$ in (4.32). In our calculations of $\mathbf{u}^{(d)}$ when $k \gg 1$ it was possible to choose a suitable vorticity distribution in the body, or for arbitrary k to choose suitable constants in the integrals (which can be regarded as equivalent) such that $\mathbf{u}^{(d)}.\mathbf{n} = 0$. Therefore $|\mathbf{u}^{(s)}| \sim |\mathbf{u}_\infty|$, and from our discussion of $|\mathbf{u}^{(d)}|$ we find that, if

$$l \gg a \text{ (or } \quad k \ll 1), \quad |\mathbf{u}^{(s)}| \gg |\mathbf{u}^{(d)}|$$

and that, if $l \ll a$ or $k \gg 1$, $|\mathbf{u}^{(s)}| \sim |\mathbf{u}^{(d)}|$.

When $k \gg 1$, the velocity produced by sources on the boundary decreases very rapidly as a function of the distance ξ from the boundary, in fact like $e^{-k\xi}$, and therefore over most of the flow can be ignored. But when $k \ll 1$, our order-of-magnitude argument shows that $\mathbf{u}^{(s)}$ is now the most important component of the flow everywhere, since $|\mathbf{u}^{(s)}| \gg |\mathbf{u}^{(d)}|$. This explains why the leading term $M_{il}^{(0)}$ in the asymptotic expansion for M_{il} as $k \to 0$, equation (5.23), is produced by the source (in this case, dipole) effect of the cylinder. In fact $M_{i1}^{(0)}$ is the velocity distribution produced by a steady velocity in the x direction far upstream and $M_{i2}^{(0)}$ is the same for an upstream velocity in the y direction. But, however small the values of k, there must be some variation of the upstream velocity over a distance of the order of the size of the body, so that there is sufficient vorticity in the upstream turbulence to be distorted and induce a velocity $O(k)$, denoted by $M_{il}^{(d,1)}$. The physical explanation for the terms $M_{il}^{(I)}$ of order $k^2 \ln k$ is partly that the velocity near the body is induced by vorticity in the far field where $kr \gg 1$, and partly that the source distribution on the body produces many higher order wavenumber components in $\mathbf{u}^{(s)}$ and therefore in $M_{il}^{(s)}$.

(iii) *Combined effects of distortion and blocking.* Having discussed the physical processes and the analytical solutions in the limits $k \gg 1$ and $k \ll 1$, it is worth

considering the range of k of order unity. There is no special reason why a maximum in M_{il} might not have occurred near $k = 1$ rather than when $k \ll 1$ or $k \gg 1$. In fact tables 1 and 2 and the results plotted in figures 6(*a*)–(*d*) show that when $k \sim 1$ M_{il} lies somewhere midway between its asymptotic values. This fact might be explained by saying that when $k \sim 1$ there is a rough balance between the distortion of the incident vorticity and the velocity produced by the source effect.

6. Spectra, correlations and variances

6.1. *Form of the incident spectrum* $\Phi_{\infty ij}$

In order to calculate the one-dimensional spectra and correlations of the turbulent flow near the body $\Theta_{ij}(\kappa_1)$ and $\overline{u_i u_j}$, we have to know the structure of the incident turbulence. In particular we need to know $\Phi_{\infty ij}(\kappa_1, \kappa_2, \kappa_3)$.

The only assumption about the incident turbulence that is required for our analysis is that it should be *homogeneous*. Only then can $\Phi_{\infty ij}$ be defined. However, in order to simplify the calculations, to bring out the physical ideas and to produce results which can be tested experimentally in the wind tunnel we make the additional hypothesis that the incident turbulence is *isotropic*. Then given $\Theta_{\infty 11}(\kappa_1)$ upstream, we can calculate $\Phi_{\infty ij}(\kappa)$.

A convenient choice for $\Theta_{\infty 11}(\kappa_1)$ is the spectrum first proposed by von Kármán (1948) as a simple expression which fits wind-tunnel measurements of turbulence behind course grids (see Bearman 1972). It has since been used by Harris (1971) to describe the spectrum in the natural wind when the atmosphere is neutrally stable or, which comes to the same thing, when the wind speed is high enough. If $\Theta^*_{\infty 11}$ and κ_1^* are the dimensional forms of $\Theta_{\infty 11}$ and κ_1 defined by

$$\Theta^*_{\infty 11}(\kappa_1^*) = \frac{1}{2\pi}\int_{-\infty}^{\infty} \overline{u'_{\infty 1}(x^*, y^*, z^*)\, u'_{\infty 1}(x^* + r_x^*, y^*, z^*)} \exp\{-i\kappa_1^* r_x^*\}\, dr_x^* \tag{6.1}$$

the von Kármán spectrum can be written as

$$\frac{\Theta^*_{\infty 11}(\kappa_1^*)}{u'^2_\infty L_x} = \left(\frac{a}{L_x}\right)\Theta_{\infty 11} = \frac{g_1}{[g_2 + (\kappa_1^* L_x)^2]^{\frac{5}{6}}}, \tag{6.2}$$

where the numerical constants g_1 and g_2 are determined by the conditions

$$\Theta^*_{\infty 11}(\kappa_1^* = 0) = L_x/\pi, \quad \int_{-\infty}^{\infty} \Theta^*_{\infty 11}\, d\kappa_1^* = u'^2_\infty,$$

and the integral scale

$$L_x = \left\{\int_0^\infty \overline{u'_{\infty 1}(x^*, y^*, z)\, u'_{\infty 1}(x^* + r_x^*, y^*, z^*)}\, dr_x^*\right\} \Big/ u'^2_\infty. \tag{6.3a}$$

It is found that

$$g_2 = \frac{\pi \Gamma^2(\frac{5}{6})}{\Gamma^2(\frac{1}{3})} = 0{\cdot}558, \quad g_1 = \frac{g_2^{\frac{5}{6}}}{\pi} = 0{\cdot}1955. \tag{6.3b}$$

To avoid the parameter a/L_x when presenting the results for $\Theta_{\infty 11}$ it is convenient to define

$$\hat{\Theta}_{11}(\hat{\kappa}_1) = (a/L_x)\,\Theta_{11}(\kappa_1); \quad \hat{\kappa}_1 = \kappa_1(L_x/a) = \kappa_1^* L_x. \tag{6.4}$$

There are two important points to be made about this formula (6.2) for the spectrum. First, it reduces to the Kolmogoroff spectrum in the inertial subrange, i.e. when $\eta_K^{-1} \gg \kappa_1^* \gg L_x^{-1}$, where $\eta_K = (\nu^3/\varepsilon)^{\frac{1}{4}}$,

$$\Theta^*_{\infty 11}(\kappa_1^*) = C_1 \varepsilon^{\frac{2}{3}} \kappa_1^{*-\frac{5}{3}}.$$

In many experimental investigations of the turbulence spectra in the subrange it has been found that $C_1 \simeq 0{\cdot}25$ (Lighthill 1970). Therefore from (6.2) and (6.3), the von Kármán spectrum implies that

$$\varepsilon = C_2 u_\infty'^3 / L_x,$$

where

$$C_2 = (g_1/C_1)^{\frac{3}{2}} = 0{\cdot}69.$$

Direct experimental measurements of ε, $\overline{u_1^2}$ and L_x are consistent with this value of C_2.

The second point to note is that when $\kappa_1^* \sim \eta_\kappa^{-1}$ viscous forces are of the same order as inertial forces, so that the analysis of this paper is not appropriate. But it is relevant to note that when $\kappa_1^* > \eta_\kappa^{-1}$ the spectrum decays very much more rapidly than $\kappa_1^{*\frac{5}{3}}$ and probably exponentially (Batchelor 1953).

Now $\Phi_{\infty ij}(\boldsymbol{\kappa})$, which is normalized in terms of u'_∞, the r.m.s. incident turbulent velocity, and the body size a, can be calculated in terms of $\Theta_{\infty 11}(\kappa_1)$, which from (6.2) is

$$\Theta_{\infty 11}(\kappa_1) = c_1/[c_2 + \kappa_1^2]^{\frac{5}{6}}, \tag{6.5}$$

where $c_1 = g_1(a/L_x)^{\frac{2}{3}}$, and $c_2 = g_2(a/L_x)^2$. We now use the fact that, if the turbulence is isotropic,

$$\Phi_{\infty ij}(\boldsymbol{\kappa}) = (E(k)/4\pi k^4)(k^2\delta_{ij} - \kappa_i\kappa_j) \tag{6.6}$$

(Batchelor 1953). $E(k)$ is the dimensionless form of energy spectrum function, and is related to $\Theta_{\infty 11}(\kappa_1)$ by the equation

$$E(k) = k^3 \frac{d}{dk}\left(\frac{1}{k}\frac{d}{dk}\Theta_{\infty 11}(k)\right)$$

(Batchelor 1953, equation (3.4.18)), so that from (6.5) and (6.6)

$$\Phi_{\infty ij}(\boldsymbol{\kappa}) = \frac{c_3[k^2\delta_{ij} - \kappa_i\kappa_j]}{(c_2 + k^2)^{\frac{17}{6}}}, \tag{6.7}$$

where $c_3 = 55c_1/36\pi$.

From (6.7), (3.31) and (3.32) it follows that

$$\hat{\Theta}_{\infty 22}(\hat{\kappa}_1) = \hat{\Theta}_{\infty 33}(\hat{\kappa}_1) = \frac{g_1(2)[1 + 5\hat{\kappa}_1^2/\{\hat{\kappa}3(g_2 + \hat{\kappa}_1^2)\}]}{(g_2 + \hat{\kappa}_1^2)^{\frac{5}{6}}}, \tag{6.8}$$

which of course shows that

$$\hat{\Theta}_{\infty 22}(0) = \hat{\Theta}_{\infty 33}(0) = \tfrac{1}{2}\hat{\Theta}_{\infty 11}(0) \quad \text{when} \quad \hat{\kappa}_1 = 0,$$

and

$$\hat{\Theta}_{\infty 22}(\hat{\kappa}_1) = \hat{\Theta}_{\infty 33}(\hat{\kappa}_1) = \tfrac{4}{3}\hat{\Theta}_{\infty 11}(\hat{\kappa}_1) \quad \text{when} \quad \hat{\kappa}_1 \to \infty.$$

It is useful to note that the autocorrelation of the incident turbulence is (from the Fourier transform of (6.2))

$$R_{\infty 11}(0, 0, 0, \tau) = R_{\infty 11}(\tau) = g_3(\tau a/L_x)^{\frac{1}{3}} K_{\frac{1}{3}}(g_2^{\frac{1}{2}}\tau a/L_x), \tag{6.9}$$

where $g_3 = 2g_1\pi^{\frac{1}{2}}/(2^{\frac{1}{3}}g_2^{\frac{1}{6}}\Gamma(\frac{5}{6}))$ and $K_{\frac{1}{3}}$ is a modified Bessel function. Note that the ratio a/L_x appears because τ has been normalized in terms of $\overline{u}_\infty$ and a, the radius of the cylinder, rather than in terms of L_x.

6.2. *Large-scale turbulence*: $(a/L_x) \ll 1$

6.2.1. *One-dimensional spectra.* It follows from (3.32), (3.36) and (6.7) that to calculate the one-dimensional spectra and thence the covariances etc., we have to evaluate the double integral

$$\Theta_{ij}(x,y;x',y';r_z;\kappa_1) = \int_{-\infty}^{\infty}\int_{-\infty}^{\infty} c_3\, M^{\dagger}_{in}(x,y;\boldsymbol{\kappa})\, M_{jm}(x',y';\boldsymbol{\kappa}) \exp(i\kappa_3 r_z) \times \frac{[k^2\delta_{nm}-\kappa_n\kappa_m]}{[g_2(a/L_x)^2+\kappa_1^2+\kappa_2^2+\kappa_3^2]^{\frac{17}{6}}}\, d\kappa_2\, d\kappa_3. \quad (6.10)$$

Now consider which part of wavenumber space provides the dominant contributions to the integral in (6.10). First it is clear that in (6.10) $\Phi_{\infty nm}$ increases as k increases until $k = O(a/L_x)$, or $k = O(\kappa_1)$ if $\kappa_1 \gg a/L_x$. Thus the major contribution to the integral comes from the region of wavenumber space where $k = O(a/L_x)$ or $k = O(\kappa_1)$, whichever is the larger. Consequently if $a/L_x \ll 1$ and $\kappa_1 = O(a/L_x)$ or $\hat{\kappa}_1 = O(1)$, the only values of $M_{in}(x,y;\boldsymbol{\kappa})$ that are required are those for which $k \ll 1$. Thus for large-scale turbulence the spectra can be calculated using the asymptotic expansion for M_{in} as $k \to 0$, defined by (5.23)–(5.25). In other words, only the large eddies need be considered if the integral scale is large. Since the expansion of $M_{in}(\boldsymbol{\kappa})$ in (5.23) is only valid to $O(k^2 \ln k)$, it follows that, as $k \to 0$, $M^{\dagger}_{in} M_{jm}$ can only be expanded to $O(k^2 \ln k)$. However, the usefulness of the expansion procedure is limited because the terms $O(k^2 \ln k)$ have the effect that the integral (6.10) only converges when $r_z \neq 0$, whatever the value of κ_1. Also we cannot evaluate the integrals analytically using the terms to this order, but it is possible to see that, if this one-dimensional spectrum is normalized in terms of L_x, the integral scale, i.e. if $\hat{\Theta}_{ij}(\hat{\kappa}_1) = (a/L_x)\,\Theta_{ij}(\kappa_1)$, then $\hat{\Theta}_{ij}(\hat{\kappa}_1)$ can be expanded as a series in terms of a/L_x:

$$\hat{\Theta}_{ij}(x,y;x',y';r_z;\hat{\kappa}_1) = \hat{\Theta}^{(0)}_{ij}(\hat{\kappa}_1) + (a/L_x)\,\hat{\Theta}^{(1)}_{ij}(\hat{\kappa}_1) + (a/L_x)^2 \ln(a/L_x)\,\hat{\Theta}^{(L)}_{ij}(\hat{\kappa}_1) + \ldots, \quad (6.11)$$

where the first three terms are calculated using the following terms in the expansion of M_{il} in (5.23): $M^{(0)}_{il}$, $M^{(0)}_{il}$ and $M^{(1)}_{il}$, $M^{(0)}_{il}$ and $M^{(L)}_{il}$ respectively for the first three terms in (6.11). Note that $\hat{\Theta}^{(0)}_{ij}$ and $\hat{\Theta}^{(2)}_{ij}$ are real, while $\hat{\Theta}^{(1)}_{ij}$ is complex.

Although $M^{(0)}_{il}$, $M^{(1)}_{il}$ and $M^{(L)}_{il}$ are known analytically a closed-form solution for only $\hat{\Theta}^{(0)}_{ij}(\hat{\kappa}_1)$ and $\hat{\Theta}^{(1)}_{ij}(\hat{\kappa}_1)$ can be given. Since from (5.24) and (5.25)

$$M^{(0)}_{il} = M^{(0)}_{il}(x,y),$$

and since $\Theta_{\infty ij}(\kappa_1) = 0$ if $i \neq j$, it follows from (6.10) that, whatever the value of r_z,

$$\hat{\Theta}^{(0)}_{ij}(\mathbf{x},\mathbf{x}';r_z;\hat{\kappa}_1) = F^{(0)}_{ijkl}\,\delta_{kl}\,\hat{\Phi}_{\infty kl}(r_z;\hat{\kappa}_1), \quad (6.12)$$

where
$$\left.\begin{aligned}
&\mathbf{x} = (x, y), \quad \mathbf{x}' = (x', y'),\\
&F^{(0)}_{ij11} = M^{(0)}_{i1}(\mathbf{x})\, M^{(0)}_{j1}(\mathbf{x}'), \quad F^{(0)}_{ij22} = M^{(0)}_{i2}(\mathbf{x})\, M^{(0)}_{j2}(\mathbf{x}'),\\
&F^{(0)}_{ij33} = M^{(0)}_{i3}(\mathbf{x})\, M^{(0)}_{j3}(\mathbf{x}') = \delta_{i3}\delta_{3j},\\
&\hat{\Theta}_{\infty 11}(r_z; \hat{\kappa}_1) = \frac{\frac{4}{3}g_1}{\Gamma(\frac{5}{6})\,(g_2+\hat{\kappa}_1^2)^{\frac{5}{6}}}\{\tfrac{11}{3}(\tfrac{1}{2}\zeta)^{\frac{5}{6}} K_{\frac{5}{6}}(\zeta) - 2(\tfrac{1}{2}\zeta)^{\frac{11}{6}} K_{\frac{11}{6}}(\zeta)\},\\
&\hat{\Theta}_{\infty 22}(r_z; \hat{\kappa}_1) = \frac{2g_1}{\Gamma(\frac{5}{6})\,(g_2+\hat{\kappa}_1^2)^{\frac{5}{6}}}\left\{\tfrac{4}{3}(\tfrac{1}{2}\zeta)^{\frac{5}{6}} K_{\frac{5}{6}}(\zeta) - \frac{(\frac{1}{2}\zeta)^{\frac{11}{6}} g_2}{(g_2+\hat{\kappa}_1^2)} K_{\frac{11}{6}}(\zeta)\right\},\\
&\zeta = r_z(a/L_x)\,(g_2+\hat{\kappa}_1^2)^{\frac{1}{2}}.
\end{aligned}\right\} \tag{6.13}$$

To obtain the cross-spectra at two points in the x, y plane or the spectrum at one point, we put $r_z = 0$ in (6.13) or use the expressions for $\hat{\Theta}_{\infty 11}(\hat{\kappa}_1)$ and $\hat{\Theta}_{\infty 22}(\hat{\kappa}_1)$ in (6.5) and (6.8). Although $M^{(1)}_{il}$ can be written in the general form

$$i(\kappa_1 p_{il}(x, y) + \kappa_2 q_{il}(x, y) + \kappa_3 \delta_{i3} r_{3l}),$$

we cannot obtain a general expression for $\hat{\Theta}^{(1)}_{ij}(\mathbf{x}, \mathbf{x}'; \hat{\kappa}_1)$ in terms of $\hat{\Theta}_{\infty ii}(r_z; \hat{\kappa}_1)$ if $r_z \neq 0$, but for our particular $\hat{\Theta}_{\infty ii}(r_z; \hat{\kappa}_1)$ it can be calculated at each point in the flow in terms of modified Bessel functions. However if $r_z = 0$

$$\hat{\Theta}^{(1)}_{ij}(\mathbf{x}, \mathbf{x}'; \hat{\kappa}_1) = i\hat{\kappa}_1 \left\{\sum_{l=1}^{3} F^{(1)}_{ijkl}(\mathbf{x}, \mathbf{x}')\, \delta_{kl}\, \Theta_{\infty kl}(\hat{\kappa}_1)\right\}, \tag{6.14}$$

where
$$\left.\begin{aligned}
&\mathbf{x} = (x, y, z), \quad \mathbf{x}' = (x', y', z'),\\
&F^{(1)}_{ij11} = -M^{(0)}_{ij}(\mathbf{x})\,[\tfrac{1}{2}q_{j2}(\mathbf{x}') + p_{j1}(\mathbf{x}')] - M^{(0)}_{j1}(\mathbf{x}')\, p_{i1}(\mathbf{x})\\
&\qquad + \tfrac{1}{2}q_{i2}(\mathbf{x})\, M^{(0)}_{j1}(\mathbf{x}') - \tfrac{1}{2}q_{j1}(\mathbf{x}')\, M_{i1}(\mathbf{x}) + \tfrac{1}{2}M^{(0)}_{j2}(\mathbf{x}')\, q_{i1}(\mathbf{x})\\
&\qquad + \tfrac{1}{2}[\delta_{i3} M_{j3}(\mathbf{x}')\, r_{31}(\mathbf{x}) - r_{31}(\mathbf{x}')\, M_{i3}(\mathbf{x})\, \delta_{3j}],\\
&F^{(1)}_{ij22} = -M^{(0)}_{j2}(\mathbf{x}')\, p_{i2}(\mathbf{x}) + M^{(0)}_{i2}(\mathbf{x})\, p_{j2}(\mathbf{x}'),\\
&F^{(1)}_{ij33} = \delta_{i3}\delta_{3j}[p_{33}(\mathbf{x}') - p_{33}(\mathbf{x})].
\end{aligned}\right\} \tag{6.15}$$

$\hat{\Theta}_{\infty 11}(\hat{\kappa}_1)$ and $\hat{\Theta}_{\infty 22}(\hat{\kappa}_1)$ are given by (6.4), (6.5) and (6.8). Note that if $i = j$, and if $\mathbf{x} = \mathbf{x}'$, then $F^{(1)}_{ijl} = \Theta^{(1)}_{ij} = 0$. As an example of these expressions, the real and imaginary parts of $\hat{\Theta}_{22}(\mathbf{x}, \mathbf{x}'; \hat{\kappa}_1)$ (co- and quad-spectra) are calculated for points on the stagnation line $\theta = \pi$ using (6.11) and (6.13). The results are plotted in figure 8. The most striking difference between the two graphs is that the unfamiliar quad-spectrum is zero when $\hat{\kappa}_1 = 0$, but decays like $|\hat{\kappa}_1|^{-\frac{8}{3}}$ when $|\hat{\kappa}_1| \to \infty$. This last point is important when integrating the spectrum to obtain cross-correlations. Note that since $\hat{\Theta}^{(1)}_{22}(\hat{\kappa}_1)$ is multiplied by a/L_x in (6.11), the imaginary part of $\hat{\Theta}_{22}(\hat{\kappa}_1)$ or the quad-spectrum is very small when $a/L_x \to 0$.

The practical conclusion to be drawn from this section is that, when $a/L_x \ll 1$, the cross-spectrum $\hat{\Theta}_{ij}(\mathbf{x}; \mathbf{x}', r_z, \hat{\kappa}_1)$ can be calculated to an accuracy of

$$O((a/L_x)^2 \ln (a/L_x)) \quad \text{if} \quad r_z \neq 0,$$

but if $r_z = 0$, it can only be calculated to $O(a/L_x)$. If $\mathbf{x} = \mathbf{x}'$ and $r_2 = 0$, then the important results for the power spectral density of one-dimensional spectra at a point $\hat{\Theta}_{ii}(\mathbf{x}, \hat{\kappa}_1)$ $(i = 1, 2, 3)$ can only be calculated to $O(1)$, so that the variation with a/L_x is not then known, nor is the error in neglecting the finite value of a/L_x. However, the qualitative effect of increasing a/L_x can be inferred from

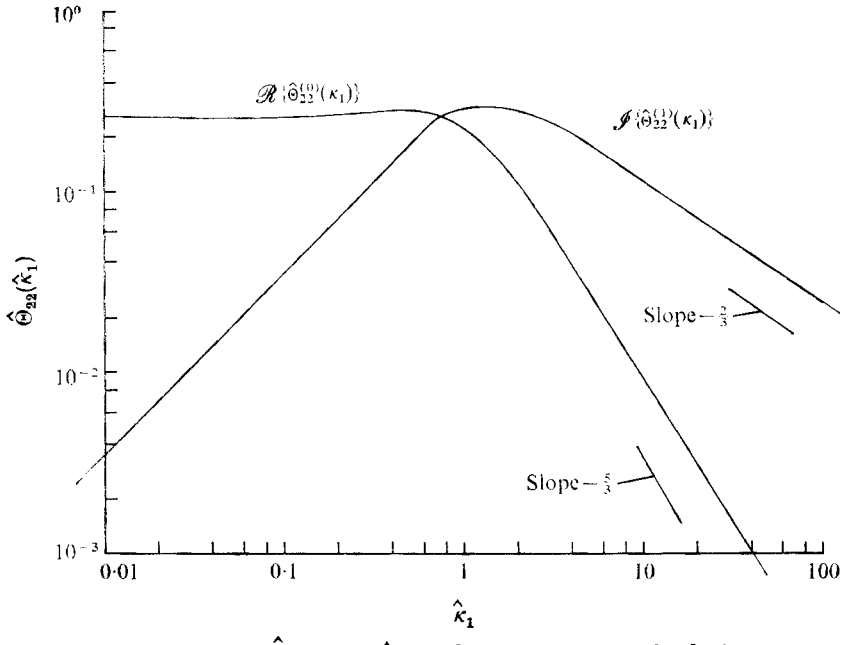

FIGURE 8. Cross-spectrum $\hat{\Theta}_{22}(\mathbf{x}, \mathbf{x}'; \hat{\kappa}_1)$ of the y component of velocity at two points on the stagnation line $\theta = \pi$, at $r = 1{\cdot}5$, $2{\cdot}5$. Note that $\hat{\Theta}_{22}(\hat{\kappa}_1) = \hat{\Theta}_{22}^{(0)}(\hat{\kappa}_1) + (a/L_x)\,\hat{\Theta}_{22}^{(1)}(\kappa_1)$, where in this case the first term is real and the second imaginary.

the difference between the values of $M_{il}^{(0)}$ and the computed values in tables 1 and 2 of M_{il} when $k \sim 1$. In figure 9 graphs are shown of $\hat{\Theta}_{11}(\hat{\kappa}_1)$ and $\hat{\Theta}_{22}(\hat{\kappa}_1)$ at $r = 2{\cdot}0$ and $\theta = \pi, \frac{3}{4}\pi$ as $a/L_x \to 0$, using (6.12). Dashed lines are drawn for comparison with the upstream spectra, $\hat{\Theta}_{\infty 11}(\hat{\kappa}_1)$ and $\hat{\Theta}_{\infty 22}(\hat{\kappa}_1)$.

6.2.2. *Correlations and variance.* From the spectra (6.12) and (6.14), the cross-correlations and the variance can be calculated throughout the flow, using (3.33). To do so we note that, since the integral is convergent,

$$\int_{-\infty}^{\infty} i\hat{\kappa}_j \hat{\Theta}_{\infty ii}(\hat{\kappa}_1) \exp\{-i\kappa_1 \tau\}\, d\kappa_1 = -\frac{d}{d\tau}\int_{-\infty}^{\infty} \Theta_{\infty ii}(\kappa_1) \exp\{-i\kappa_1 \tau\}\, d\kappa_1$$

$$= -d\,[R_{\infty ii}(\tau)]/d\tau, \tag{6.16}$$

where $R_{\infty ii}(\tau) = R_{\infty ii}(0, 0, 0, \tau)$, as defined in § 3.3. Therefore we can evaluate the cross-covariance of the velocity at two points at different times, namely

$$\overline{u_i(x, y; t)\, u_j(x', y'; t+\tau)} = \sum_{l=1}^{3} \left\{ F_{ijkl}^{(0)} \delta_{kl} R_{\infty kl}(\tau) - F_{ijkl}^{(1)} \delta_{kl} \frac{d}{d\tau} R_{\infty kl}(\tau) \right\}. \tag{6.17}$$

In the special case where (x', y') is another point lying on the mean streamline through (x, y) and $\tau\,(= \Delta_T(x', y') - \Delta_T(x, y) + x' - x)$ is the time taken to travel from (x, y) to (x', y'), then the above covariance has been termed the 'pseudo-Lagrangian' covariance by Hunt & Mulhearn (1973) and forms the basis for a statistical theory of turbulent diffusion from a source near a two-dimensional body. Note that the expression (6.17) has been deduced by assuming that the

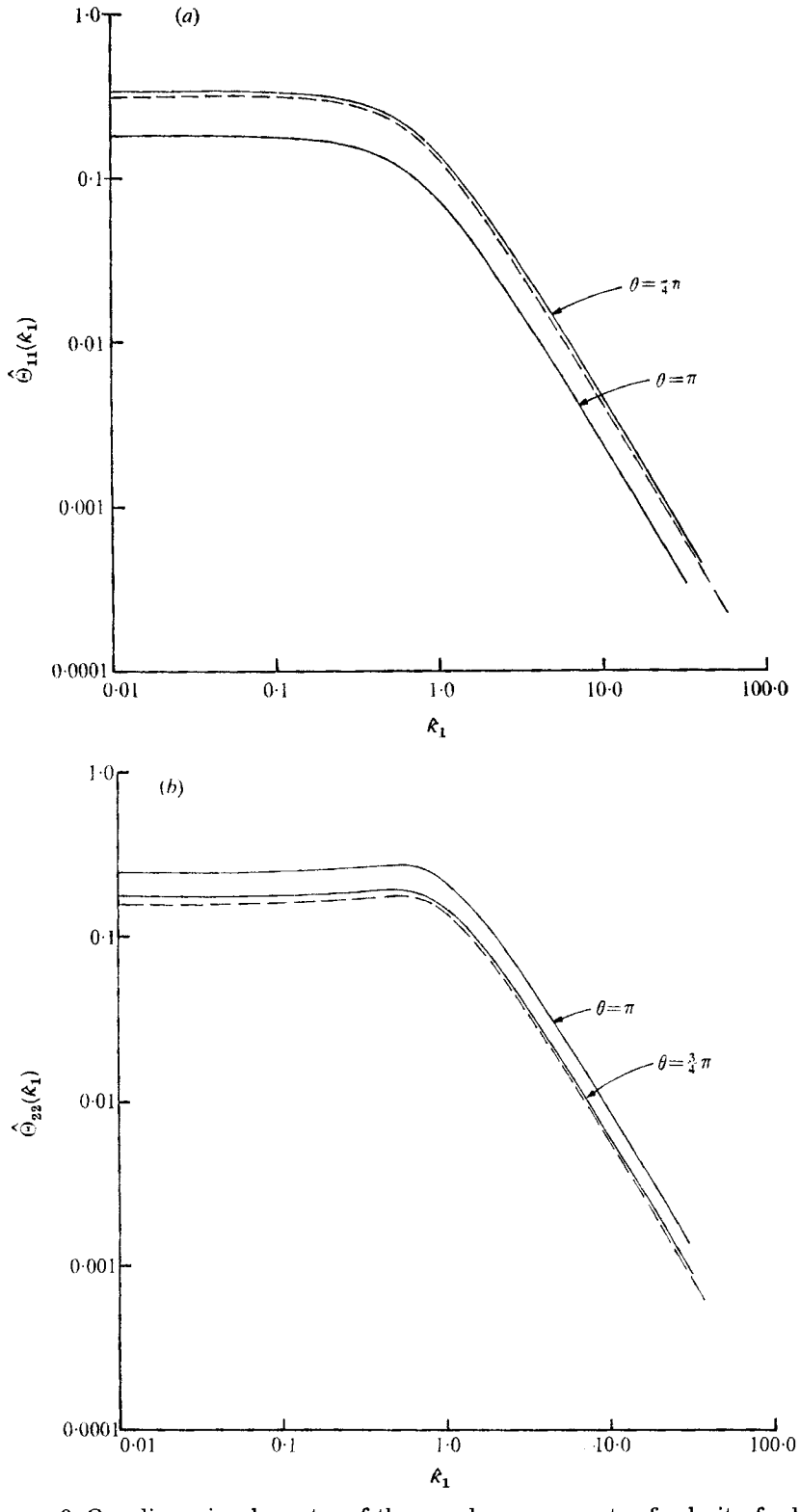

FIGURE 9. One-dimensional spectra of the x and y components of velocity for large-scale turbulence, i.e. $a/L_x \to 0$. (*a*) $\hat{\Theta}_{11}(\kappa_1)$. (*b*) $\hat{\Theta}_{22}(\kappa_1)$. — — —, $r \to \infty$; ———, $r = 2{\cdot}0$.

incident turbulence is isotropic, but without assuming any particular form of the spectrum. To obtain the order of magnitude of the second term we use the expression in (6.9) for $R_{\infty 11}(\tau)$, and if we take $\tau = O(1)$, as $a/L_x \to 0$, then this term can be seen to be $O(\overline{u_{\infty 1}^2}\,(a/L_x)^{\frac{2}{3}}\tau^{-\frac{1}{3}})$, as compared with the first term, which is $O(\overline{u_{\infty 1}^2})$. Thus (6.17) is not valid as $\tau \to 0$; in fact the condition for its validity is that $\tau \gg \eta_K/(a)$. However, the result is useful because it can be used to indicate the effect of turbulence scale on diffusion.

The cross-variances, without time delay, the covariances and variances can only be calculated to zero order as $a/L_x \to 0$, since the terms $O(a/L_x)$ in the integral (6.10) are identically zero. We find that

$$R_{ij}(\mathbf{x}, \mathbf{x}'; r_z) = F_{ijkl}^{(0)}(\mathbf{x}, \mathbf{x}')\,\delta_{kl} R_{\infty kl}(0, 0, r_z, 0). \tag{6.18}$$

When $r_z = 0$, (6.18) becomes

$$\overline{u_i(\mathbf{x})\,u_j(\mathbf{x}')} = F_{ijkl}^{(0)}(\mathbf{x}, \mathbf{x}')\,\delta_{kl}\,\overline{u_{\infty k}\,u_{\infty l}}, \tag{6.19}$$

which can usefully be expanded to give the variances

$$\left.\begin{aligned} \overline{u_1^2}(\mathbf{x}) &= (M_{11}^{(0)}(\mathbf{x}))^2\,\overline{u_{\infty 1}^2} + (M_{12}^{(0)}(\mathbf{x}))^2\,\overline{u_{\infty 2}^2}, \\ \overline{u_2^2}(\mathbf{x}) &= (M_{21}^{(0)}(\mathbf{x}))^2\,\overline{u_{\infty 1}^2} + (M_{22}^{(0)}(\mathbf{x}))^2\,\overline{u_{\infty 2}^2}, \\ \overline{u_3^2}(\mathbf{x}) &= \overline{u_{\infty 3}^2}. \end{aligned}\right\} \tag{6.20}$$

These results are valid for any homogeneous incident turbulence; they do not depend upon any assumptions of isotropy. To recapitulate, M_{11} and M_{21} are equal to the normalized *mean* x and y velocities over the body, and M_{21} and M_{22} are equal to the normalized mean x and y velocities caused by an upstream velocity in the y direction. Alternatively $M_{12}u_{\infty 2}$, $M_{22}u_{\infty 2}$ can be regarded as the x and y perturbation velocity components due to a change in the direction of the incident flow from $\theta = 0$ to $\theta = u_{\infty 2}$. Using this idea the zero-order values of the variances can be calculated for a turbulent flow with a large scale over *any body*, given the mean velocity around the body (i.e. M_{i1}) and the rate of change of that mean velocity due to small changes in the direction of the incident flow (i.e. M_{i2}). One benefit of the higher order analysis of this paper is that it gives an idea of the limitations of such quasi-steady analyses.

6.3. *Small-scale* ($a/L_x \gg 1$) *and high-frequency* ($\kappa_1 \gg 1$) *turbulence*

If $a/L_x \gg 1$ or $\kappa_1 \gg 1$, then the dominant contribution to the integral in (6.10) comes from the region of wavenumber space where $k \gg 1$. Therefore the asymptotic expansion for $M_{in}(x, y; \boldsymbol{\kappa})$ as $k \to \infty$, given by (5.43)–(5.45), should be used in (6.10). In this case only small eddies need be considered, because the integral scale is small. Since we were not able to obtain a solution for M_{in} as $k \to \infty$ valid everywhere in the flow, except when $\kappa_1 = 0$, we have to consider whether $k\xi \gg 1$ or $k\xi \ll 1$. Interpreting these criteria in terms of a/L_x, it follows from (6.10) that, if $a/L_x \gg 1$ and $\kappa_1 \lesssim O(a/L_x)$, i.e. $\hat{\kappa}_1 = O(1)$, then these two regions can be defined more conveniently as $(a/L_x)\,\xi \gg 1$, or $(a/L_x)\,\xi \ll 1$. But if $a/L_x \lesssim O(1)$, then the expressions for M_{in} as $k \to \infty$ can only be used in (6.10) when $\kappa_1 \gg 1$, or $\hat{\kappa}_1(a/L_x) \gg 1$; then the two regions can be defined as $\kappa_1\xi = (a/L_x)\,\hat{\kappa}_1\xi \gg 1$ or $\kappa_1\xi \ll 1$, respectively.

Before calculating Θ_{ij} for these two cases, it is useful to simplify the integrand in (6.10). Since when $k \gg 1$, the expression for M_{il} can be reduced to $M_{il}^{(d)}$, where $M_{il}^{(d)} = ia_{ij}^{(d)}\epsilon_{jkl}\kappa_k$, as shown for example in (5.45b),

$$M_{in}^{\dagger}(x,y;\boldsymbol{\kappa})M_{jm}(x',y';\boldsymbol{\kappa})\,(k^2\delta_{nm}-\kappa_n\kappa_m) = a_{in}^{(d)\dagger}(x,y;\boldsymbol{\kappa})\,a_{jm}^{(d)}(x',y';\boldsymbol{\kappa})\,(k^2\delta_{nm}-\kappa_n\kappa_m)\,k^2. \quad (6.21)$$

6.3.1. *Spectra when* $(a/L_x)\xi \gg 1$ *or* $\kappa_1\xi \gg 1$. The spectra away from the immediate vicinity of the body, such that $k\xi \gg 1$, are calculated using the result for $a_{ij}^{(d)}$, given by (5.31). We first express $a_{il}^{(d)}$ as

$$a_{il}^{(d)}(\mathbf{x},\boldsymbol{\kappa}) = iL_{il}(\mathbf{x},\boldsymbol{\kappa})\exp\{i(\kappa_1 T_0(\mathbf{x})-\kappa_2\Psi(\mathbf{x}))\},$$

where $$\mathbf{x} = (x,y), \quad T_0(\mathbf{x}) = x+\Delta_T(\mathbf{x}), \quad \Psi(\mathbf{x}) = -y+\Delta_y(\mathbf{x}),$$

$$L_{il} = \epsilon_{ijk}\chi_j(\mathbf{x},\boldsymbol{\kappa})\gamma_{kl}(\mathbf{x})/\chi^2 \text{ (and is real)},$$

then

$$a_{in}^{(d)\dagger}(\mathbf{x},\boldsymbol{\kappa})\,a_{jm}^{(d)}(\mathbf{x}',\boldsymbol{\kappa}) = L_{in}(\mathbf{x},\boldsymbol{\kappa})\,L_{jm}(\mathbf{x}',\boldsymbol{\kappa})\exp\{i\kappa_1(T_0(\mathbf{x}')-T_0(\mathbf{x}))\} \times\exp\{-i\kappa_2(\Psi(\mathbf{x}')-\Psi(\mathbf{x}))\}. \quad (6.22)$$

Analytic expressions for $\Theta_{ij}(\kappa_1)$ cannot, in general, be obtained from the integral (6.10). However, on the stagnation line $\theta = \pi$, $U_y = \partial\Delta_T/\partial y = 0$, so that the computation of the integral (6.10) is greatly simplified. The distortion of turbulence on $\theta = \pi$ is an interesting special case because the vortex lines are only stretched by the mean flow and not twisted. This symmetric distortion was one of the cases studied by Batchelor & Proudman (1954). Substituting (6.22) into (6.10) leads to the spectrum at a point $(x, 0)$ on the stagnation line:

$$\Theta_{11}(\kappa_1) = \int_{-\infty}^{\infty}\int_{-\infty}^{\infty}\frac{c_3k^2(\gamma_{22}^2\chi_3^2(\kappa_1^2+\kappa_3^2)+\chi_2^2(\kappa_1^2+\kappa_2^2)+2\chi_2\chi_3\gamma_{22}\kappa_2\kappa_3)\,d\kappa_2\,d\kappa_3}{(c_2+\kappa_1^2+\kappa_2^2+\kappa_3^2)^{\frac{17}{6}}(\chi_1^2+\chi_2^2+\chi_3^2)^2}.$$

From (5.27) $\chi_1 = \kappa_1/U_1, \chi_2 = \kappa_2 U_1$ and $\chi_3 = \kappa_3$, and from (3.11), $\gamma_{22} = 1+\partial\Delta_T/\partial x = 1/U_1$, whence

$$\hat{\Theta}_{11}(\hat{\kappa}_1) = 2g_3 I_{11}(\hat{\kappa}_1)/U_1^2\hat{\kappa}_1^{\frac{5}{3}},$$

where

$$I_{11}(\hat{\kappa}_1) = \int_0^{\infty}\int_0^{\frac{1}{2}\pi}\frac{b(1+b)\,[b(\sin^2\phi^{\times}+U_1^2\cos^2\phi^{\times})^2+U_1^4\cos^2\phi^{\times}+\sin^2\phi^{\times}]\,d\phi^{\times}\,db}{[1/U_1^2+b(U_1^2\cos^2\phi^{\times}+\sin^2\phi^{\times})]^2\,[g(\hat{\kappa}_1)+b]^{\frac{17}{6}}}, \quad (6.23)$$

$$g(\hat{\kappa}_1) = 1+c_2/\kappa_1^2 = 1+g_2/\hat{\kappa}_1^2, \quad b = (\kappa_2^2+\kappa_3^2)/\kappa_1^2.$$

Since

$$\int_0^{\frac{1}{2}\pi}\frac{\cos^2\phi^{\times}d\phi^{\times}}{[(a^2-b^2)\cos^2\phi^{\times}+b^2]^2} = \frac{\pi}{4a^3b}, \quad \int_0^{\frac{1}{2}\pi}\frac{d\phi^{\times}}{[(a^2-b^2)\cos^2\phi^{\times}+b^2]^2} = \frac{\pi(a^2+b^2)}{4a^3b^3} \quad (6.24)$$

(Gröbner & Hofreiter 1968), $I_{11}(\hat{\kappa}_1)$ can be reduced to the integral

$$I_{11}(\hat{\kappa}_1) = \tfrac{1}{2}\pi\int_0^{\infty}\frac{(1+b)\,db}{(g(\hat{\kappa}_1)+b)^{\frac{17}{6}}}\left\{1-\frac{2+bU_1^2(3+2U_1^2-U_1^6)+b^2U_1^6(4-U_1^4-U_1^2)}{2[(1+U_1^2b)\,(1+U_1^4b)]^{\frac{3}{2}}}\right\}. \quad (6.25)$$

Now this integral cannot be re-expressed in terms of known functions, however we can examine its main properties close to and far from the cylinder. When

$r \to \infty$, $U_1 = 1$ and $I_{11}(\hat{\kappa}_1) = \frac{1}{2}\pi \times \frac{36}{55} g(\hat{\kappa}_1)^{-\frac{5}{6}}$, whence $\hat{\Theta}_{11}(\hat{\kappa}_1) = \hat{\Theta}_{\infty 11}(\hat{\kappa}_1)$, as expected. When $r - 1 = \xi \to 0$, $U_1 \to 0$, and the asymptotic form for $I^{(d)}$ can be obtained for small and large values of $\hat{\kappa}_1$. As $\hat{\kappa}_1 \to 0$, so that $g(\hat{\kappa}_1) \to \infty$,

$$I_{11}(\hat{\kappa}_1) \sim \left(\frac{\pi}{2}\right)\left(\frac{36}{55}\right) g(\hat{\kappa}_1)^{-\frac{5}{6}}. \tag{6·26}$$

Now when $\hat{\kappa}_1 \to \infty \quad (g(\hat{\kappa}_1) \to 1)$,

$$I_{11}(\hat{\kappa}_1) \sim \tfrac{1}{2}\pi[\tfrac{6}{5}(1 + O(g(\hat{\kappa}_1) - 1)) - \Delta I], \tag{6.27}$$

where, as $U_1 \to 0$,

$$\Delta I \sim \int_0^\infty \frac{[1 + (\frac{3}{2}U_1^2 + U_1^4)\, b + O(U_1^6)]\, db}{(1+b)^{\frac{11}{6}}(1 + U_1^2 b)^{\frac{3}{2}}(1 + U_1^4 b)^{\frac{3}{2}}}.$$

First integrate by parts, and then use the power series expansion of the integral

$$F(U_1^2) = \int_0^\infty \frac{db}{(1+b)^{\gamma_1}(1+U_1^2 b)^{\gamma_2}} \quad (0 < \gamma_1 < 1, \gamma_1 + \gamma_2 > 1)$$

$$= \frac{1}{U_1^{2(1-\gamma_1)}(1-U_1^2)^{\gamma_1+\gamma_2-1}}\left[\frac{\Gamma(\gamma_1+\gamma_2-1)\,\Gamma(1-\gamma_1)}{\Gamma(\gamma_2)} - \Sigma(-1)^n \binom{\gamma_3}{n} \frac{U_1^{2(n+1-\gamma_1)}}{n+1-\gamma_1}\right],$$

where $\gamma_3 = \gamma_1 + \gamma_2 - 2$,

$$\binom{\gamma_3}{n} = \frac{\gamma_3!}{n!(\gamma_3 - n)!}.$$

Thence $$\Delta I \sim \tfrac{6}{5} - \tfrac{1}{10} G_1 U_1^{\frac{5}{3}} + O(U_1^{\frac{11}{3}}),$$

where $$G_1 = \Gamma(\tfrac{4}{3})\,\Gamma(\tfrac{1}{6})/\Gamma(\tfrac{3}{2}) = 5{\cdot}6. \tag{6.28}$$

Therefore, in the formal limits $\xi \to 0$, $\xi(a/L_x) \to \infty$, $\hat{\kappa}_1 \to 0$,

$$\hat{\Theta}_{11}(\hat{\kappa}_1) = \frac{1}{\pi U_1^2} = \frac{0{\cdot}319}{(2\xi)^2}, \tag{6.29a}$$

and as $\xi \to 0$, $\hat{\kappa}_1(a/L_x)\,\xi \to \infty$, $\hat{\kappa}_1 \to \infty$,

$$\hat{\Theta}_{11}(\hat{\kappa}_1) \sim 0{\cdot}167/\hat{\kappa}_1^{\frac{5}{3}} U_1^{\frac{1}{3}} = 0{\cdot}167/\hat{\kappa}_1^{\frac{5}{3}}(2\xi)^{\frac{1}{3}}. \tag{6.29b}\dagger$$

These formulae show that the shape of the $\hat{\Theta}_{11}(\hat{\kappa}_1)$ spectrum is likely to be unchanged near the body but that as $\hat{\kappa}_1 \to 0$ the spectrum is very much more amplified than in the region where $\hat{\kappa}_1 \to \infty$. The physical implications of these results are discussed later. But the results are also useful in checking computations of the integrals (6.23) and (6.24), the results of which are shown as a graph in figure 10 of $\hat{\Theta}_{11}(\hat{\kappa}_1)$ on $\theta = \pi$, where $a/L_x \gg 1$. The spectrum has been evaluated at three positions, $r = 2{\cdot}0$, $1{\cdot}5$, $1{\cdot}1$, at the third of which comparison with the asymptotic results (6.29) shows approximate agreement. (Higher order terms in the two asymptotic series have been obtained and then much better agreement is found.) Note that the results at $r = 1{\cdot}1$ are strictly only valid if $a/L_x \gg 10$.

† In this and subsequent formulae for spectra in the limit $\hat{\kappa}_1 \to \infty$ the form of the result does not depend on the particular spectrum taken for $\Phi_{\infty ij}$ in (6.7). It only depends on the spectrum satisfying the Kolmogoroff law that $E(k) \propto k^{-\frac{5}{3}}$ as $k \to \infty$, for $k < a/\eta_K$.

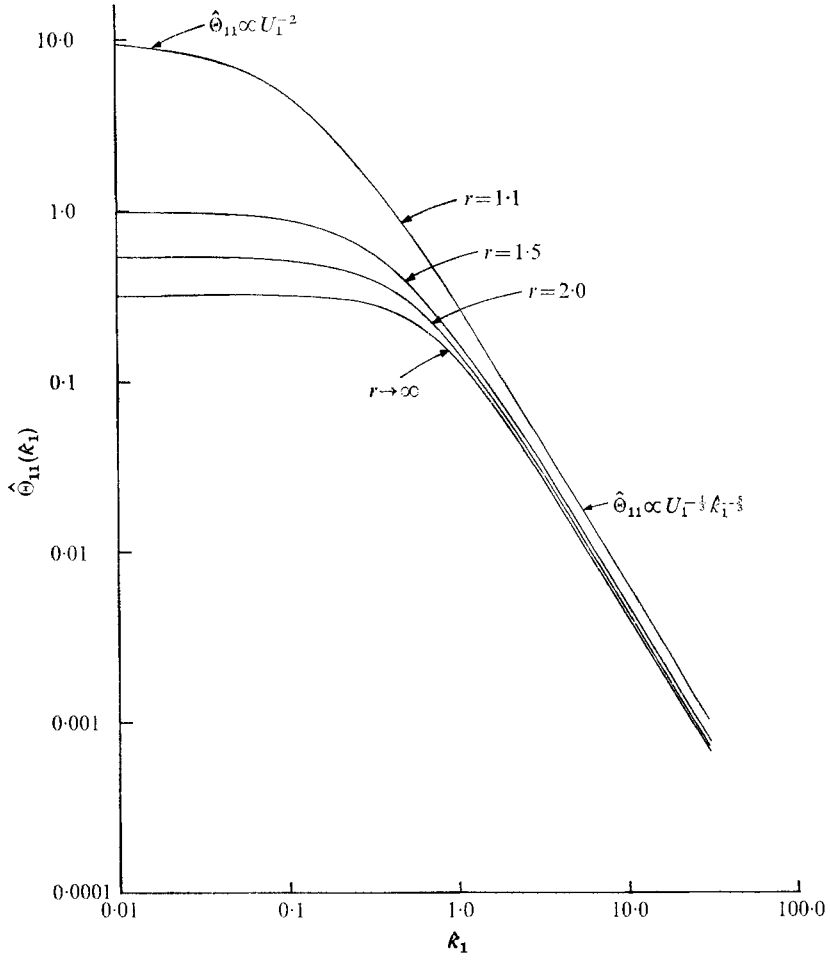

FIGURE 10. One-dimensional spectra of the component of velocity on the stagnation line for small-scale turbulence not very close to the body; i.e. $\hat{\Theta}_{11}(\hat{\kappa}_1)$ on $\theta = \pi$ when

$$a/L_x \to \infty, \ (a/L_x)\,\xi \gg 1.$$

$\hat{\Theta}_{22}(\hat{\kappa}_1)$ on $\theta = \pi$ can similarly be found, the relevant expression to be evaluated being

$$\hat{\Theta}_{22}(\hat{\kappa}_1) = 2g_3 I_{22}(\hat{\kappa}_1)/U_1^2 \hat{\kappa}_1^{\frac{5}{3}}, \tag{6.30}$$

where

$$I_{22}(\hat{\kappa}_1) = \int_0^\infty \int_0^{\frac{1}{2}\pi} \frac{[(1+bU_1^2\sin^2\phi^\times)^2 + b\cos^2\phi(bU_1^4\sin^2\phi^\times + 1)]\,(1+b)\,d\phi^\times\,db}{(g(\hat{\kappa}_1)+b)^{\frac{1}{6}}[b(\sin^2\phi^\times + U_1^2\cos^2\phi^\times) + 1/U_1^2]^2}.$$

Using the integrals (6.24),

$$I_{22}(\hat{\kappa}_1) = \frac{\pi U_1^4}{4}\int_0^\infty \frac{(1+b)\,[2+(1+U_1^2+U_1^4)\,b + U_1^6 b^2]\,db}{(g(\hat{\kappa}_1)+b)^{\frac{17}{6}}(1+U_1^4 b)^{\frac{3}{2}}(1+U_1^2 b)^{\frac{1}{2}}}, \tag{6.31}$$

which, as before, cannot be evaluated exactly. However, it can be shown that, as $r \to \infty$, $U_1 \to 1$ and $\hat{\Theta}_{22}(\hat{\kappa}_1) \sim \hat{\Theta}_{\infty 22}(\hat{\kappa}_1)$. When $r \sim 1 = \xi \to 0$, $U_1 \to 0$, $(a/L_x)\,\xi \to \infty$ there are two asymptotic regions as $\hat{\kappa}_1 \to 0$.

(i) $\hat{\kappa}_1 \ll U_1^{\frac{3}{2}}$ (or $U_1^6 g^2(\kappa_1) \gg 1$), when

$$\hat{\Theta}_{22}(\hat{\kappa}_1) = U_1/(2\pi) = U_1 \hat{\Theta}_{\infty 22}(\hat{\kappa}_1 = 0). \tag{6.32a}$$

(ii) $U_1^{\frac{3}{2}} \ll \hat{\kappa}_1 \ll U_1$ (or $g(\hat{\kappa}_1) \gg U_1^2 g(\hat{\kappa}_1) \gg 1 \gg U_1^6 g^2(\hat{\kappa}_1)$), when

$$I_{22}(\hat{\kappa}_1) \sim \frac{\pi U_1^3}{4[g(\kappa_1)]^{\frac{1}{3}}} \frac{\Gamma(\frac{5}{2})\,\Gamma(\frac{4}{3})}{\Gamma(\frac{17}{6})}$$

and

$$\hat{\Theta}_{22}(\hat{\kappa}_1) \sim 0{\cdot}369 U_1/\hat{\kappa}_1. \tag{6.32b}$$

When $\xi \to 0$, $U_1 \to 0$, $(a/L_x)\hat{\kappa}_1 \xi \to \infty$ and $\hat{\kappa}_1 \to \infty$,

$$\hat{\Theta}_{22}(\hat{\kappa}_1) \sim \left(\frac{55\Gamma(\frac{1}{3})\,\Gamma(\frac{1}{6})}{72\Gamma(\frac{1}{2})} g_1\right) \frac{U_1^{\frac{5}{3}}}{\hat{\kappa}_1^{\frac{5}{3}}}, \quad 0{\cdot}823 U_1^{\frac{5}{3}} \hat{\kappa}_1^{-\frac{5}{3}}.$$

Clearly the shape of the $\hat{\Theta}_{22}(\hat{\kappa}_1)$ spectrum is drastically changed near the body, one part, region (ii), being amplified, while as $\hat{\kappa}_1 \to 0$ or $\hat{\kappa}_1 \to \infty$ the spectrum is diminished. Thus in the limit $U_1 \to 0$, $\hat{\Theta}_{22}(\hat{\kappa}_1)$ approximates to a weak delta function. These unexpected phenomena are demonstrated in the graphs shown in figure 11 of $\hat{\Theta}_2(\hat{\kappa}_1)$ on $\Theta = \pi$ when $a/L_x \gg 1$. The graphs have been computed from (6.30) and (6.31), and agree with the form of the asymptotic results (6.32).

The results for $\hat{\Theta}_{22}(\hat{\kappa}_1)$ on $\theta = \pi$ near $\xi = 0$ suggest that it would be interesting to compare the spectra $\hat{\tilde{\Theta}}_{22}(\hat{\kappa}_1)$ of the tangential component of velocity $\tilde{u}_2$, at say $\xi = 0{\cdot}05$ for $\theta = \pi$, $\frac{3}{4}\pi$ and $\frac{1}{2}\pi$. Calculating $\tilde{a}_{2j}^{(d)}$ from (5.31) and (5.34) and substituting (6.21) and (6.22) into (6.10) it follows that, when $\xi \ll 1$,

$$\hat{\tilde{\Theta}}_{22}(\kappa_1) = c_3(\tilde{I}_1 + \tilde{I}_2 + \tilde{I}_3), \tag{6.33}$$

where

$$\tilde{I}_1 = \left(\frac{1+\cos\theta}{2\sin\theta}\right)^2 \iint_{-\infty}^{\infty} \frac{k^2 \chi_z^2 (\kappa_1^2 + \kappa_3^2)\, d\kappa_2 d\kappa_3}{(c_2 + k^2)^{\frac{17}{6}} \chi^4},$$

$$\tilde{I}_2 = \iint_{-\infty}^{\infty} \frac{k^2 \chi_r^2 (\kappa_1^2 + \kappa_2^2)\, d\kappa_3 d\kappa_3}{(c_2 + k^2)^{\frac{17}{6}} \chi^4},$$

$$\tilde{I}_3 = \frac{1+\cos\theta}{2\sin\theta} \iint_{-\infty}^{\infty} \frac{2\chi_r \chi_z \kappa_2 \kappa_3 k^2\, d\kappa_2 d\kappa_3}{(c_2 + k^2)^{\frac{17}{6}} \chi^4},$$

$$\chi_r = \kappa_1 \partial T/\partial r - \kappa_2 U_\theta = \kappa_1[-1/2\xi + \tfrac{1}{4}(4\cos\theta + 1)] + 2\kappa_2 \sin\theta,$$

$$\chi_\theta = -\tfrac{1}{2}\kappa_1 \cot(\tfrac{1}{2}\theta), \quad \chi_z = \kappa_3, \quad \chi^2 = \chi_r^2 + \chi_\theta^2 + \chi_z^2.$$

The spectra are given in figure 12, which shows that the peak in the low-frequency part of the spectrum decreases as the flow moves round the cylinder from the stagnation point. On the other hand, the high-frequency part increases. In this as in all cases where $(a/L_x)\,\xi \gg 1$ as $\hat{\kappa}_1 \to \infty$, $\hat{\Theta}_{ii}(\hat{\kappa}_1) \propto \hat{\kappa}_1^{-\frac{5}{3}}$.

6.3.2. *Spectra when* $(a/L_x)\,\xi \ll 1$. In general the calculation of one-dimensional spectra of the velocity very close to the body cannot be done simply by using the results for $a_{ij}^{(d)}(\boldsymbol{\kappa})$ when $k\xi \ll 1$, and $k \gg 1$, given by (5.43), because integrating with respect to κ_2 and κ_3 to evaluate $\Theta_{ii}(\kappa_1)$ leads to a divergent integral. Therefore, in general, $a_{ij}^{(d)}(\boldsymbol{\kappa})$ must be evaluated in the region of wavenumber space where $k\xi = O(1)$, which can only be done by numerical calculation of the integral (5.38), followed by numerical calculation of the spectrum integral (6.10).

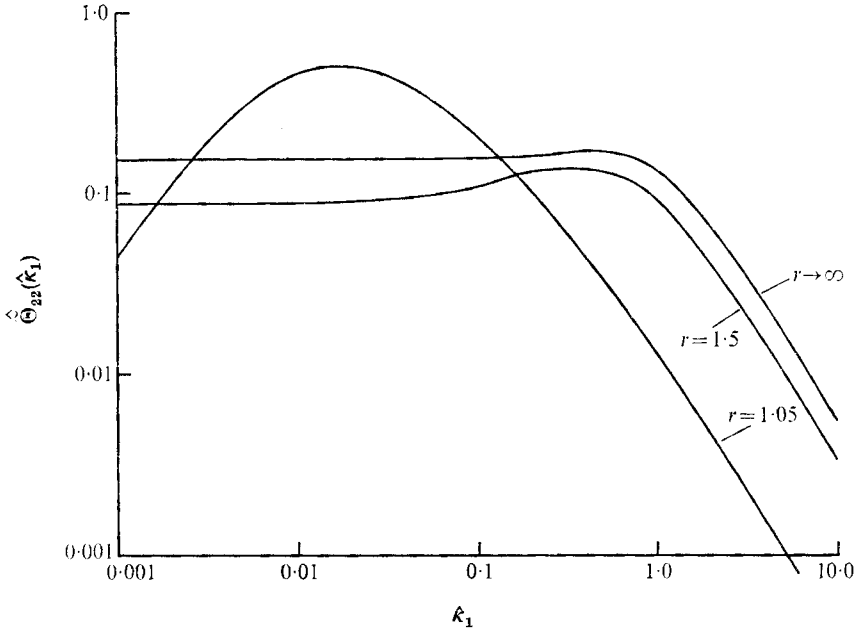

FIGURE 11. One-dimensional spectra of the θ (or y) component of velocity, i.e. $\hat{\hat{\Theta}}_{22}(\kappa_1)$, on $\theta = \pi$ when $a/L_x \to \infty$, $(a/L_x)\,\xi \gg 1$.

However in two important special cases which provide valuable physical insight into the turbulence at this close distance from the body, the integrals converge. In the first case we consider $\Theta_{11}(\kappa_1)$ on $\Theta = \pi$ in the limit $\kappa_1 \to 0$, $k \to \infty$ because in this limit M_{1n} is known for $k\xi = O(1)$. M_{1n} is given by (5.46), whence from (6.10) on $\theta = \pi$, $r = 1+\xi$,

$$\Theta_{11}(\kappa_1 = 0) = \frac{c_3}{16}\int_{-\infty}^{\infty}\int_{-\infty}^{\infty} \frac{\kappa_3^2 f(\kappa_3\xi)\,(\kappa_2^2+\kappa_3^2)\,d\kappa_2 d\kappa_3}{[c_2+\kappa_2^2+\kappa_3^2]^{\frac{17}{6}}}$$
$$= \tfrac{1}{8}c_3 g_2^{\frac{1}{2}}\,(a/L_x)^{\frac{1}{3}}\,G_2[(\tfrac{1}{2}+\tfrac{4}{3})\,I_A - \tfrac{4}{3}I_B], \tag{6.34}$$

where

$$\left.\begin{aligned} g_2 &= 0{\cdot}558, \quad G_2 = \Gamma(\tfrac{1}{2})\,\Gamma(\tfrac{4}{3})/\Gamma(\tfrac{17}{6}),\\ I_A &= \int_0^\infty \frac{b^2 f^2(b\bar{\xi})\,db}{(1+b^2)^{\frac{4}{3}}}, \quad I_B = \int_0^\infty \frac{b^2 f^2(b\bar{\xi})\,db}{(1+b^2)^{\frac{7}{3}}},\\ \bar{\xi} &= (\xi a/L_x)\,g_2^{\frac{1}{2}}, \quad b = \kappa_3/[(a/L_x)\,g_2^{\frac{1}{2}}],\\ f(b) &= e^b E_1(b) + e^{-b}E_i(b). \end{aligned}\right\} \tag{6.35}$$

Again the integrals in (6.35) can only be evaluated in two asymptotic limits. Consider the limit $\bar{\xi} \to 0$; substituting the asymptotic value of $f(b)$ as $b \to 0$ (given in (5.46b)) into (6.35) we find that the integral I_A diverges, in other words does not converge for $b < (a/\eta_K)$, η_K being the Kolmogoroff dissipation scale. However, the infinite integrals I_A and I_B may be rewritten as

$$I_A = \lim_{\substack{\Xi\to\infty\\ \bar{\xi}\to 0}} \left\{\frac{1}{\bar{\xi}^{\frac{1}{3}}}\int_0^\Xi \frac{\bar{b}^2 f^2(\bar{b})\,d\bar{b}}{(\bar{\xi}^2+\bar{b}^2)^{\frac{4}{3}}}\right\}, \quad I_B = \lim_{\substack{\Xi\to\infty\\ \bar{\xi}\to 0}} \left\{\bar{\xi}^{\frac{4}{3}}\int_0^\Xi \frac{\bar{b}^2 f^2(\bar{b})\,d\bar{b}}{(\bar{\xi}^2+\bar{b}^2)^{\frac{7}{3}}}\right\},$$

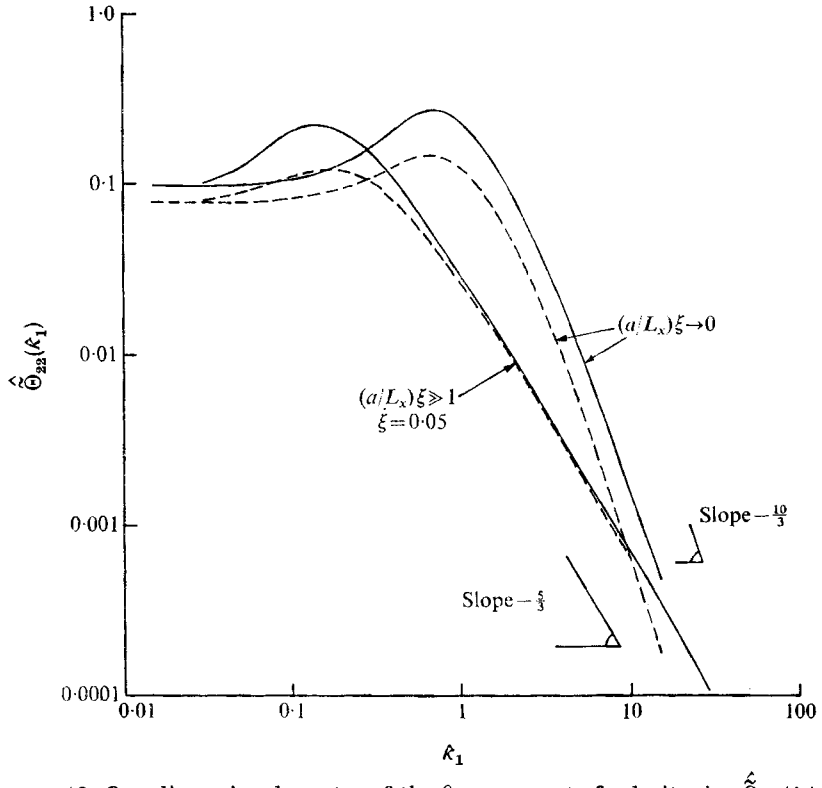

FIGURE 12. One-dimensional spectra of the θ component of velocity, i.e. $\hat{\Theta}_{22}(\hat{\kappa}_1)$, for small-scale turbulence on and near to the surface of the cylinder away from the stagnation point, i.e. when $a/L_x \gg 1$ and $(a/L_x)\,\xi \to 0$ or $(a/L_x)\,\xi \gg 1$ and $\xi \ll 1$. — —, $\theta = \frac{1}{2}\pi$; ———, $\theta, = \frac{3}{4}\pi$.

where $\Xi < \xi a/\eta_K$. Therefore, in the limit

$$\bar{\xi} = \xi(a/L_x)\,g_2^{\frac{1}{2}} \to 0, \quad \xi a/\eta_K \to \infty,$$

$$I_A \sim \bar{\xi}^{-\frac{1}{3}} \int_0^\infty \bar{b}^{-\frac{2}{3}} f^2(\bar{b})\,d\bar{b}, \quad I_B \sim \bar{\xi}^{\frac{8}{3}} \int_0^\infty \bar{b}^{-\frac{8}{3}} f^2(\bar{b})\,d\bar{b}, \tag{6.36a}$$

whence, by evaluating I_A numerically, we find in this limit

$$\hat{\Theta}_{11}(\hat{\kappa}_1 = 0) \sim \frac{(a/L_x)^2\,0{\cdot}0788}{(\xi a/L_x)^{\frac{1}{3}}}. \tag{6.36b}$$

Note that this result is only valid if $\xi \gg \eta_K/a$, in other words it is not valid at a distance from the body equal to the Kolmogoroff dissipation scale. However, this is only of academic interest because, as shown in (5.52*a*), this solution is only valid outside the boundary layer at the stagnation point, i.e. $\xi \gg Re^{-\frac{1}{2}}$. Since $aRe^{-\frac{1}{2}} \gg \eta_K$ for typical laboratory or large-scale flows, (6.36*b*) is valid up to a distance from the body of the order of the boundary-layer thickness. Thus the limitation (6.36*b*) is that (5.52*a*) must be satisfied.

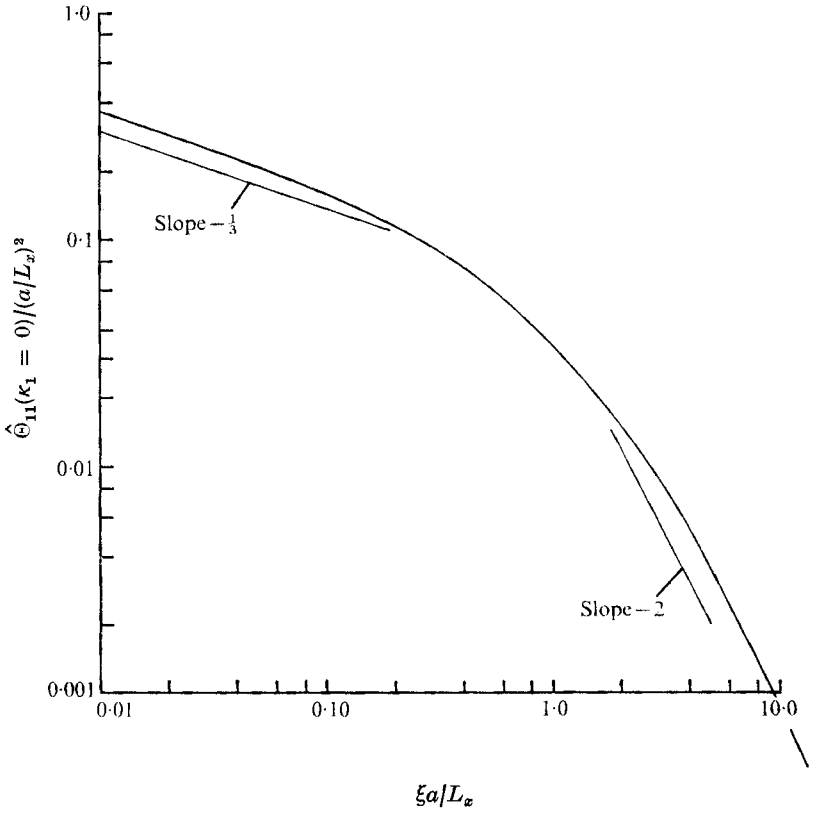

FIGURE 13. The variation with distance from the surface of the zero-frequency value of the spectrum of the x component of velocity on the stagnation line for small-scale turbulence, i.e. $\hat{\Theta}(\hat{\kappa}_1 = 0)$ on $\theta = \pi$ as a function of $\xi a/L_x$ when $a/L_x \gg 1$.

Now consider the limit $\bar{\xi} = \xi(a/L_x)g_2^{\frac{1}{3}} \to \infty$. Since, as $b \to \infty$, $f(b) \sim 2/b$, it follows immediately from (6.34) that, as $\xi(a/L_x) \to \infty$,

$$\hat{\Theta}_{11}(\hat{\kappa}_1 = 0) \sim 1/\pi(2\xi)^2 = 1/\pi U_1^2. \tag{6.37}$$

This result of course agrees with (6.29).

The expression for $\hat{\Theta}_{11}(\hat{\kappa}_1 = 0)$ in the two limiting cases can now be compared with the computed values of $\hat{\Theta}_{11}(\hat{\kappa}_1 = 0)$ in the range $0{\cdot}01 < \xi(a/L_x) < 10{\cdot}0$ shown in figure 13.

The second special case which we consider is $\tilde{\Theta}_{22}(\kappa_1)$ as $\xi(a/L_x) \to 0$, when $a/L_x \gg 1$. Using the value of $\tilde{M}_{2n}(\boldsymbol{\kappa})$ at $\xi = 0$ given in (5.47), and the methods for calculating Θ_{22} in (6.10) and (6.21),

$$\tilde{\Theta}_{22}(\kappa_1) = \frac{c_3\kappa_1^2}{4}\left|\Gamma(-\tfrac{1}{2}i\kappa_1)\right|^2\left[I_C + \left(\frac{1+\cos\theta}{2\sin\theta}\right)^2 I_D\right], \tag{6.38a}$$

where

$$I_C = \int_{-\infty}^{\infty}\int_{-\infty}^{\infty} \frac{e^{\kappa_1\phi}(\kappa_1^2+\kappa_2^2)\,k^2\,d\kappa_2\,d\kappa_3}{(c_2+k^2)^{\frac{17}{6}}(\tilde{\chi}_{23}^2+\tilde{\chi}_1^2)}, \tag{6.38b}$$

$$I_D = \int_{-\infty}^{\infty}\int_{-\infty}^{\infty} \frac{e^{\kappa_1\phi}\kappa_3^2(\kappa_1^2+\kappa_3^2)\,k^2\,d\kappa_2\,d\kappa_3}{(c_2+k^2)^{\frac{17}{6}}(\tilde{\chi}_{23}^2+\tilde{\chi}_1^2)\chi_{23}^2}, \tag{6.38c}$$

$$\phi = \tan^{-1}(\tilde{\chi}_1/\tilde{\chi}_{23}), \quad (-\tfrac{1}{2}\pi < \phi < \tfrac{1}{2}\pi), \quad \tilde{\chi}_1 = 2\kappa_2 \sin\theta + \tfrac{1}{4}\kappa_1(4\cos\theta + 1),$$

$$\tilde{\chi}_{23} = (\kappa_3^2 + \tfrac{1}{4}\kappa_1^2 \cot^2(\tfrac{1}{2}\theta))^{\frac{1}{2}}.$$

These integrals (6.38*b*, *c*) can be performed analytically in two limiting cases: as $\kappa_1 \to 0$, given $\xi a/L_x \to 0$, $a/L_x \gg 1$ $(\theta \neq \pi)$

$$\hat{\tilde{\Theta}}_{22}(\hat{\kappa}_1 = 0) = \frac{1}{2\pi} \frac{1 + 2(\cos\theta + \sin\theta) + \cos^2\theta}{4\sin^2\theta(1 + 2\sin\theta)}. \tag{6.39}$$

Note that this result is independent of a/L_x as $a/L_x \to \infty$. When $\kappa_1 \to \infty$, the evaluation of I_C and I_D is a little more complicated, but since the major contribution to I_C and I_D occurs in the region of wavenumber space where $\phi \simeq \frac{1}{2}\pi$, i.e. $\tilde{\chi}_1 \gg \chi_{23}$ or $\kappa_2 \gg \kappa_1, \kappa_3$, then using (5.48) it follows that as $(a/L_x)\hat{\kappa}_1 = \kappa_1 \to \infty$, and $\xi(a/L_x) \to 0$ $(\theta \neq \pi)$

$$\hat{\tilde{\Theta}}_{22}(\hat{\kappa}_1) \sim G_3 \frac{(2\sin\theta)^{\frac{2}{3}}}{(\frac{1}{2}\cot\frac{1}{2}\theta)^{\frac{5}{3}}} (a/L_x)^{-\frac{5}{3}} \hat{\kappa}_1^{-\frac{10}{3}}, \tag{6.40}$$

where

$$G_3 = \frac{55 \times 0{\cdot}1955}{36\pi \times 4\pi} \frac{\Gamma(\frac{8}{3})\Gamma(\frac{1}{4})\pi^{\frac{1}{2}}}{\Gamma(\frac{3}{4})} = 0{\cdot}0598.$$

For both these limits the important case of $\theta = \pi$ has been excluded. In the case of $\kappa_1 \to 0$, the reason is that for the particular limit $\kappa_1 \to 0$, $\kappa_3 \to 0$, $\kappa_2 \to \infty$ $\tilde{M}_{2n}$ on $\theta = \pi$ is not given by (5.47) (as mentioned in the footnote on page 660). Therefore, if $\theta = \pi$, $\kappa_1 = 0$ and $\kappa_3 \to 0$ the integrand of (6.38*b*) is singular and not valid. $\tilde{M}_{2n}$ in this particular region of wavenumber space has yet to be studied, but it is clear from (6.39) that as $\theta \to \pi$, $\hat{\tilde{\Theta}}_{22}(\hat{\kappa}_1 = 0)$ becomes very large in the limit $a/L_x \gg 1$. In the case $\kappa_1 \to \infty$, at $\theta = \pi$, I_C can be evaluated, the dominant contribution occurring where $\phi \simeq 0$ and $\kappa_3 \gg \kappa_1$, whence as $(a/L_x)\hat{\kappa}_1 = \kappa_1 \to \infty$ and $\xi(a/L_x) \to 0$, on $\theta = \pi$

$$\hat{\tilde{\Theta}}_{22}(\hat{\kappa}_1) \sim G_4 (a/L_x)^{-\frac{8}{3}} \kappa_1^{-\frac{7}{3}} e^{-\frac{1}{2}\pi\kappa_1}, \tag{6.41}$$

where

$$G_4 = \frac{55 \times 0{\cdot}1955 \times \pi^{\frac{1}{2}}\Gamma(\frac{1}{3})\Gamma(\frac{5}{3})}{36\pi \times 4\pi \times (\frac{3}{4})^{\frac{5}{3}}\Gamma(\frac{11}{6})} = 0{\cdot}0566.$$

Note the striking difference in $\hat{\tilde{\Theta}}_{22}(\hat{\kappa}_1)$ as $(a/L_x)\hat{\kappa}_1 \to \infty$ between the stagnation-point region $\theta = \pi$ in (6.41) and the flow further round the cylinder where $\theta < \pi$, shown in (6.40).

Where $\theta < \pi$, $\hat{\tilde{\Theta}}_{22}(\hat{\kappa}_1)$ decreases algebraically as a power of $\hat{\kappa}_1$, in this case $\hat{\kappa}_1^{-\frac{10}{3}}$, whereas at $\theta = \pi$ we find the unusual phenomenon of an exponential decay of the non-dimensional spectrum. However the $\hat{\tilde{\Theta}}_{22}(\hat{\kappa}_1)$ spectrum near $\theta = \pi$ is even more strange because, as (6·40) shows, $\hat{\tilde{\Theta}}_{22}(\hat{\kappa}_1)$ *increases* as $\theta \to \pi$. Therefore near $\theta = \pi$, where $\hat{\kappa}_1 \to \infty$, a sudden *decrease* in $\hat{\tilde{\Theta}}_{22}(\hat{\kappa}_1)$ must occur. (This corresponds to the dominant contribution in integral I_C shifting from the region of $\phi = \frac{1}{2}\pi$ to $\phi = 0$.) Equation (6.39) shows that as $\hat{\kappa}_1 \to 0$ $\Theta_{22}(\hat{\kappa}_1)$ behaves quite differently, between $\theta = \pi$ and $\theta \neq \pi$ in that $\hat{\tilde{\Theta}}_{22}(\hat{\kappa}_1 = 0)$ rapidly increases as $\theta \to \pi$. These surprising phenomena are demonstrated by the graphs of $\hat{\tilde{\Theta}}_{22}(\hat{\kappa}_1)$ as $\xi(a/L_x) \to 0$ at various values of θ shown in figures 12 and 14.

6.3.3. *Variance.* When $a/L_x \gg 1$ and $(a/L_x)\xi \gg 1$, the cross-variance at two

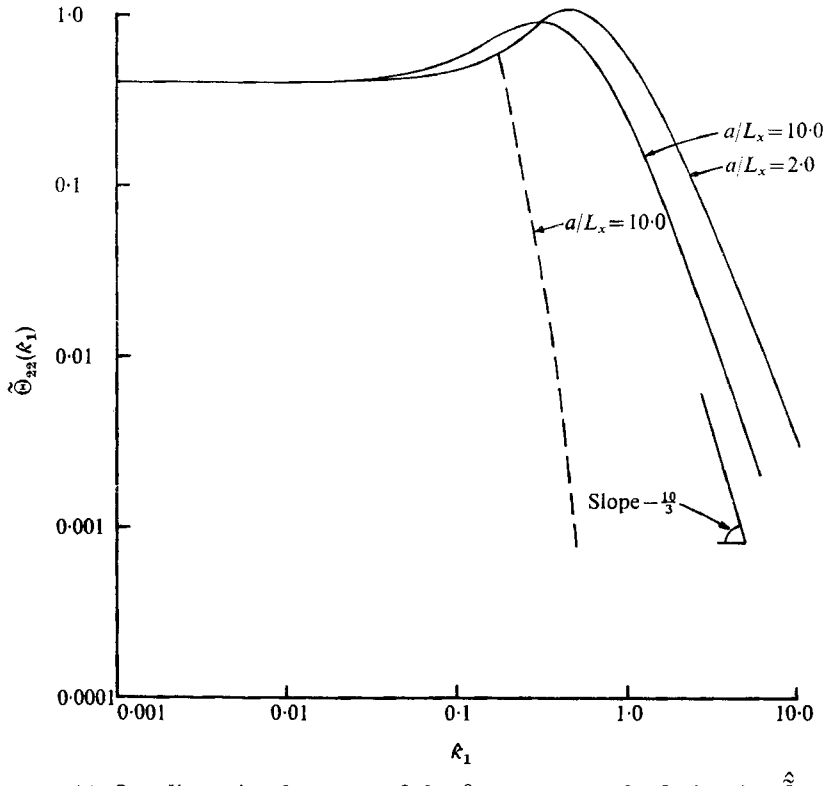

FIGURE 14. One-dimensional spectra of the θ component of velocity, i.e. $\hat{\tilde{\Theta}}_{22}(\kappa_1)$, in the region of the stagnation point at $\xi = 0$ when $a/L_z \gg 1$ (spectrum not calculated when $\kappa_1 \ll 1, \theta = \pi$). — — —, $\theta = \pi$, ——— $\theta = \frac{11}{12}\pi$.

points with time delay is obtained from the definition in (3.33) by using the definition of $\Theta_{ij}(\kappa_1)$ in (6.10) and the simplifying formulae (6.21):

$$R_{ip}(x,y;x',y';r_z,\tau) = c_3 \iiint_{-\infty}^{\infty} \frac{a_{il}^{(d)\dagger}(\mathbf{x},\boldsymbol{\kappa})\, a_{ps}^{(d)}(\mathbf{x}',\boldsymbol{\kappa})\, e^{-i\kappa_1\tau} \exp(i\kappa_3 r_z)\,(k^2\delta_{ls}-\kappa_l\kappa_s)\, d\kappa_1 d\kappa_2 d\kappa_3}{(c_2+k^2)^{\frac{17}{6}}}. \quad (6.42)$$

In general a triple integral must be evaluated to calculate R_{ip}, but there are some important cases where only double integrals need be evaluated.

The 'pseudo-Lagrangian' covariance we defined in §6.2.2 is the one case, where $\tau \neq 0$, in which (6.42) reduces to a double integral. In this case since

$$\Psi'(\mathbf{x}') = \Psi'(\mathbf{x}), \quad \tau = T(\mathbf{x}') - T(\mathbf{x}) \quad \text{and} \quad r_z = 0$$

it follows from (6.22) that (6.42) becomes

$$R_{ip}(x,y;x',y';0,\tau) = c_3 \iiint_{-\infty}^{\infty} \frac{L_{il}(\mathbf{x},\boldsymbol{\kappa})\, L_{ps}(\mathbf{x}',\boldsymbol{\kappa})\,(k^2\delta_{ls}-\kappa_l\kappa_s)\, k^2 d\kappa_1 d\kappa_2 d\kappa_3}{(c_2+k^2)^{\frac{17}{6}}}. \quad (6.43)$$

Since from (6.22) $L_{in}(\mathbf{x}, \boldsymbol{\kappa})$ is linear in χ_j, which in turn is linear in κ_j, and if κ_i is written in spherical polar co-ordinates $\kappa_i = k\kappa_i^{\times}$, where

$$\kappa_i^{\times} = (\cos\sigma_1, \sin\sigma_1\cos\sigma_2, \sin\sigma_1\sin\sigma_2),$$

then $\chi_i = k\chi_i^{\times}(\sigma_1, \sigma_2)$ may be defined and (6.43) becomes

$$R_{ip}(x, y; x', y'; 0, \tau) = \int_0^{\infty} \frac{E(k)\,dk}{4\pi} \left[\int_0^{\pi} \left\{ \int_0^{2\pi} \epsilon_{ijk}\epsilon_{pqr}\chi_j^{\times}(\mathbf{x})\chi_q^{\times}(\mathbf{x}')\gamma_{kl}(\mathbf{x})\gamma_{rs}(\mathbf{x}') \times \frac{(\delta_{ls} - \kappa_l^{\times}\kappa_s^{\times})\sin\sigma_1\,d\sigma_2}{\chi^{\times 2}(\mathbf{x})\chi^{\times 2}(\mathbf{x}')} \right\} d\sigma_1 \right], \quad (6.44)$$

where

$$\chi_1^{\times} = \cos\sigma_1\,\partial T/\partial x - \sin\sigma_1\cos\sigma_2\,U_2, \quad \chi_2^{\times} = \cos\sigma_1\,\partial T/\partial y + \sin\sigma_1\cos\sigma_2\,U_1,$$

$$\chi_3^{\times} = \sin\sigma_1\sin\sigma_2, \quad (\chi^{\times})^2 = \sum_{i=1}^{3} (\chi_i^{\times})^2.$$

Note that

$$\int_0^{\infty} E(k)\,dk = \tfrac{3}{2}u_{\infty}'^2,$$

so that the result (6.44) is independent of the form of the upstream spectrum. The technique is due to Batchelor & Proudman (1954). The integral has been evaluated and will be published in its relevant context of turbulent diffusion.

Restricting the calculation to the variance at a point and using the notation of (6.44),

$$\frac{\overline{u_i(x,y)\,u_p(x,y)}}{\overline{u_{\infty 1}^2}} = \frac{3}{8\pi}\int_0^{\pi}\int_0^{2\pi} \frac{\epsilon_{ijk}\epsilon_{pqr}\chi_j^{\times}\chi_q^{\times}\gamma_{kl}\gamma_{rs}(\delta_{ls} - \kappa_l^{\times}\kappa_s^{\times})}{\chi^{\times 4}} \sin\sigma\,d\sigma_2\,d\sigma_1. \quad (6.45)$$

Note that, unlike the symmetrical flows considered by Batchelor & Proudman (1954), $\overline{u_i u_p} \neq 0$ if $i \neq j$, except on $\theta = \pi$. We now use (6.45) to evaluate $\overline{u_1^2}$ on $\theta = \pi$ and $\theta = \frac{1}{2}\pi$.

On $\theta = \pi$,

$$\overline{u_1^2}/\overline{u_{\infty 1}^2} = \frac{3}{8\pi U_1^2}\int_0^{\pi} \sin\sigma_1 \left(\int_0^{2\pi} (I_E + I_F)\,d\sigma_2 \right) d\sigma_1, \quad (6.46)$$

where

$$I_E = \sin^4\sigma_1(\sin^2\sigma_2 + U_1^2\cos^2\sigma_2)^2/\chi^{\times 4},$$

$$I_F = \sin^2\sigma_1\cos^2\sigma_1(\sin^2\sigma_2 + U_1^4\cos^2\sigma_2)/\chi^{\times 4},$$

$$\chi^{\times 2} = \cos^2\sigma_1 + \sin^2\sigma_2\cos^2\sigma_1\,U_1^4 + \sin^2\sigma_1\sin^2\sigma_2\,U_1^2.$$

Batchelor & Proudman (1954) showed that this double integral can be found exactly in terms of elliptic integrals, but it is equally convenient to examine its asymptotic properties and compute intermediate values. They found that as $r \to \infty$ (or $U_1 \to 1$)

$$\overline{u_1^2}/\overline{u_{\infty 1}^2} = 1,$$

and in the limit

$$\left.\begin{aligned} (a/L_x) \to \infty, \quad (a/L_x)\,\xi \to \infty, \quad \xi \to 0 \quad (\text{or } U_1 \to 0) \\ \overline{u_1^2}/\overline{u_{\infty 1}^2} = \tfrac{3}{4}[1/U_1 + \tfrac{1}{2}U_1\ln(4/U_1) + \ldots]. \end{aligned}\right\} \quad (6.47)$$

This result is in fact valid for any stagnation-line flow, and was used by Bearman (1972) for comparison with his experimental results. The results of computing

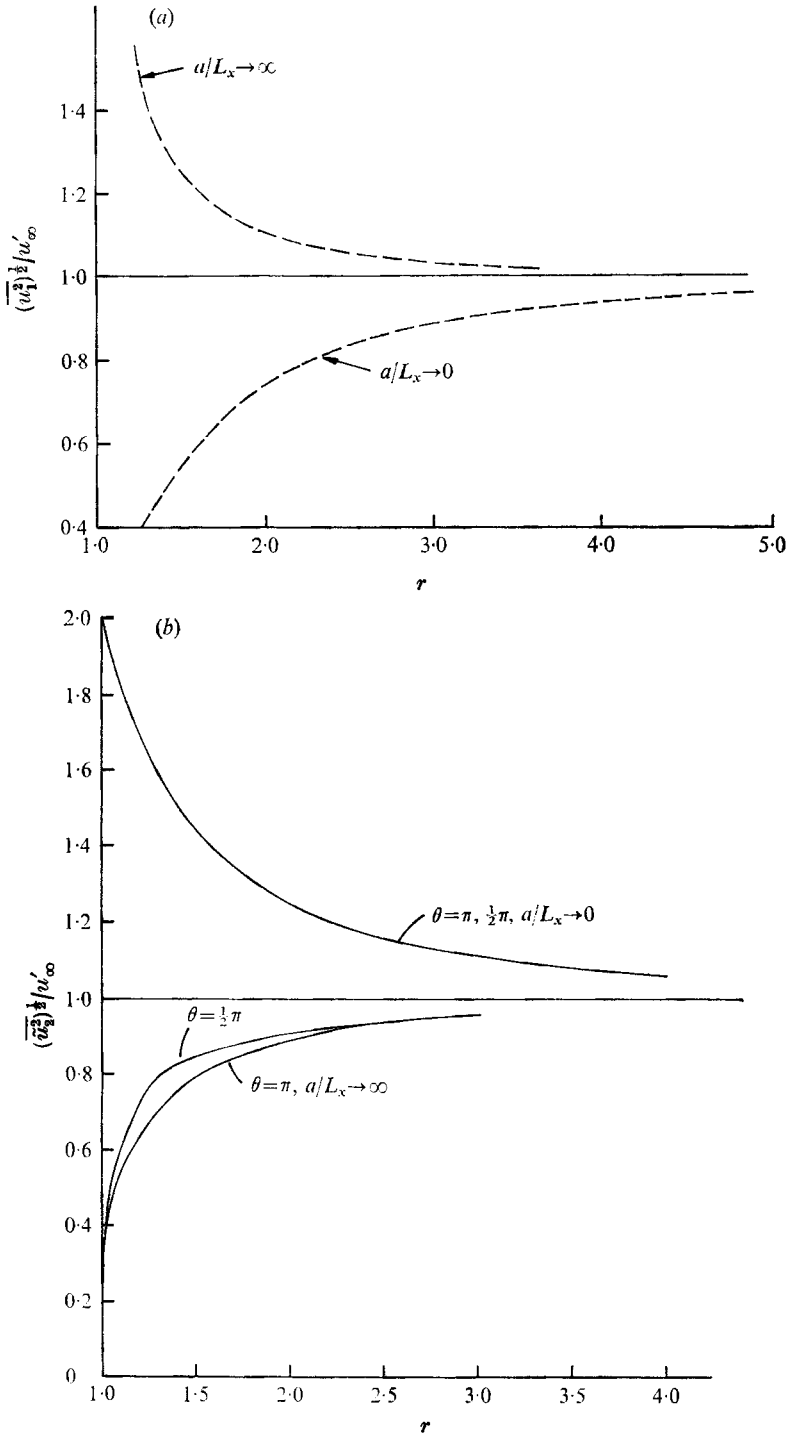

FIGURE 15. Variation of the r.m.s. turbulent velocity components in the radial and tangential directions for the limiting cases of very large and very small scales of turbulence. (*a*) $[(\overline{u_1^2})^{\frac{1}{2}}/u'_\infty](r)$ on $\theta = \pi$ when $a/L_x \to 0$, and $a/L_x \to 0$, $(a/L_x)\,\xi \to \infty$. (*b*) $[(\overline{u_2^2})^{\frac{1}{2}}/u'_\infty](r)$ at $\theta = \pi$, $\theta = \frac{1}{2}\pi$ when $a/L_x \to 0$, and $a/L_x \to \infty$, $(a/L_x)\,\xi \to \infty$.

(6.46) in the form of a curve of $(\overline{u_1^2}/\overline{u_{\infty 1}^2})^{\frac{1}{2}}(r)$ on $\theta = \pi$ in the limit $a/L_x \to \infty$, $(a/L_x)\,\xi \gg 1$ is shown in figure 15(*a*). Also shown is the curve of $(\overline{u_1^2}/\overline{u_{\infty 1}^2})^{\frac{1}{2}}(r)$ when $a/L_x \to 0$, taken from (6.20). Results for $\overline{u_2^2}/\overline{u_{\infty 1}^2} = \overline{\tilde{u}_2^2}/\overline{u_{\infty 1}^2}$ and $\overline{u_3^2}/\overline{u_{\infty 1}^2}$, using Batchelor & Proudman's results, are shown in figure 15(*b*) and Bearman's paper respectively. It is useful to restate the asymptotic results that in the limit $a/L_x \to \infty$, $(a/L_x)\,\xi \to \infty$ as $\xi \to 0$ ($U_1 \to 0$)

$$\left.\begin{aligned} \overline{u_2^2}/\overline{u_{\infty 1}^2} &\sim \tfrac{3}{4}U_1(\ln(4/U_1) - 1), \\ \overline{u_3^2}/\overline{u_{\infty 1}^2} &\sim \tfrac{3}{4}(1/U_1 - \tfrac{1}{2}U_1 \ln(4/U_1)\ldots). \end{aligned}\right\} \tag{6.48}$$

On $\theta = \frac{1}{2}\pi$ from (6.45)

$$\frac{\overline{u_1^2}}{\overline{u_{\infty 1}^2}} = \frac{\overline{\tilde{u}_2^2}}{\overline{u_{\infty 1}^2}} = \frac{3}{8\pi}[I_G + I_H + I_J], \tag{6.49}$$

where

$$I_G = \frac{1}{U_1^2}\int_0^{\pi}\int_0^{2\pi} \frac{\sin^2\phi \sin^2\sigma_1(\cos^2\sigma_1 + \sin^2\sigma_1 \sin^2\sigma_2)}{\chi^{\times 4}} \sin\sigma_1 \, d\sigma_2 \, d\sigma_1,$$

$$I_H = \frac{2}{U_1}\int_0^{\pi}\int_0^{2\pi} \frac{(\cos\sigma_1 \, \partial T/\partial y + U_1 \sin\sigma_1 \cos\sigma_2)}{\chi^{\times 4}} \sin^4\sigma_1 \cos\sigma_2 \sin^2\sigma_2 \, d\sigma_2 \, d\sigma_1,$$

$$I_J = \int_0^{\pi}\int_0^{2\pi} \frac{(\cos^2\sigma_1 + \sin^2\sigma_1 \cos^2\sigma_2)[(\partial T/\partial y)\cos\sigma_1 + U_1 \sin\sigma_1 \cos\sigma_2]^2}{\chi^{\times 4}} \sin\sigma_1 \, d\sigma_2 \, d\sigma_1,$$

$$\chi^{\times 2} = \cos^2\sigma_1/U_1^2 + \sin^2\sigma_1 \sin^2\sigma_2 + [(\partial T/\partial y)\cos\sigma_1 + U_1 \sin\sigma_1 \cos\sigma_2]^2.$$

Note that the form of these integrals is different from those required to find $\overline{u_1^2}$ on $\theta = \pi$ because in travelling to $\theta = \frac{1}{2}\pi$ the vortex lines have been rotated as well as strained. The effect of rotation leads to terms like

$$(\partial T/\partial y \cos\sigma_1 + U_1 \sin\sigma_1 \cos\sigma_2)$$

in $\chi^{\times 2}$. It is easily seen that, as $\tau \to 1$, $\overline{u_1^2}/\overline{u_{\infty 1}^2} \to 1$. Close to the surface of the cylinder, in the limit $(a/L_x)\,\xi \to \infty$, $\xi \to 0$, where $U_1 \to 2$ and $\partial T/\partial y \sim -1/(2\xi)$,

$$\frac{\overline{u_1^2}}{\overline{u_{\infty 1}^2}} \sim \frac{G_5}{|\partial T/\partial y|} \ln|\partial T/\partial y| = -2G_5 \xi \ln\xi, \tag{6.50}$$

where $G_5 = \frac{3}{4}$.

The results of computing (6.49) are presented in a graph of $(\overline{\tilde{u}_2^2}/\overline{u_{\infty 1}^2})^{\frac{1}{2}}(r)$ on $\theta = \pi$, $\frac{1}{2}\pi$ in figure 15(*b*). Curves are also presented for large-scale turbulence $a/L_x \to 0$ using (6.20), and show no difference between $\theta = \pi$, $\frac{1}{2}\pi$! (In reality there will be less amplification at $\theta = \frac{1}{2}\pi$.) Note that the asymptotic forms at $\theta = \frac{1}{2}\pi$, as $\xi \to 0$, are similar when $a/L_x \to \infty$, which is also borne out by (6.48) and (6.50).

When $a/L_x \gg 1$, but $(a/L_x)\,\xi = O(1)$, the only complete spectrum which can be straightforwardly obtained is $\tilde{\Theta}_{22}(\kappa_1)$ at $\zeta = 0$. Even then to calculate $\overline{\tilde{u}_2^2}$ at $\xi = 0$ requires considerable further computing, which has not yet been performed. Since $\Theta_{11}(\kappa_1)$ has not yet been calculated over the full range $0 < \kappa_1 < \infty$ when $(a/L_x)\,\xi = O(1)$, neither has $\overline{u_1^2}$.

6.3.4. *Physical interpretation of results for small-scale turbulence.* Although some comments have already been made in §5.3.3 on the physical effects which

give rise to changes in the velocity tensor $M_{in}(\mathbf{x}, \boldsymbol{\kappa})$ it is now interesting to consider the spectra of the velocity to see which of the various effects are dominant, or equivalently which part of wavenumber space is dominant.

Consider first the results for the spectrum of the normal component of the velocity $\hat{\Theta}_{11}(\hat{\kappa}_1)$ close to the body on the stagnation line. If the distance from the body is large compared with a typical eddy size (i.e. $(a/L_x)\,\xi \gg 1$) then at low frequencies the amplification of u_1 by vortex stretching, discussed in §5.3.3, leads to the result that $\hat{\Theta}_{11}(\hat{\kappa}_1 = 0) \propto 1/U_1^2$. At high frequencies the 'piling-up' effect diminishes the vortex stretching and consequently the amplification of $\hat{\Theta}_{11}(\hat{\kappa}_1 \to \infty)$ is only proportional to $U_1^{-\frac{1}{3}}$. The more surprising result is that at the low-frequency end of the spectrum $\hat{\Theta}_{11}(\kappa_1 = 0)$ continues to increase as the body is approached even when the distance from the body is small compared with a typical eddy size ($(a/L_x)\,\xi \ll 1$, equation (6.36*b*)). The reason is that, although for each wavenumber the normal component of the velocity tensor $\tilde{M}_{1l} = 0$ at the surface $\xi = 0$ (owing to the blocking effect), for a given value of $\xi > 0$, $\tilde{M}_{1l}$ increases as κ_3 (or the intensity of the vorticity) increases. In other words, at a point however close to the body there is a value of κ_3 such that $|\tilde{M}_{1l}| > 0$. Therefore in our inviscid approximation $\hat{\Theta}_{11}(\hat{\kappa}_1 \to 0)$ increases as $\xi \to 0$, although it increases more slowly when $(a/L_x)\,\xi \ll 1$, being proportional to $U_1^{-\frac{1}{3}}$, as compared with U_1^{-2} when $(a/L_x)\,\xi \gg 1$. However, for a viscous fluid this singular amplification is halted at the outer edge of the stagnation-point boundary layer. Note that at sufficiently high frequencies ($\kappa_1 \to \infty$), $\hat{\Theta}_{11}(\hat{\kappa}_1)$ behaves in the same way as in the region where $(a/L_x)\,\xi \gg 1$, and increases like $U_1^{-\frac{1}{3}}$. Qualitatively similar results may be expected for $\hat{\Theta}_{11}(\hat{\kappa}_1)$ when $\theta \neq \pi$.

The main result for the $\overline{u_1^2}$ on the stagnation line, obtained from integrating the spectrum, is that, when $(a/L_x)\,\xi \gg 1$, $\overline{u_1^2}$ increases in proportion to U_1^{-1}. The amplification, as might be expected, is less than that at low frequencies and greater than at high frequencies. Since the complete spectrum when $(a/L_x)\,\xi \ll 1$ has not been computed, it is only possible to speculate that in this region $\overline{u_1^2}$ increases approximately in proportion to $U_1^{-\frac{1}{3}}$, this reduction in the rate of increase being due to the blocking effect.

The spectrum $\hat{\Theta}_{22}(\hat{\kappa}_1)$ of the tangential component of the velocity close to the body has a very different behaviour from $\hat{\Theta}_{22}(\hat{\kappa}_1)$ upstream and is quite different at the stagnation point $\theta = \pi$ compared with elsewhere round the cylinder. When $(a/L_x)\,\xi \gg 1$ and at low frequencies the spectrum exhibits a flattish peak, which at the maximum point may be three times the maximum value of the incident spectrum (figure 11). This peak occurs where $\kappa_1 \simeq U_1$ and is induced by the axial component of vorticity ω_3. It has the same form all round the surface. At high frequencies the spectrum decays with a $-\frac{5}{3}$ law, but with no vortex stretching to amplify the velocity, $\hat{\Theta}_{22}(\hat{\kappa}_1)$ is much smaller than $\hat{\Theta}_{11}(\kappa_1)$ as $\hat{\kappa}_1 \to \infty$. Equation (6.32*c*) shows that on $\theta = \pi$ $\hat{\Theta}_{22}(\hat{\kappa}_1) \propto U_1^{\frac{5}{3}} \hat{\kappa}_1^{-\frac{5}{3}}$. Figure 12 shows that at high frequencies $\hat{\Theta}_{22}(\hat{\kappa}_1)$ is larger downstream of the stagnation point. Within an eddy size of the body, i.e. $(a/L_x)\,\xi \ll 1$, the spectrum changes considerably. In figures 12 and 14 the spectra have also been calculated at $\xi = 0$, i.e. at the outer edge of the boundary layer, and they showed marked differences between $\theta = \pi$ and $\theta \neq \pi$. It was mentioned in §5.3.3 that at low frequencies the θ component of

velocity $\tilde{M}_{2n}$ is $O(1)$, except at $\theta = \pi$ when $\kappa_1 = \kappa_3$ and $\kappa_2 \to \infty$. Then $\tilde{M}_{2n}$ is $O(k^{\frac{1}{2}})$ and $\hat{\tilde{\Theta}}_{22}(\hat{\kappa}_1 \to 0)$ becomes very large. The details of this singular region of wavenumber space have not all been worked out yet. It is interesting that at $\xi = 0$ when $\theta \neq \pi$ the maximum value in the spectrum of $\hat{\tilde{\Theta}}_{22}(\hat{\kappa}_1)$ does not occur at $\hat{\kappa}_1 = 0$, as shown by the spectra at $\theta = \frac{11}{12}\pi$ (or 15° from the stagnation point) and $\theta = \pi$ in figure 14. This figure also shows how the turbulence close to the surface in the region of the stagnation point changes very rapidly when $\kappa_1 \to \infty$. Then the fact that on $\theta = \pi$ the Fourier transform, $\tilde{M}_{2j}$ of $\tilde{u}_2$ has an exponential decay with κ_1 for all values of κ_2 and κ_3 inevitably implies that $\hat{\tilde{\Theta}}_{22}(\hat{\kappa}_1)$ has an exponential decay, as shown in figure 14. But when $\theta \neq \pi$, $|\tilde{M}_{2j}|$ only decays exponentially with κ_1 over a limited range of values of κ_2 and κ_3. For other values of κ_2 and κ_3, $|\tilde{M}_{2j}|$ increase with κ_1. Therefore $\hat{\tilde{\Theta}}_{22}(\hat{\kappa}_1)$ decays with κ_1 much more slowly for $\theta \neq \pi$ than at $\theta = \pi$. In fact we find in (6.40) the interesting result that

$$\hat{\tilde{\Theta}}_{22}(\hat{\kappa}_1) \propto \hat{\kappa}_1^{-\frac{10}{3}}.$$

6.4. *Validity of spectra*

Although we discussed in §5.3.1 the distance from the body and the range of wavenumber space in which our solutions for $M_{ij}(\boldsymbol{\kappa})$ are valid, it is also important to determine how these limitations affect the validity of the calculations of spectra, in §§6.2 and 6.3. It has been shown how these calculations give different weight to different parts of wavenumber space depending on the values of a/L_x and κ_1. In particular the energy-containing part of the spectrum is where

$$\hat{\kappa}_1 \lesssim 1 \quad \text{or} \quad \kappa_1 \lesssim a/L_x.$$

Therefore if $a/L_x \lesssim 1$, using the result (5.5.2a), it follows that the solutions for the velocity spectra in §6.2 are valid if

$$\xi \gg Re^{-\frac{1}{2}}. \tag{6.51}$$

On the other hand, if $a/L_x \gg 1$, so that much of the energy occurs when $\kappa_1 \gg 1$, it follows from (5.52b) that the solutions for the velocity spectra in §6.3 are only valid if

$$\xi \gg \kappa_1^{\frac{1}{2}} Re^{-\frac{1}{2}} \quad \text{or} \quad \xi \gg (a/L_x)^{\frac{1}{2}} Re^{-\frac{1}{2}}. \tag{6.52}$$

This implies that if $a/L_x \gg 1$ viscous dissipation affects the distortion of the turbulence well outside the boundary layer on the body's surface, a phenomenon which was observed by Sadeh, Sutera & Maeder (1970b). A further implication of (6.52) is that the results of §6.3.2 for spectra sufficiently close to the surface that $(a/L_x)\,\xi \ll 1$ are only valid if

$$(a/L_x)^{-1} \gg \xi \gg (a/L_x)^{\frac{1}{2}} Re^{-\frac{1}{2}},$$

whence

$$a/L_x \ll Re^{\frac{1}{3}}. \tag{6.53}$$

It was shown in §5.3.1 that nonlinear terms in the equations for two components of vorticity could not be ignored close to the surface, unless as $\xi \to 0$,

$$\left.\begin{aligned} &\alpha \ll \xi \quad \text{if} \quad \kappa_1 = O(1), \\ \text{or} \quad &\beta \kappa_1^{-1} \ll \xi \quad \text{if} \quad \kappa_1 \gg 1. \end{aligned}\right\} \tag{6.54}$$

We were not able to show whether or not this condition also had to be satisfied for the r and θ velocity components to be correctly evaluated. Thus a *sufficient* condition for $\tilde{\Theta}_{11}$ and $\tilde{\Theta}_{22}$ to be valid as $\xi \to 0$ is that (6.54) be satisfied, but this condition probably underestimates the magnitude of α that is strictly necessary. On the other hand Θ_{33} is valid as $\xi \to 0$ provided that $\beta \ll 1$ and (6.53) is satisfied.

For small scales of turbulence at low frequencies, at points further from the body than one or two eddy sizes (i.e. $a/L_x \gg 1$, $\kappa_1 \ll 1$ and $\xi(a/L_x) \gg 1$) it has been assumed that, when integrating over all wavenumber space for κ_2 and κ_3, there is a negligible contribution from the region of wavenumber space where κ_2, $\kappa_3 \ll 1$. The reason for this assumption is that, when $k \to 0$, $M_{il}(\boldsymbol{\kappa})$ is regular everywhere in the flow, so that any error in $\hat{\Theta}_{11}(\hat{\kappa}_1 \to 0)$ is $O((a/L_x)^{-4})$. This error is much smaller than that caused by neglecting the higher order terms in the expression for Ω_{ij} in (5.27), which typically are $O[(a/L_x)^{-2}]$.

Another assumption that has been made in the calculations of spectra is that, when $(a/L_x)\,\xi \ll 1$ and $a/L_x \gg 1$ or $\kappa_1 \xi \ll 1$ and $\kappa_1 \gg 1$, the condition (5.39) that $\kappa_1 \ll (\tilde{\chi}_1^2 + \tilde{\chi}_{23}^2)^{\frac{1}{2}}$ is satisfied. If $(a/L_x) \gg 1$ and $\kappa_1 \ll (1a/L_x)$, then inspection of (6.34) and (6.38) reveals that the dominant contributions to the spectra come from the region in wavenumber space where $(\kappa_3^2 + \kappa_2^2)^{\frac{1}{2}} \sim a/L_x$. For high frequencies, $\kappa_1 \gg 1$ where $\kappa_1 \xi \ll 1$, the dominant contribution to $\hat{\tilde{\Theta}}_{22}(\hat{\kappa}_1)$ comes from the region in wavenumber space where $\kappa_3 \gg \kappa_1$ when $\theta = \pi$, but, when $\theta \neq \pi$, $\kappa_2 \gg \kappa_3, \kappa_1$. Thus in these limiting situations the basic assumption for our calculation of $M_{il}(\boldsymbol{\kappa})$ when $k\xi \ll 1$ is satisfied.

Another criterion for the validity of the analysis which must be satisfied is the statistical uniformity of the incident turbulence. It would appear that, if $a/L_x \ll 1$, then the turbulence must be uniform over a distance large compared with L_x, but that, if $a/L_x \gg 1$, then this distance is a. By recasting the analysis it may be possible to calculate the turbulence when the incident turbulence is non-uniform over a distance comparable with the body size.

7. Discussion

7.1. *Interpolation and approximation*

Although the calculations of spectra and variances in § 6 were only performed for the limiting cases of turbulence of very large scale and very small scale, it is possible to draw some conclusions about the behaviour of turbulence which has a scale comparable with the size of the body, i.e. $a/L_x \sim 1$. Consider $\hat{\tilde{\Theta}}_{11}(\hat{\kappa}_1)$ on the stagnation line say at $r = 1{\cdot}1$ when $a/L_x \simeq 0{\cdot}1$. Then, when $\hat{\kappa}_1 \ll 1$, it might be expected that $\hat{\tilde{\Theta}}_{11} \gtrsim \hat{\tilde{\Theta}}_{11}^{(0)}$ because $|M_{11}|$ increases rapidly as κ_3 increases, but on the other hand at very high frequencies such that $\hat{\kappa}_1(a/L_x) = \kappa_1 \gg 1$, i.e. $\hat{\kappa}_1 \gg 10$, $\hat{\tilde{\Theta}}_{11}(\hat{\kappa}_1)$ would be given by the result for small-scale or high-frequency turbulence. Interpolating between these two limits and using the fact that the tabulated results show that $|M_{11}(\boldsymbol{\kappa})|$ lies between the asymptotic values for $k \to 0$ and $k \to \infty$, we can draw a dashed line to suggest the probable form of $\hat{\tilde{\Theta}}_{11}(\hat{\kappa}_1)$, as shown on figure 16. To take another example, when $a/L_x = 2{\cdot}0$, we can estimate $\hat{\tilde{\Theta}}_{11}(\hat{\kappa}_1 = 0)$ using the result for $a/L_x \gg 1$ and $(a/L_x)\,\xi \ll 1$ given by (6.36*b*), and when $\hat{\kappa}_1 \gg 5$ use the results for the case where $\kappa_1 \gg 1$ and $\kappa_1 \xi \gg 1$, given by

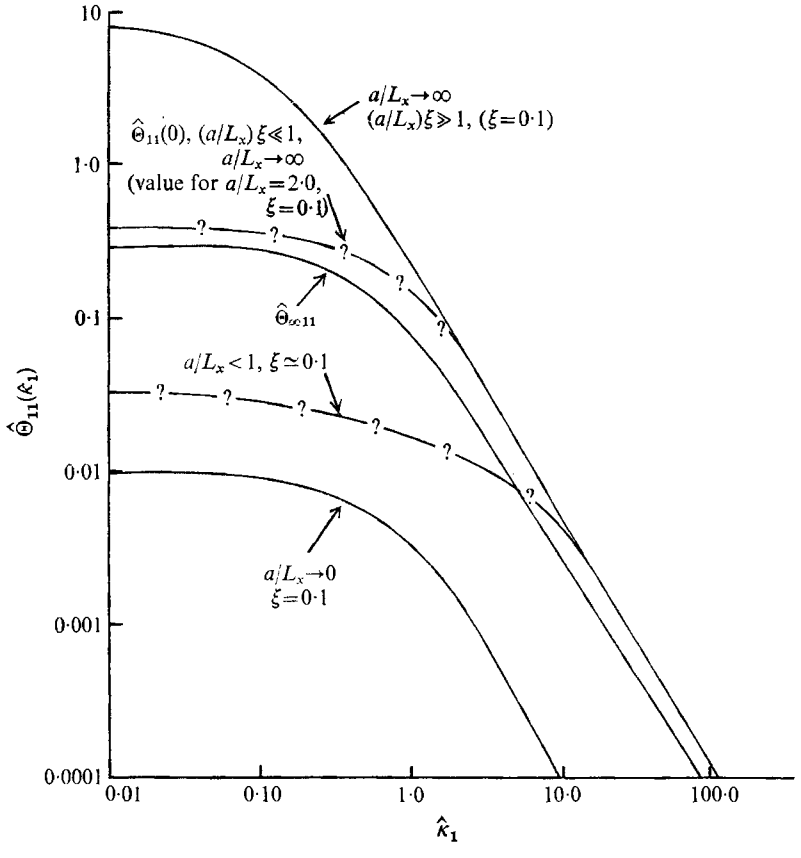

FIGURE 16. One-dimensional spectrum of the x component of velocity on the stagnation line, i.e. $\hat{\Theta}_{11}(\hat{\kappa}_1)$, showing the asymptotic limits $a/L_x \to 0$ and $a/L_x \to \infty$, and the approximate forms expected for intermediate values of a/L_x.

(6.23). The interpolation is again shown in figure 16. A similar investigation can be performed with $\hat{\hat{\Theta}}_{22}(\hat{\kappa}_1)$ and will be presented in a later paper when comparing experimental and theoretical results.

The important result of this examination of the limiting cases and of the tabulations of M_{ll} for $k \sim 1$ is that it *suggests* that for most of the range of $\hat{\kappa}_1$ on the line $\theta = \pi$

$$\lim_{a/L_x \to \infty} \{\hat{\Theta}_{11}(\hat{\kappa}_1)\} \geqslant \hat{\Theta}_{11}(\kappa_1) \geqslant \lim_{a/L_x \to 0} \{\hat{\Theta}_{11}(\kappa_1)\} \tag{7.1}$$

and consequently

$$\lim_{a/L_x \to \infty} \{\overline{u_1^2}(x)\} \geqslant \overline{u_1^2}(x) \geqslant \lim_{a/L_x \to 0} \{\overline{u_1^2}(x)\}.$$

Although plausible interpolations are possible for $\hat{\hat{\Theta}}_{22}(\hat{\kappa}_1)$ on the stagnation line, because of the hump in the solution for $\hat{\hat{\Theta}}_{22}(\kappa_1)$ as $\xi \to 0$ no criterion such as (7.1) can be proposed.

This qualitative interpolation argument can be quantified but not made any more rigorous by making the approximation that over the wavenumber range

$\kappa < \kappa_t$ $M_{ll}(\kappa)$ is equal to its asymptotic value as $k \to 0$, given by (5.39). The transition wavenumber κ_t is defined by inspecting the computed and asymptotic results in tables 1 and 2. It is found that $|\kappa_t|$ lies between 1·0 and 2·0.

For $\kappa > \kappa_t$ $M_{ll}(\kappa)$ could be approximated by the asymptotic solutions for M_{ll} as $k \to \infty$, (5.43) or (5.45) depending on whether $k\xi < 1$ or $k\xi > 1$. The tabulated values of $M_{ll}(\kappa)$ can be used to determine the value of κ_t. This procedure can be adopted to provide highly approximate numerical values for all wavenumbers and integral scales. Some provisional results using this method were published by Hunt (1971). However, it may be preferable to make experimental measurements rather than devise an elaborate calculation procedure such as this.

7.2. *Applicability of the theory*

The actual turbulent flow which has been analysed in this paper is not of course physically realizable at all points around the body, However, there are reasons to believe that the velocities predicted over certain parts of the flow can be used to predict experimental results. Consider the particular case studied here of a circular cylinder, where on account of the assumption (As 1) that no separation occurs, the expression for the mean velocity **U** is only a good representation of a real flow in the region near the front stagnation point (and even then is not very accurate because the wake also affects the flow in this region). Near $\theta = \frac{1}{2}\pi$ the theoretical mean velocity is a very poor representation, and consequently so are the expressions for Δ_T and Δ_y. In addition, the boundary condition on the turbulence must be wrong because here the flow separates. However, the direction and variation with radius of the mean velocity is approximately represented near $\theta = \frac{1}{2}\pi$ and therefore the correct qualitative predictions might be expected from the theory. Having ignored the existence of the wake by (As 1), it was necessary to make further artificial assumptions about the turbulent vorticity downstream of the body, (As 2) and (As 3). These assumptions will have much less effect on the calculations of turbulent velocities upstream of the separation point than (As 1) has on mean velocities. Thus (As 1) is the most critical assumption. It is probably worth abandoning this assumption and using a wake model to represent the mean velocity (such as used by Bearman 1972) only in order to calculate turbulent velocities more accurately near $\theta = \frac{1}{2}\pi$ for the limiting cases of $a/L_x \ll 1$ and $a/L_x \gg 1$, because only then are the boundary conditions known: in the former case they are the same as for the mean velocity and in the latter case upstream of separation the boundary condition remains $\mathbf{u}.\mathbf{n} = 0$.

If $a/L_x \sim 1$ the flow can be accurately calculated near $\theta = \frac{1}{2}\pi$ only when the interaction of the wake boundary and the incident turbulence is understood. As a first step, we have made the assumption in § 2 that if $u'_\infty/\overline{u}_\infty \ll 1$ the incident turbulence and the turbulence induced by the wake are statistically independent, an assumption which should be fairly accurate in the stagnation region for all values of a/L_x. This assumption has some experimental support even when $a/L_x \sim 1$ and $\theta = \frac{1}{2}\pi$ (Petty 1974). There are some exceptional situations, when the theory will not be valid anywhere in the flow, one of which occurs if the Reynolds number and $u'_\infty/\overline{u}_\infty$ are sufficiently large that the incident turbulence induces transition in the body's boundary layer. Then rapid changes in the

position of separation and the position of mean separation may occur and result in $O(1)$ changes in the mean velocity. Another exceptional situation is where the body (e.g. a rectangular prism) is such that a small change in the angle of incidence of the mean velocity of $O(u'_\infty/\overline{u}_\infty)$ produces an $O(1)$ change in the mean velocity near the body by including a large change in the position of separation. Clearly these particular cases need a careful study.

The theory of this paper is well worth applying to turbulent flows over other two-dimensional bodies. In principle the most suitable application is for bodies from which no separation occurs but which introduce significant distortions into the flow, for example a flat plate normal to a stream with a filled-in wake (Bearman 1972) or an aerofoil at incidence, or a 'Rankine solid' Note that a stagnation point where Δ_T is singular may not always occur, for example for a square prism at 45° to the flow. In these and other flows where the mean velocity is known it is simple to calculate velocities and pressures to zero order in the limits as $a/L_x \to 0$, assuming the result of §6.2 that quasi-steady solutions give this limiting solution can be generalized and as $a/L_x \to \infty$. In particular this means that in these limits, given that the conditions (2.7)–(2.10) are satisfied, $\overline{u_i^2}$ and $\hat{\Theta}_{ii}$ ($i = 1, 2, 3$; with the exception of $\overline{u_2^2}$ when $a/L_x \to 0$) can be calculated on the stagnation line approaching any symmetrical body just by knowing U_1. When $a/L_x \sim 1$ then wake boundary conditions are always important and we do not know what they are, but even assuming they can be ignored to a first approximation, then lengthy numerical calculations are needed. These in general will be even more lengthy than for a circular cylinder.

7.3. *Comparison with experiments*

No detailed comparisons of the theory with experimental results will be given here except for a brief discussion of those of Bearman (1972), who has recently published his experimental measurements of turbulent velocity on the stagnation line and fluctuating pressure at the stagnation point of a bluff body (already described in §7.2). He compared his measurements of $\overline{u_i^2}$ ($i = 1, 2, 3$) and $\hat{\Theta}_{11}(\hat{\kappa}_1)$ with theoretical results for the limiting cases $a/L_x \to 0$ and $a/L_x \to \infty$, which were calculated from the measured values of $\overline{u_1}$, using the result of §7.2. In his experiments the scale of turbulence was in the range $0{\cdot}21 < a/L_x < 0{\cdot}42$, where a is the half-width of the plate normal to the flow.

The qualitative predictions for $\hat{\Theta}_{ii}$ and $\overline{u_1^2}$ made in §7.1 for values of $aL_x < 1$ are borne out by Bearman's experimental results. In fact he found that for all three velocity components $\overline{u_i^2}$ lay between the asymptotic values for very large and very small scales of turbulence. The one-dimensional spectrum $\hat{\Theta}_{11}(\hat{\kappa}_1)$ (figure 5 of Bearman's paper) demonstrates the important physical result that when $a/L_x < 1$ low-frequency components of the turbulent velocity u_1 are reduced on the stagnation line but high-frequency components are amplified, and in particular his results approximately agree with the prediction that when $\kappa_1 \gg 1$ values of $\hat{\Theta}_{11}(\hat{\kappa}_1)$ for all wavenumbers fall onto the same curve. Further comparisons between this theory and his experiments will be made when $\hat{\Theta}_{11}(\hat{\kappa}_1)$ and $\hat{\Theta}_{22}(\hat{\kappa}_1)$ have been calculated near the stagnation point in the limit $\kappa_1 \gg 1$,

$\kappa_1 \xi \ll 1$. An extensive comparison between experiments for turbulent flow round a circular cylinder and the theory will be given by Petty (1974).

7.4. *Extensions of the theory*

We hope that this paper has demonstrated that the study of turbulent flows round a bluff body is an important and fruitful theoretical research problem. Some of the further problems that will be tackled are (i) extending the theory to other two-dimensional and to three-dimensional bodies, (ii) completing the investigations of $\hat{\Theta}_{ii}(\hat{\kappa}_1)$ when $(a/L_x)\,\xi \ll 1$, (iii) calculating the spectra for $\hat{\Theta}_{33}(\hat{\kappa})$, (iv) examining the effect of viscosity on the turbulence near the surface of the body and (v) calculating fluctuating pressures on the body. We shall not be undertaking a numerical calculation for all the wavenumbers necessary to calculate spectra and variances when $a/L_x \sim 1$. This remains an important task to be done by someone else!

There is also a great need for further experimental work on this problem particularly in exploring the nonlinear effects due to finite intensity of turbulence, and in investigating in detail the effect of incident turbulence on the velocities in the boundary layers and wake of a bluff body.

The work described here was begun in the Central Electricity Research Laboratories, Leatherhead, where I was encouraged to pursue this academic approach to a practical problem and where I received many valuable ideas and much mathematical assistance from J. Armitt and R. A. Scriven. Continuing at Cambridge I have been greatly helped by the criticisms and suggestions of G. K. Batchelor and H. K. Moffatt. I am also grateful for many rewarding discussions with P. W. Bearman and D. G. Petty, and for extensive computing assistance from J. C. Mumford, with support from the Science Research Council.

Appendix

General expressions for $\tilde{M}_{ii}^{(s)}$ when $k \to 0$, $r\kappa_1 = o(1)$, $r\kappa_2 = o(1)$, $r\kappa_3$ is arbitrary

$$\tilde{M}_{11}^{(s)} = \tfrac{1}{2}i\kappa_3\kappa_1 K_0'(|r\kappa_3|) + \kappa_3^2 K_1'(|r\kappa_3|)\cos\theta\,(1+\tfrac{1}{2}\kappa_3^2\ln(\tfrac{1}{2}|\kappa_3|)) + \tfrac{1}{8}i\kappa_1\kappa_3^2 K_2'(|r\kappa_3|)\cos 2\theta + \tfrac{1}{8}i\kappa_2\kappa_3^2 K_2'(|r\kappa_3|)\sin 2\theta + O(k^2), \quad (A\,1)$$

$$\tilde{M}_{12}^{(s)} = \tfrac{1}{2}i\kappa_2\kappa_3 K_0'(|r\kappa_3|) + \kappa_3^2 K_1'(|r\kappa_3|)\,(1+\tfrac{1}{2}\kappa_3^2\ln(\tfrac{1}{2}|\kappa_3|))\sin\theta - \tfrac{1}{8}i\kappa_2\kappa_3^2 K_2'(|r\kappa_3|)\cos 2\theta + \tfrac{1}{8}i\kappa_1\kappa_3^2 K_2'(|r\kappa_3|)\sin 2\theta + O(k^2), \quad (A\,2)$$

$$\tilde{M}_{13}^{(s)} = 0, \quad (A\,3)$$

$$\tilde{M}_{21}^{(s)} = -\frac{\kappa_3 K_1(|r\kappa_3|)}{r}\left(1+\frac{\kappa_3^2}{2}\ln\left(\frac{|\kappa_3|}{2}\right)\right)\sin\theta + \frac{i\kappa_2\kappa_3^2 K_2(|r\kappa_3|)\cos 2\theta}{4r} - \frac{i\kappa_1\kappa_3^2 K_2(|r\kappa_3|)}{4r}\sin 2\theta + O(k^2), \quad (A\,4)$$

$$\tilde{M}_{22}^{(s)} = \frac{\kappa_3 K_1(|r\kappa_3|)}{r}\left(1+\frac{\kappa_3^2}{2}\ln\left(\frac{|\kappa_3|}{2}\right)\right)\cos\theta + \frac{i\kappa_1\kappa_3^2}{r}K_2(|r\kappa_3|)\cos 2\theta + \frac{i\kappa_2\kappa_3^2 K_2(|r\kappa_3|)}{4r}\sin 2\theta + O(k^2), \quad (A\,5)$$

$$\tilde{M}^{(s)}_{23} = 0, \tag{A 6}$$

$$\tilde{M}^{(s)}_{31} = -\tfrac{1}{2}\kappa_1\kappa_3 K_0(|r\kappa_3|) + i\kappa_3 K_1(|r\kappa_3|)\,(1+\tfrac{1}{2}\kappa_3^2 \ln(\tfrac{1}{2}|\kappa_3|))\cos\theta$$
$$-\tfrac{1}{8}\kappa_1\kappa_3^3 K_2(|r\kappa_3|)\cos 2\theta - \tfrac{1}{8}\kappa_2\kappa_3^3 K_2(|r\kappa_3|)\sin 2\theta, \tag{A 7}$$

$$\tilde{M}^{(s)}_{32} = -\tfrac{1}{8}\kappa_2\kappa_3 K_0(|r\kappa_3|) + i\kappa_3 K_1(|r\kappa_3|)\,(1+\tfrac{1}{2}\kappa_3^2 \ln(\tfrac{1}{2}|\kappa_3|))\sin\theta$$
$$+\tfrac{1}{8}\kappa_2\kappa_3^3 K_2(|r\kappa_3|)\cos 2\theta - \tfrac{1}{8}\kappa_1\kappa_3^3 K_2(|r\kappa_3|)\sin 2\theta, \tag{A 8}$$

$$\tilde{M}^{(s)}_{33} = 0. \tag{A 9}$$

Note

$$K_0'(|r\kappa_3|) = -K_1(|r\kappa_3|) \sim -(1/|r\kappa_3| + \tfrac{1}{2}|\kappa r_3|\,|\ln(\tfrac{1}{2}|r\kappa_3|)),$$
$$K_1'(|r\kappa_3|) = -K_0(|r\kappa_3|) - |r\kappa_3|^{-1} K_1(|r\kappa_3|) \sim -1/r^2\kappa_3^2 + \tfrac{1}{2}\ln(\tfrac{1}{2}|r\kappa_3|),$$
$$K_2'(|r\kappa_3|) = -K_1(|r\kappa_3|)/r - (2/r\kappa_3)\,K_2(|r\kappa_3|),$$
$$K_2(r\kappa_3) \sim (2/r^2\kappa_3^2)\,(1+O(k^4)).$$

	$r = 1{\cdot}01$				$r = 3{\cdot}6$			
$\kappa_1 = \kappa_2$	$(\Omega_{11}^{cn})_{\max}$		$n_{\max}$	λ_c	$(\Omega_{11}^{cn})_{\max}$		$n_{\max}$	λ
0·1	−0·975	0·005	1	$1{\cdot}6\times10^{3}$	−0·694	0·017	1	$4{\cdot}5\times10$
1·0	−0·560	0·009	1	$7{\cdot}1\times10^{2}$	0·104	−0·094	3	$1{\cdot}0\times10$
3·0	0·327	−0·001	5	$1{\cdot}6\times10$	0·230	0·100	1	3·8
10·0	−0·002	0·287	4	$1{\cdot}3\times10$	−0·074	0·418	2	1·5

TABLE 3. Properties of the series Ω_{11}^{cn}: the largest term $(\Omega_{11}^{cn})_{\max}$, the value of n $(n_{\max})$ at which $\Omega_{11}^{cn} = (\Omega_{11}^{cn})_{\max}$, and the ratio $\lambda_c = (\Omega_{11}^{cn})_{\max}/|\Omega_{11}^{c20}|$

			$r = 1{\cdot}1$				$r = 2{\cdot}0$			
κ_1	κ_2	κ_3	$(a_{12}^{cn})_{\max}$		$n_{\max}$	λ	$(a_{12}^{cn})_{\max}$		$n_{\max}$	λ
0·1	0·1	0·1	−0·001	0·012	0	$5{\cdot}2\times10$	−0·003	0·037	0	$4{\cdot}0\times10^{4}$
1·0	1·0	—	−0·003	−0·006	1	$2{\cdot}2\times10$	−0·022	0·016	1	$1{\cdot}3\times10^{4}$
3·0	0·1	—	0·002	−0·003	1	7·3	−0·001	0·007	1	$9{\cdot}0\times10^{2}$
0·1	0·1	1·0	−0·010	0·093	0	$9{\cdot}0\times10^{3}$	−0·011	0·151	0	$4{\cdot}5\times10^{4}$
1·0	1·0	—	−0·023	−0·070	1	$2{\cdot}3\times10^{3}$	−0·157	0·054	1	$1{\cdot}0\times10^{4}$
0·1	3·0	—	−0·012	0·128	1	$1{\cdot}1\times10^{4}$	Not computed			
0·1	0·1	3·0	−0·020	0·182	0	$5{\cdot}3\times10^{3}$	−0·006	0·097	0	$3{\cdot}0\times10^{3}$
1·0	1·0	—	−0·025	−0·164	1	$1{\cdot}8\times10^{4}$	−0·141	0·016	1	$3{\cdot}0\times10^{3}$
3·0	3·0	—	0·032	0·071	1	$1{\cdot}8\times10^{2}$	−0·014	−0·253	1	$1{\cdot}8\times10^{3}$

TABLE 4. Properties of the series a_{12}^{cn}: the largest term $(a_{12}^{cn})_{\max}$, the value of n $(n_{\max})$ at which $a_{12}^{cn} = (a_{12}^{cn})_{\max}$, and the ratio $\lambda_c = |a_{12}^{cn}|/|a_{12}^{c20}|$

Nomenclature

An equation number following a symbol indicates the equation where it is defined or the equation immediately following or preceding its definition.

a	radius of circular cylinder (or typical dimension of a body)
a_{ij}	velocity tensor in terms of upstream vorticity, (4.30)
b	integration variable used in § 6

c_1, c_2, c_3	(6.5), (6.7)
$f(b)$	(5.46a), (6.35)
$f_{ij}(\theta)$	(5.11)
$g(\hat{\kappa}_1)$	(6.23)
g_1, g_2, g_3	(6.3b), (6.7)
$g_{ij}(x, y)$	(5.27)
$g_{ij}^{(1)}, g_{ij}^{(\infty)}(r, \theta)$	(5.4), (5.6)
$g_{ijl}(\theta)$	(5.11)
h_{ij}	(5.27)
$k = \lvert\boldsymbol{\kappa}\rvert$	modulus of wavenumber
$\tilde{k}$	(5.43)
l	a length scale of turbulence (§2) or an eddy size (§5)
$\mathbf{n}$	outward normal to body
n	integer variable
p	pressure
p_{il}	(6.12)
q_{il}	(6.12)
r	radial co-ordinate
r_x, r_y, r_z	(3.30)
$\bar{r} = rk$	(5.7)
r_{il}	(6.12)
$s_{\infty i}$	vorticity Fourier transform, (3.24), (3.26)
t	time
$\mathbf{u}', \mathbf{u}$	dimensional and dimensionless turbulent velocity
$\bar{u}_\infty, u'_\infty$	dimensional mean velocity and root-mean-square turbulent velocity (in x direction) upstream
(x, y, z)	Cartesian co-ordinates
A	constant, (5.34)
(B)	boundary layers (§2)
$B(\theta_0)$	(5.36)
C_1, C_2	(6.5)
C_{ij}^{cn}, C_{ij}^{sn}	(4.14), (4.18)
(E)	external flow region (§2)
$E(k)$	(6.6)
$E_L(\theta, \zeta), E_L(\zeta)$	(4.4)
$E_1(t), E_i(t)$	(5.46a)
$F(\theta, \zeta)$	(4.4)
F_{ij}	(4.13)
$F_{ijll}^{(0)}, F_{ijll}^{(1)}$	(6.12), (6.15)
$G_1 \ldots, G_6$	constants in §6
G_i^{cn}, G_i^{sn}	(4.25)
I	(4.26)
I_1, I_2, I_3	(6.33)
$I_A, \ldots, I_J$	integrals used in §6
$I_n(\ )$	modified Bessel function (first kind)
$I_{ij}, I_{Aij}, I_{Bij}, I_{cij}$	(5.38), (5.40)

$I_{11}(\hat{\kappa}_1), I_{22}, (\hat{\kappa}_1)$	(6.25), (6.30)
$\mathscr{I}(\ )$	'imaginary part of'
$J_n(\ )$	Bessel function (first kind)
$K(\zeta)$	(4.4)
$K_n(\ )$	modified Bessel function (second kind)
L_x	integral scale of incident turbulence, (6.3a)
L_{ij}	(6.22)
M_{il}	velocity tensor in terms of upstream velocity, (3.28), (4.32)
R	(2.24)
Re	Reynolds number, (2.7)
R_{ij}	cross-variance, (3.30), (3.31)
$\mathscr{R}(\ )$	'real part of'
S	surface of the body
$S_{\infty i}$	velocity Fourier transform, (3.24), (3.26)
T^*	averaging time, (2.5)
T_x	(3.3)
T	'Drift' time, (3.8)
$\mathscr{T}$	(3.24), (3.27)
$\mathbf{U}, (U_x, U_y, U_z), (U_1, U_2, U_3)$	dimensionless mean velocity in Cartesian co-ordinates
(U_r, U_θ, U_z)	dimensionless mean velocity in cylindrical co-ordinates
(W)	wake region (§2)
$\hat{\hat{W}}$	pressure Fourier transform
X	(5.32)
Y	(5.32)
$\mathscr{Y}$	(3.24)
$\mathscr{Z}$	(3.24), (3.27)
α	(2.8)
α_{ij}	(4.2)
$\alpha_{ij}^{cn}, \alpha_{ij}^{sn}$	(4.6)
β	(2.9)
β_i	(4.20)
$\beta_i^{cn}, \beta_i^{sn}$	(4.21)
γ	Euler's constant
γ_1, γ_2	(6.30)
$\gamma_{ij}, \gamma_{\infty ij}$	(3.11)
δ_{ij}	Kronecker delta
δ_b	boundary-layer thickness
$\delta(\ )$	delta function
$\delta\theta$	(As 3) in §2
ε	energy dissipation density, (2.16)
ϵ	(5.33)
ϵ_{ijk}	alternating tensor, (3.25)
ζ	(6.13)
η	co-ordinate parallel to surface
η_K	(6.4)
θ	angular co-ordinate

$\boldsymbol{\kappa}, \kappa_i, (\kappa_1 \kappa_2, \kappa_3)$	wavenumber vector
$\kappa_i^\times = \kappa_i/k$	(5.7)
$\tilde{\kappa}_2$	(5.43)
$\lambda, \lambda^\times$	(5.3), (5.32)
λ_c	§4.3
μ, μ_i	(4.3)
$\mu_{ij}^{(n)} (n = 1, 2, 3, 4)$	(5.10)
$\tilde{\mu}, \tilde{\mu}^\times$	(5.40*b*)
ν	kinematic viscosity, (2.1)
ν_{ijk}	(5.1)
ξ	co-ordinate normal to surface
ρ	density (2.1)
$\rho^\times$	(5.32)
σ	(3.24)
σ_1, σ_2	(6.44)
σ_3	(4.26)
τ	time difference (dimensionless)
ϕ	(5.42)
$\phi^\times$	integration variable in §6
χ	(5.30), (6.33)
$\chi_i^\times = \chi_i/k$	(6.44)
$\tilde{\chi}$	(5.42)
$\chi^\times$	(6.49)
$\chi_t, (\chi_1, \chi_2, \chi_3)$	(5.27)
$\chi_r, \chi_\theta, \chi_z$	(6.33)
$\tilde{\chi}_1, \tilde{\chi}_2, \tilde{\chi}_{23}$	(5.36)
$\boldsymbol{\psi}, \psi_i, (\psi_r, \psi_\theta, \psi_z)$	(3.17)
$\boldsymbol{\omega}', \boldsymbol{\omega}$	dimensional and dimensionless turbulent vorticity
$\Gamma( )$	gamma function
$\Gamma_{ij}, \Gamma_{ij}^{(\infty)}$	(5.26)
$\Gamma_{ij}^{cn}, \Gamma_{ij}^{sn}$	(4.19)
$\Delta\mathbf{u}, \Delta\boldsymbol{\omega}$	(3.14)
$\Delta\gamma_{ij}$	(5.1)
Δ_T	(3.8)
Δ_y	(3.9)
$\Theta_{ij}(\kappa_1)$	(3.32)
$\hat{\Theta}_{ij}(\hat{\kappa}_1), \hat{\tilde{\Theta}}_{ij}(\hat{\kappa}_1)$	(6.4), (6.33)
Ξ	(6.36)
Φ	(3.17)
$\Phi_{\infty ij}$	(3.30)
Ψ	(3.2)
Ψ_{ij}	(3.31)
$\boldsymbol{\Omega}$	(2.12)
Ω_{ij}	(4.2)
$\Omega_{ij}^{cn}, \Omega_{ij}^{sn}$	(4.7)

Superscripts

*	dimensional variable
†	complex conjugate
——	time mean
′	unsteady component of a random variable
^	variable normalized with respect to L_x
^^	Fourier transforms with respect to t and z
~	vector or tensor in cylindrical co-ordinates
(d), (s), (∞)	distortion, source, undisturbed values of M_{il}
(b)	term affected by presence of the body
(0,) (1), (2), (L)	terms in expansion of Θ_{ij}, M_{il}, α_{ij}, a_{ij}

Subscripts

∞	upstream or undisturbed value
w	effect of wake
max	maximum value

REFERENCES

ABRAMOWITZ, M. & STEGUN, I. A. 1964 *Handbook of Mathematical Functions*. Washington: Nat. Bur. Stand.

BATCHELOR, G. K. 1953 *Homogeneous Turbulence*. Cambridge University Press.

BATCHELOR, G. K. 1967 *An Introduction to Fluid Dynamics*. Cambridge University Press.

BATCHELOR, G. K. & PROUDMAN, I. 1954 The effect of rapid distortion of a fluid in turbulent motion. *Quart. J. Mech. Appl. Math.* **7**, 83.

BEARMAN, P. W. 1968. The flow around a circular cylinder in the critical Reynolds number regime. *Nat. Phys. Lab. Aero. Rep.* no. 1257.

BEARMAN, P. W. 1972 Some measurements of the distortion of turbulence approaching a two-dimensional body. *J. Fluid Mech.* **53**, 451.

CERMAK, J. E. & HORN, J. D. 1968 Tower shadow effect *J. Geophys. Res.* **73**, 1869.

DARWIN, C. G. 1953 Note on hydrodynamics. *Proc. Camb. Phil. Soc.* **49**, 342.

DAVENPORT, A. G. 1971 The response of six building shapes to turbulent wind. *Phil. Trans. Roy. Soc.* A **269**, 385.

DEISSLER, R. G. 1965 The problem of steady state shear flow turbulence. *Phys. Fluids*, **8**, 391.

DEISSLER, R. G. 1967 Weak locally homogeneous turbulence and heat transfer with uniform normal strain. *N.A.S.A. Tech. Note*, D-3779.

ERDÉLYI, A., MAGNUS, W. & OBERHETTINGER, F. 1954 *Tables of Integral Transforms*, vol. 1. McGraw-Hill.

GRÖBNER, W. & HOFREITER, N. 1968 *Integral Tafel*, vol. 1. Springer.

HALITSKY, J. 1968 Gas diffusion near buildings. In '*Meteorology and Atomic Energy*'. U.S. Atomic Energy Commission.

HARRIS, I. 1971 The nature of the wind. *Proc. Seminar at Inst. Civil Engrs, June* 1970.

HUNT, J. C. R. 1971 The effect of single buildings and structures. *Phil. Trans. Roy. Soc.* A **269**, 457.

HUNT, J. C. R. 1973 A theory for fluctuating pressures on bluff bodies in turbulent flows. *Proc. IUTAM/IAHR Symp. on Flow Induced Vibrations, Karlsruhe*, 1972. Springer.

HUNT, J. C. R. & MULHEARN, P. J. 1973 The dispersion of pollution by the wind near two-dimensional obstacles. *J. Fluid Mech.* **61**, 245.

KESTIN, J. 1966 The effect of free stream turbulence on heat transfer rates. *Adv. in Heat Transfer*, **3**, 1.

KESTIN, J. & WOOD, R. T. 1970 On the stability of two-dimensional stagnation flow. *J. Fluid Mech.* **44**, 461.

LIGHTHILL, M. J. 1954 The response of laminar skin friction and heat transfer to fluctuations in the stream velocity. *Proc. Roy. Soc.* A **224**, 1.

LIGHTHILL, M. J. 1956 Drift. *J. Fluid Mech.* **1**, 31.

LIGHTHILL, M. J. 1970 Turbulence. In *Osborne Reynolds and Engineering Science To-day*, chap. 2. Manchester University Press.

MOFFATT, H. K. 1965 The interaction of turbulence with strong wind shear. *Proc. URSI–IUGG Int. Coll. on 'Atmospheric Turbulence & Radio wave Propagation'*. Moscow: Nauka.

OWEN, P. R. 1965 Buffeting excitation of boiler tube vibration. *J. Mech. Engng Sci.* **7**, 431.

PEARSON, J. R. A. 1959 The effect of uniform distortion on weak homogeneous turbulence. *J. Fluid Mech.* **5**, 274.

PETTY, D. G. 1974 The distortion of turbulence by a circular cylinder. To be published.

PIERCY, N. A. V. & RICHARDSON, E. G. 1930 The turbulence in front of a body moving through a viscous fluid. *Phil. Mag.* **9**, 1038.

PRANDTL, L. 1933 Attaining a steady air stream in wind tunnels. *N.A.C.A. Tech. Memo.* no. 726.

RIBNER, H. S. & TUCKER, M. 1953 Spectrum of turbulence in a contracting stream. *N.A.C.A. Tech. Note*, no. 19, p. 1113.

SADEH, W. Z., SUTERA, S. P. & MAEDER, P. F. 1970*a* Analysis of vorticity amplification in the flow approaching a two-dimensional stagnation point. *Z. angew. Math. Phys.* **21**, 699.

SADEH, W. Z., SUTERA, S. P. & MAEDER, P. F. 1970*b* An investigation of vorticity amplification in stagnation flow. *Z. angew. Math. Phys.* **21**, 717.

SUTERA, S. P., MAEDER, P. F. & KESTIN, J. 1963 On the sensitivity of heat transfer in the stagnation point boundary layer to free stream vorticity. *J. Fluid Mech.* **16**, 497.

TAYLOR, G. I. 1935 Turbulence in a contracting stream. *Z. angew. Math. Mech.* **15**, 91.

TOWNSEND, A. A. 1954 The uniform distortion of homogeneous turbulence. *Quart. J. Mech. Appl. Math.* **7**, 118.

TOWNSEND, A. A. 1970 Entrainment and the structure of turbulent flow. *J. Fluid Mech.* **41**, 13.

TUCKER, H. S. & REYNOLDS, A. J. 1968 The distortion of turbulence by irrotational plane strain. *J. Fluid Mech.* **32**, 657.

UBEROI, M. S. 1956 The effect of wind tunnel contraction on free stream turbulence. *J. Aero. Sci.* **23**, 754.

VON KÁRMÁN, T. 1948 Progress in the statistical theory of turbulence. *J. Mar. Res.* **7**, 252.